FOREST ECOLOGY

Plant diversity increases with the strength of negative density dependence at the global scale

Joseph A. LaManna,[1,2]* Scott A. Mangan,[2] Alfonso Alonso,[3] Norman A. Bourg,[4,5] Warren Y. Brockelman,[6,7] Sarayudh Bunyavejchewin,[8] Li-Wan Chang,[9] Jyh-Min Chiang,[10] George B. Chuyong,[11] Keith Clay,[12] Richard Condit,[13] Susan Cordell,[14] Stuart J. Davies,[15,16] Tucker J. Furniss,[17] Christian P. Giardina,[14] I. A. U. Nimal Gunatilleke,[18] C. V. Savitri Gunatilleke,[18] Fangliang He,[19,20] Robert W. Howe,[21] Stephen P. Hubbell,[22] Chang-Fu Hsieh,[23] Faith M. Inman-Narahari,[14] David Janík,[24] Daniel J. Johnson,[25] David Kenfack,[15,16] Lisa Korte,[3] Kamil Král,[24] Andrew J. Larson,[26] James A. Lutz,[17] Sean M. McMahon,[27,28] William J. McShea,[4] Hervé R. Memiaghe,[29] Anuttara Nathalang,[6] Vojtech Novotny,[30,31,32] Perry S. Ong,[33] David A. Orwig,[34] Rebecca Ostertag,[35] Geoffrey G. Parker,[28] Richard P. Phillips,[12] Lawren Sack,[22] I-Fang Sun,[36] J. Sebastián Tello,[37] Duncan W. Thomas,[38] Benjamin L. Turner,[13] Dilys M. Vela Díaz,[2] Tomáš Vrška,[24] George D. Weiblen,[39] Amy Wolf,[21,40] Sandra Yap,[41] Jonathan A. Myers[1,2]

Theory predicts that higher biodiversity in the tropics is maintained by specialized interactions among plants and their natural enemies that result in conspecific negative density dependence (CNDD). By using more than 3000 species and nearly 2.4 million trees across 24 forest plots worldwide, we show that global patterns in tree species diversity reflect not only stronger CNDD at tropical versus temperate latitudes but also a latitudinal shift in the relationship between CNDD and species abundance. CNDD was stronger for rare species at tropical versus temperate latitudes, potentially causing the persistence of greater numbers of rare species in the tropics. Our study reveals fundamental differences in the nature of local-scale biotic interactions that contribute to the maintenance of species diversity across temperate and tropical communities.

One of the most prominent and ubiquitous patterns of life on Earth is the systematic increase in species diversity from temperate to tropical latitudes (*1*). For nearly half a century, ecologists have hypothesized that higher species diversity in the tropics is maintained by negative density–dependent interactions among species and their specialized natural enemies (*2*–*6*). Conspecific negative density dependence (CNDD) is the process by which population growth rates decline at high densities as a result of natural enemies (e.g., predators, pathogens, or herbivores) and/or competition for space and resources (*2*–*4*, *7*). Numerous studies have documented the existence of CNDD in one or several plant species (*8*–*12*), and most of these studies explicitly or implicitly assume that stronger CNDD maintains higher species diversity in communities. However, only a handful of studies have explicitly examined the link between CNDD and species diversity (*4*, *11*, *13*, *14*), and no study has examined this relationship across temperate and tropical latitudes. Despite decades of study, our understanding of how processes at local scales—such as density-dependent biotic interactions—influence global patterns of biodiversity remains in flux (*1*, *15*).

Both species-specific and more generalized mechanisms can cause CNDD, but only CNDD caused by species-specific mechanisms can maintain diversity (*2*, *3*, *16*, *17*). Species-specific causes of CNDD include intraspecific competition or pressure from host-specific natural enemies (*6*, *9*, *10*, *16*). These specialized interactions stabilize populations of individual species, causing population growth rates to decrease when a species is locally common and increase when a species is locally rare (*6*, *9*, *10*, *17*). Thus, CNDD caused by specialized interactions results in the maintenance of diversity via negative frequency dependence at local scales (*17*–*19*). However, negative density dependence may also result from interactions that are more generalized with respect to species identity, such as interspecific competition or pressure from generalist natural enemies (*6*, *16*, *20*). In this case, high densities of either conspecifics or heterospecifics similarly reduce population growth rates of a given species, and one or a few better-performing species could exclude others (*6*, *16*, *20*). Thus, negative effects of conspecific densities on the recruitment or survival of a given species (i.e., CNDD) are expected to maintain diversity only when they are stronger relative to any negative effects from heterospecific densities [hereafter, heterospecific negative density dependence (HNDD)] (*17*). Increases in CNDD

[1]Tyson Research Center, Washington University in St. Louis, St. Louis, MO, USA. [2]Department of Biology, Washington University in St. Louis, St. Louis, MO, USA. [3]Center for Conservation and Sustainability, Smithsonian Conservation Biology Institute, National Zoological Park, Washington, DC, USA. [4]Conservation Ecology Center, Smithsonian Conservation Biology Institute, National Zoological Park, Front Royal, VA, USA. [5]National Research Program - Eastern Branch, U.S. Geological Survey, Reston, VA, USA. [6]Ecology Laboratory, BIOTEC, National Science and Technology Development Agency, Science Park, Pathum Thani, Thailand. [7]Institute of Molecular Biosciences, Mahidol University, Salaya, Nakhon Pathom, Thailand. [8]Research Office, Department of National Parks, Wildlife and Plant Conservation, Bangkok, Thailand. [9]Taiwan Forestry Research Institute, Taipei 10066, Taiwan. [10]Department of Life Science, Tunghai University, Taichung, Taiwan. [11]Department of Botany and Plant Physiology, University of Buea, Buea, Cameroon. [12]Department of Biology, Indiana University, Bloomington, IN, USA. [13]Smithsonian Tropical Research Institute, Balboa, Ancon, Republic of Panama. [14]Institute of Pacific Islands Forestry, U.S. Department of Agriculture Forest Service, Hilo, HI, USA. [15]Center for Tropical Forest Science–Forest Global Earth Observatory, Smithsonian Tropical Research Institute, Panama City, Republic of Panama. [16]Department of Botany, National Museum of Natural History, Washington, DC, USA. [17]Wildland Resources Department, Utah State University, Logan, UT, USA. [18]Department of Botany, Faculty of Science, University of Peradeniya, Peradeniya, Sri Lanka. [19]Joint Lab for Biodiversity Conservation, Sun Yat-sen University (SYSU)–University of Alberta, State Key Laboratory of Biocontrol, School of Life Sciences, SYSU, Guangzhou 510275, China. [20]Department of Renewable Resources, University of Alberta, Edmonton, Alberta, Canada. [21]Department of Natural and Applied Sciences, University of Wisconsin–Green Bay, Green Bay, WI, USA. [22]Department of Ecology and Evolutionary Biology, University of California, Los Angeles, Los Angeles, CA, USA. [23]Institute of Ecology and Evolutionary Biology, National Taiwan University, Taipei, Taiwan. [24]Department of Forest Ecology, Silva Tarouca Research Institute, Brno, Czech Republic. [25]Los Alamos National Laboratory, Los Alamos, NM, USA. [26]Department of Forest Management, College of Forestry and Conservation, University of Montana, Missoula, MT, USA. [27]Center for Tropical Forest Science–Forest Global Earth Observatory, Smithsonian Environmental Research Center, Edgewater, MD, USA. [28]Forest Ecology Group, Smithsonian Environmental Research Center, Edgewater, MD, USA. [29]Institut de Recherche en Ecologie Tropicale, Centre National de la Recherche Scientifique et Technologique, Libreville, Gabon. [30]New Guinea Binatang Research Centre, P.O. Box 604, Madang, Papua New Guinea. [31]Biology Centre, Academy of Sciences of the Czech Republic, Prague, Czech Republic. [32]Faculty of Science, University of South Bohemia, Branisovska 31, Ceske Budejovice 370 05, Czech Republic. [33]Institute of Biology, University of the Philippines Diliman, Quezon City, Philippines. [34]Harvard Forest, Harvard University, Petersham, MA, USA. [35]Department of Biology, University of Hawaii, Hilo, HI, USA. [36]Department of Natural Resources and Environmental Studies, National Dong Hwa University, Hualian, Taiwan. [37]Center for Conservation and Sustainable Development, Missouri Botanical Gardens, St. Louis, MO, USA. [38]School of Biological Sciences, Washington State University, Vancouver, WA, USA. [39]Department of Plant and Microbial Biology, University of Minnesota, St. Paul, MN, USA. [40]Department of Biology, University of Wisconsin–Green Bay, Green Bay, WI, USA. [41]Institute of Arts and Sciences, Far Eastern University Manila, Manila, Philippines.
*Corresponding author. Email: joe.a.lamanna@gmail.com

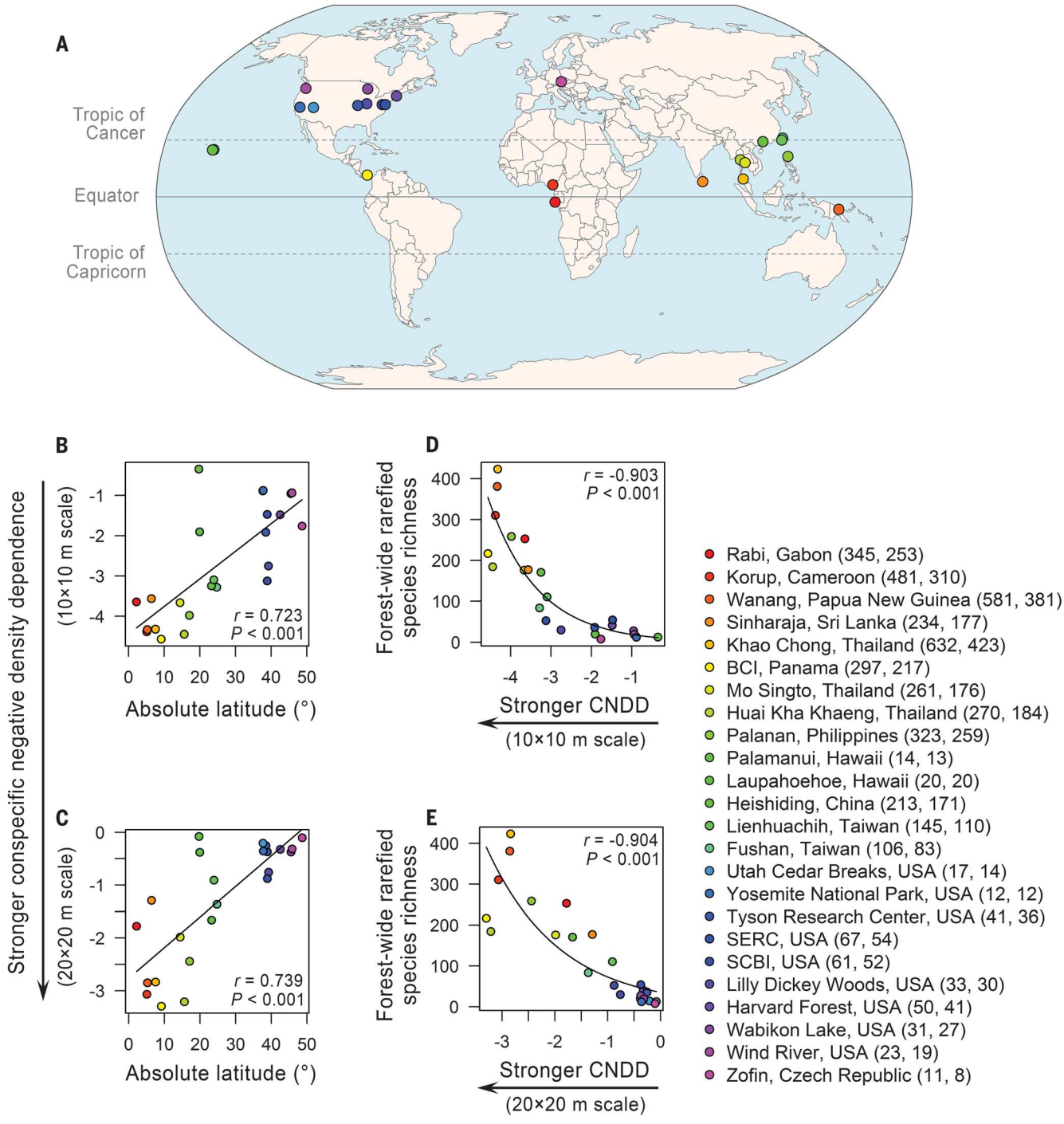

Fig. 1. Species richness increased with the strength of conspecific negative density dependence (CNDD) across tropical and temperate forests. (**A**) World map of stem-mapped forest plots (n = 24 forest plots) examined, which are part of the Smithsonian Center for Tropical Forest Science–Forest Global Earth Observatory (CTFS-ForestGEO) network. The median strength of CNDD measured at (**B**) 10-m–by–10-m and (**C**) 20-m–by–20-m scales declined (lower values indicate stronger CNDD) with increasing distance from the equator. Forest-wide rarefied species richness increased across latitudes with the median strength of CNDD measured at (**D**) 10-m–by–10-m or (**E**) 20-m–by–20-m scales. Patterns were similar for observed (nonrarefied) species richness and diversity (figs. S1 and S2). Density dependence was estimated with the Ricker model, but qualitatively similar results were obtained using another functional form (*25*) (figs. S5 and S6). Numbers next to plots (at right) are observed and rarefied species richness, respectively, of live trees. Plots are colored by increasing distance from the equator. Lines are best fits from linear [(B) and (C)] or Poisson [(D) and (E)] regression, and correlation coefficients (r) are from Spearman-rank tests. BCI, Barro Colorado Island; SERC, Smithsonian Environmental Research Center; SCBI, Smithsonian Conservation Biology Institute.

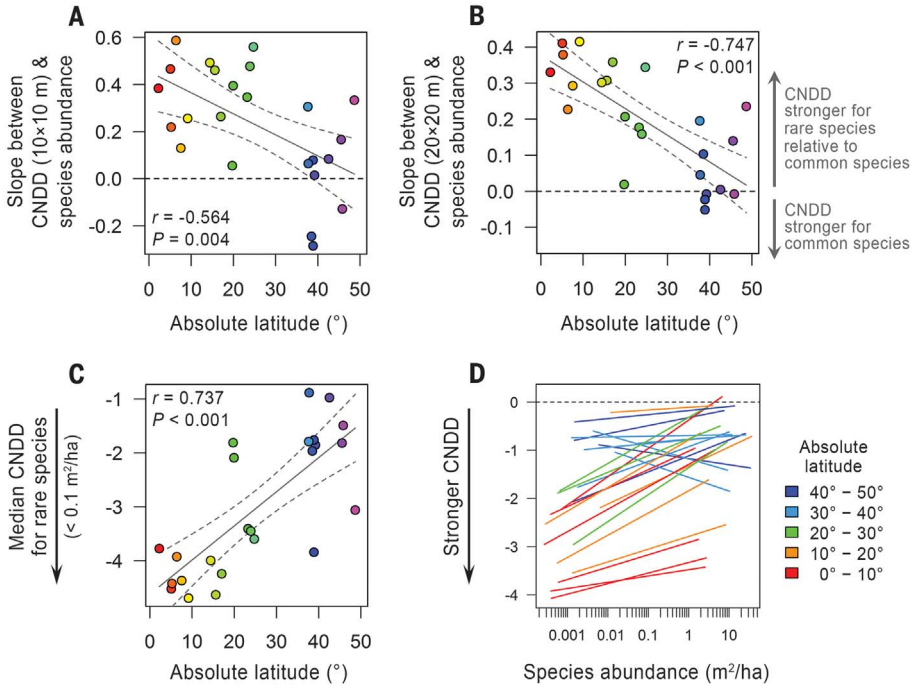

Fig. 2. Latitudinal shift in the strength of CNDD among common and rare species. Slopes and best-fit linear regression lines (±95% confidence interval) between species abundance [measured by basal area (square meters per hectare)] and CNDD measured at the (**A**) 10-m–by–10-m and (**B**) 20-m–by–20-m scales across species within each forest plot (n = 24 forest plots). Because lower values of CNDD reflect stronger CNDD, positive slopes indicate stronger CNDD for rare as compared with common species, and negative slopes indicate stronger CNDD for common versus rare species. (**C**) The median strength of CNDD for rare species (species with basal area less than 0.1 m^2/ha) was stronger at tropical than at temperate latitudes. CNDD for rare species is shown at the 10-m–by–10-m scale, but results were similar at the 20-m–by–20-m scale. For (A) to (C), plots are colored as in Fig. 1. (**D**) Best-fit linear regression relationships between the strength of CNDD (measured at the 10-m–by–10-m scale) and species abundance (square meters per hectare) within each forest plot (n = 24 forest plots) (table S8). Colors in (D) represent the latitudinal band a forest plot occupies, from tropical (red) to temperate (blue) latitudes. Species abundance is shown on a log scale. Density dependence was estimated with the Ricker model, but qualitatively similar results were found using another functional form (*25*) (fig. S7). Test statistics in (A) and (B) are Pearson correlation coefficients (r) from linear regression models, and the statistic in (C) is from a Spearman-rank test.

relative to HNDD indicate greater specificity of the mechanisms underlying CNDD and are expected to maintain higher levels of species diversity (*9*, *10*, *17*–*19*).

The relative strength of CNDD can also vary among common and rare species in a community (*9*, *10*), with important implications for the maintenance of diversity across latitudes. A notable feature of many tropical communities is that they harbor extremely large numbers of rare species (*1*). Assuming that CNDD is stronger than HNDD and limits local abundances of common species, the maintenance of diversity may depend on the degree to which populations of rare species are stabilized by CNDD. First, strong CNDD caused by host-specific enemies or intraspecific competition can reduce extinction risk by stabilizing the population dynamics of rare species (*10*, *18*, *21*, *22*), leading to the persistence of greater numbers of rare species in a community. For example, strong CNDD caused by soilborne pathogens may allow tropical tree species to recover from low population density (*23*). These types of specialized interactions may not only explain why so many species are rare in the tropics (*9*, *10*) but also why large numbers of rare species persist in tropical communities. In contrast, weak (or nonexistent) CNDD for rare species will not favor their recovery from very low densities, making these species more prone to local extinction from interspecific competition, generalist natural enemies, or demographic stochasticity (*16*, *18*, *20*) and potentially resulting in the erosion of diversity. Individual studies in either temperate or tropical latitudes have found evidence for stronger CNDD in either common or rare species (*9*, *10*, *13*, *14*, *24*). A global test of these alternatives would advance our understanding of the extent to and mechanisms by which CNDD contributes to the latitudinal-diversity gradient.

We tested the contribution of CNDD to changes in tree species diversity across temperate and tropical latitudes by using 24 globally distributed forest plots (Fig. 1A and tables S1 and S2) that are part of the Smithsonian Center for Tropical Forest Science–Forest Global Earth Observatory (CTFS-ForestGEO) network (*25*). In each large plot (mean size ± SD = 27.5 ± 13.7 ha, range = 4 to 50 ha), all stems ≥1 cm in diameter at breast height have been mapped, measured, and identified using standardized protocols (table S1) (*25*). For each plot, we measured species richness and diversity (Shannon diversity index), as well as rarefied species richness (species richness given a standardized number of individuals) to account for differences in plot size and total numbers of individuals (*25*). We measured the effects of CNDD and HNDD on sapling recruitment at both the 10-m–by–10-m and 20-m–by–20-m scales because effects of adult trees on younger trees decline with distance (*14*, *25*, *26*). By including heterospecific adult and sapling densities in our models, we explicitly measured the influence of increasing heterospecific densities on local sapling recruitment. Then, to quantify CNDD for each species in each plot, we measured the degree to which increasing adult conspecific densities suppress local recruitment of saplings, independent from the effects of heterospecific densities (*25*). Thus, we isolated conspecific density effects (CNDD) relative to heterospecific effects (HNDD) (*14*, *25*). We compared the relative magnitude of CNDD to HNDD to evaluate the extent to which CNDD is caused by species-specific mechanisms and the degree to which it is expected to maintain diversity (*17*). In addition, differences in tree densities, measurement error, and dispersal rates across forest plots might bias estimates of CNDD (*27*). Although simulation tests indicated that our results are generally robust to these potential biases (*25*), we used nonparametric Spearman-rank correlation tests to accommodate potential biases in our estimates of CNDD across latitudes.

The strength of CNDD declined with increasing distance from the equator (Fig. 1, B and C). Moreover, rarefied species richness (Figs. 1, D and E, and tables S3 to S6), nonrarefied species richness (figs. S1 and S2), and Shannon diversity (figs. S1 and S2) all increased with the strength of CNDD across temperate and tropical forests. The relationship between rarefied species richness and CNDD was equally strong whether CNDD was measured at the 10-m–by–10-m (Fig. 1D) or 20-m–by–20-m scale (Fig. 1E), indicating that CNDD operating at the scale of local tree neighborhoods can strongly contribute to large-scale diversity gradients. In contrast, density dependence from heterospecifics was relatively weak, nonexistent (i.e., HNDD ≈ 0), or slightly positive (tables S3 and S4). Consequently, species richness and diversity also increased with the relative strength of CNDD to HNDD (table S7). Although differences in CNDD between eastern and western hemispheres might influence our results (*25*), a simple linear-regression model including both latitude and a binary variable for eastern and western hemispheres showed that the strength of

CNDD still significantly decreased with latitude (at the 10-m–by–10-m scale: $F_{1,22} = 16.16$, $P < 0.001$; at the 20-m–by–20-m scale: $F_{1,22} = 25.28$, $P < 0.001$) but did not differ between eastern and western hemispheres (at the 10-m–by–10-m scale: $F_{1,22} = 0.013$, $P = 0.910$; at the 20-m–by–20-m scale: $F_{1,22} = 0.90$, $P = 0.354$). These results support the hypothesis that stronger CNDD caused by species-specific mechanisms—such as intraspecific competition or specialized host-enemy interactions—contributes to higher diversity in the tropics than at temperate latitudes (*2*, *3*).

The strength of CNDD was also associated with species abundance within forest communities, but the slope of this relationship changed systematically across latitudes. As compared with common species, rare species had stronger CNDD in the tropics (Fig. 2, A and B, and table S8). At temperate latitudes, in contrast, rare species had similar—and in some cases weaker—CNDD relative to common species (Figs. 2, A and B, and table S8). This latitudinal shift in the relationship between species abundance and CNDD was largely driven by a strong increase in the mean strength of CNDD for rare species (species with basal area < 0.1 m^2/ha) at tropical latitudes (Figs. 2, C and D). Because HNDD was relatively weak compared with CNDD across latitudes and species (tables S3 and S4), the latitudinal shift in the relationship between species abundance and CNDD was qualitatively similar if the relative strength of CNDD to HNDD was evaluated instead (at the 10-m–by–10-m scale: $r = -0.560$, $P = 0.004$; at the 20-m–by–20-m scale: $r = -0.742$, $P < 0.001$) (*25*).

Our global analysis is consistent with, and resolves apparent contradictions among, previous studies conducted within temperate or tropical latitudes documenting either stronger CNDD for rare versus common species or vice versa (*9*, *10*, *14*, *24*). Common species exhibited CNDD in both tropical and temperate forests (Fig. 2D), satisfying a basic condition for CNDD to maintain diversity (*5*, *28*). However, our results from tropical forests suggest that even stronger density-dependent regulation of rare species may cause their rarity and/or maintain diversity by stabilizing their population dynamics (*9*, *10*, *18*, *21*, *22*). Two previous studies from one of the tropical forest plots in our analysis (Barro Colorado Island, Panama) have shown that species abundance decreases with the strength of CNDD (*9*, *10*). Strong CNDD could also promote the persistence of rare species and reduce their risk of local extinction from demographic stochasticity by allowing them to recover from low densities (e.g., by escaping their specialized enemies) (*17*, *18*, *23*). Thus, stronger CNDD resulting from local biotic interactions may prevent erosion of biodiversity in tropical forests by limiting populations of common species and more strongly stabilizing populations of rare species. In contrast, our results from temperate forests suggest that CNDD maintains diversity by limiting populations of common species, but not by strongly stabilizing populations of rare species. These apparent differences in the ways in which local biotic interactions maintain diversity in temperate and tropical communities may contribute to the persistence of greater numbers of species in the tropics (*1*).

To confirm that these patterns were not influenced by differences in total numbers of individuals and/or species across forest plots, we used a neutral model to simulate the expected patterns of CNDD in the absence of density dependence. In this model, the observed total numbers of individuals and species were retained for each plot, but spatial patterns determined by recruitment, mortality, and dispersal limitation were all neutral with respect to species identity (*25*). Relationships between measures of species diversity and CNDD, as well as between species abundance and CNDD, across latitudes did not qualitatively change with the use of standardized effect sizes from this neutral model (table S9 and fig. S3 and S4).

Several mechanisms could explain shifts in CNDD across species and latitudes. First, stronger CNDD relative to HNDD at tropical versus temperate latitudes suggests that species-specific mechanisms, such as intraspecific competition for limiting resources or pressure from specialized enemies, might be stronger in the tropics (*29*, *30*). Second, strong dispersal limitation for both trees and their specialized enemies can lead to more intense host-enemy interactions or intraspecific competition and might explain stronger CNDD for rare species in the tropics (*22*, *31*). Third, stronger CNDD for rare as compared with common species at tropical latitudes may reflect greater susceptibility of rare tropical species to their specialized enemies (e.g., weaker defenses or immune responses relative to common tropical species) (*32*). Finally, differences in biogeographic history, climate, and speciation across latitudes likely have a direct influence on global patterns of species diversity (*1*, *15*), but these factors may also influence diversity indirectly by altering the composition of enemy communities, the ways in which enemies interact with their hosts, and the strength of intraspecific competition (*1*, *29*, *30*). These examples illustrate that global patterns of biodiversity cannot be understood without simultaneously considering local biotic interactions and regional processes (*1*, *15*). Our results suggest that regional processes interface with local biotic interactions to determine the strength of CNDD across species and the maintenance of biodiversity across tropical and temperate latitudes.

REFERENCES AND NOTES

1. G. G. Mittelbach *et al.*, *Ecol. Lett.* **10**, 315–331 (2007).
2. D. H. Janzen, *Am. Nat.* **104**, 501–528 (1970).
3. J. H. Connell, in *Dynamics of Populations*, P. J. den Boer, G. R. Gradwell, Eds. (Centre for Agricultural Publishing and Documentation, 1971), vol. 298, pp. 298–312.
4. K. E. Harms, S. J. Wright, O. Calderón, A. Hernández, E. A. Herre, *Nature* **404**, 493–495 (2000).
5. C. Wills *et al.*, *Science* **311**, 527–531 (2006).
6. J. W. Terborgh, *Proc. Natl. Acad. Sci. U.S.A.* **112**, 11415–11422 (2015).
7. Note that CNDD here refers to a per-neighbor or per-capita effect (the negative effect of an increase in the number of conspecific neighbors) that is species-specific and may be due to life-history differences among species. This is different from a community compensatory trend, where all species may have equivalent per-neighbor CNDD, but common species experience lower recruitment or survival on average because they encounter higher densities of conspecific neighbors.
8. A. Packer, K. Clay, *Nature* **404**, 278–281 (2000).
9. L. S. Comita, H. C. Muller-Landau, S. Aguilar, S. P. Hubbell, *Science* **329**, 330–332 (2010).
10. S. A. Mangan *et al.*, *Nature* **466**, 752–755 (2010).
11. R. Bagchi *et al.*, *Nature* **506**, 85–88 (2014).
12. L. S. Comita *et al.*, *J. Ecol.* **102**, 845–856 (2014).
13. D. J. Johnson, W. T. Beaulieu, J. D. Bever, K. Clay, *Science* **336**, 904–907 (2012).
14. J. A. LaManna, M. L. Walton, B. L. Turner, J. A. Myers, *Ecol. Lett.* **19**, 657–667 (2016).
15. R. E. Ricklefs, F. He, *Proc. Natl. Acad. Sci. U.S.A.* **113**, 674–679 (2016).
16. J. Terborgh, *Am. Nat.* **179**, 303–314 (2012).
17. G. Yenni, P. B. Adler, S. K. M. Ernest, *Glob. Ecol. Biogeogr.* **26**, 513–523 (2017).
18. G. Yenni, P. B. Adler, S. K. Ernest, *Ecology* **93**, 456–461 (2012).
19. A. Miranda, L. M. Carvalho, F. Dionisio, *PLOS ONE* **10**, e0127260 (2015).
20. R. D. Holt, *Am. Nat.* **124**, 377–406 (1984).
21. R. A. Chisholm, H. C. Muller-Landau, *Theor. Ecol.* **4**, 241–253 (2011).
22. K. M. Mack, J. D. Bever, *J. Ecol.* **102**, 1195–1201 (2014).
23. Y. Liu, S. Fang, P. Chesson, F. He, *Nat. Commun.* **6**, 10017 (2015).
24. K. Zhu, C. W. Woodall, J. V. Monteiro, J. S. Clark, *Ecology* **96**, 2319–2327 (2015).
25. See supplementary materials and methods.
26. S. P. Hubbell, J. A. Ahumada, R. Condit, R. B. Foster, *Ecol. Res.* **16**, 859–875 (2001).
27. R. P. Freckleton, A. R. Watkinson, R. E. Green, W. J. Sutherland, *J. Anim. Ecol.* **75**, 837–851 (2006).
28. R. K. Kobe, C. F. Vriesendorp, *Ecol. Lett.* **14**, 503–510 (2011).
29. L. A. Dyer *et al.*, *Nature* **448**, 696–699 (2007).
30. M. L. Forister *et al.*, *Proc. Natl. Acad. Sci. U.S.A.* **112**, 442–447 (2015).
31. F. R. Adler, H. C. Muller-Landau, *Ecol. Lett.* **8**, 438–447 (2005).
32. J. H. Marden *et al.*, *Mol. Ecol.* **26**, 2498–2513 (2017).

ACKNOWLEDGMENTS

We thank everyone involved in the collection of the vast quantity of data in the CTFS-ForestGEO network (see table S20 for site-specific acknowledgments). This work was carried out during the 2016 CTFS-ForestGEO Workshop in Hainan, China, and was supported by NSF grant DEB-1545761 to S.J.D. This work was also supported by NSF grants DEB-1256788 and -1557094 to J.A.M., NSF grant DEB-1257989 to S.A.M., and the Tyson Research Center. We thank K. Harms, R. Chisholm, T. Fung, members of the Myers Lab, and three anonymous reviewers for helpful comments and discussions. We declare no conflicts of interest. The data used in the primary analyses will be available at the Smithsonian Institution's CTFS-ForestGEO database portal: www.forestgeo.si.edu/group/Data/Access+the+data.

SUPPLEMENTARY MATERIALS

www.sciencemag.org/content/356/6345/1389/suppl/DC1
Materials and Methods
Figs. S1 to S12
Tables S1 to S20
R Scripts 1 to 3
References (*33*–*73*)

9 December 2016; resubmitted 14 March 2017
Accepted 16 May 2017
10.1126/science.aam5678

Science

Plant diversity increases with the strength of negative density dependence at the global scale

Joseph A. LaManna, Scott A. Mangan, Alfonso Alonso, Norman A. Bourg, Warren Y. Brockelman, Sarayudh Bunyavejchewin, Li-Wan Chang, Jyh-Min Chiang, George B. Chuyong, Keith Clay, Richard Condit, Susan Cordell, Stuart J. Davies, Tucker J. Furniss, Christian P. Giardina, I. A. U. Nimal Gunatilleke, C. V. Savitri Gunatilleke, Fangliang He, Robert W. Howe, Stephen P. Hubbell, Chang-Fu Hsieh, Faith M. Inman-Narahari, David Janík, Daniel J. Johnson, David Kenfack, Lisa Korte, Kamil Král, Andrew J. Larson, James A. Lutz, Sean M. McMahon, William J. McShea, Hervé R. Memiaghe, Anuttara Nathalang, Vojtech Novotny, Perry S. Ong, David A. Orwig, Rebecca Ostertag, Geoffrey G. Parker, Richard P. Phillips, Lawren Sack, I-Fang Sun, J. Sebastián Tello, Duncan W. Thomas, Benjamin L. Turner, Dilys M. Vela Díaz, Tomás Vrska, George D. Weiblen, Amy Wolf, Sandra Yap and Jonathan A. Myers

Science **356** (6345), 1389-1392.
DOI: 10.1126/science.aam5678

Maintaining tree diversity

Negative interaction among plant species is known as conspecific negative density dependence (CNDD). This ecological pattern is thought to maintain higher species diversity in the tropics. LaManna *et al.* tested this hypothesis by comparing how tree species diversity changes with the intensity of local biotic interactions in tropical and temperate latitudes (see the Perspective by Comita). Stronger local specialized biotic interactions seem to prevent erosion of biodiversity in tropical forests, not only by limiting populations of common species, but also by strongly stabilizing populations of rare species, which tend to show higher CNDD in the tropics.

Science, this issue p. 1389; see also p. 1328

www.sciencemag.org/content/356/6345/1389/suppl/DC1

Supplementary Materials for

Plant diversity increases with the strength of negative density dependence at the global scale

Joseph A. LaManna,* Scott A. Mangan, Alfonso Alonso, Norman A. Bourg, Warren Y. Brockelman, Sarayudh Bunyavejchewin, Li-Wan Chang, Jyh-Min Chiang, George B. Chuyong, Keith Clay, Richard Condit, Susan Cordell, Stuart J. Davies, Tucker J. Furniss, Christian P. Giardina, I. A. U. Nimal Gunatilleke, C. V. Savitri Gunatilleke, Fangliang He, Robert W. Howe, Stephen P. Hubbell, Chang-Fu Hsieh, Faith M. Inman-Narahari, David Janík, Daniel J. Johnson, David Kenfack, Lisa Korte, Kamil Král, Andrew J. Larson, James A. Lutz, Sean M. McMahon, William J. McShea, Hervé R. Memiaghe, Anuttara Nathalang, Vojtech Novotny, Perry S. Ong, David A. Orwig, Rebecca Ostertag, Geoffrey G. Parker, Richard P. Phillips, Lawren Sack, I-Fang Sun, J. Sebastián Tello, Duncan W. Thomas, Benjamin L. Turner, Dilys M. Vela Díaz, Tomáš Vrška, George D. Weiblen, Amy Wolf, Sandra Yap, Jonathan A. Myers

*Corresponding author. Email: joe.a.lamanna@gmail.com

Published 30 June 2017, *Science* **356**, 1389 (2017)
DOI: 10.1126/science.aam5678

This PDF file includes:

Materials and methods:

Data

We used intensive survey data of woody-plant species from 24 large stem-mapped forest plots that are part of the Smithsonian Center for Tropical Forest Science-Forest Global Earth Observatory (CTFS-ForestGEO) network *(33)*. These 24 forest plots spanned a latitudinal gradient from 5.25° S to 48.66° N. Despite this large latitudinal range (53.9° of latitude), only two forest plots were south of the equator and no forest plots were in the south-temperate zone (below 23° S). Thus, our results and inferences may only apply to latitudinal-diversity gradients among tropical and temperate latitudes in the northern hemisphere. All plots use identical methodologies to map, tag, measure, and identify all woody-plant individuals ≥ 1 cm diameter at breast height, or dbh (see Table S1 for summary statistics of plots; brief forest-type descriptions are given in Table S2). CTFS-ForestGEO plots are censused at a large enough spatial extent to accurately sample species richness *(15)*. These censuses also survey and map smaller size classes (1-10 cm dbh) whose recruitment is thought to be influenced by densities of neighboring conspecific adults *(12)*. We included data from live stems in the most recent complete census for each plot. We classified stems as either adults or saplings for analyses. Saplings were defined as trees smaller than 10 cm dbh. If this threshold resulted in fewer than 20% of individuals of a given species being classified as adults, then the threshold was lowered to 5 cm dbh for those species. Similarly, if a 5 cm dbh threshold for adults resulted in fewer than 20% of individuals of a given species being classified as adults, then the threshold was lowered to 2 cm dbh for those species. Such species represent small-stature understory species (e.g., shrubs & understory trees) that never or rarely reach 10 cm dbh or 5 cm dbh respectively *(34)*. Because stems smaller than 1 cm dbh are not sampled under the standard CTFS-ForestGEO protocol, 2 cm dbh was the lowest adult threshold size used. Adults were defined as individuals larger than the sapling size class for each species. Lianas were removed for analyses of those plots that survey lianas. Differences in average adult threshold size (2 cm, 5 cm, or 10 cm) were not associated with our estimates of CNDD measured at the 10×10 m scale (Pearson correlation coefficient [hereafter r_p] = 0.095; $p = 0.658$) or the 20×20 m scale ($r_p = 0.123$; $p = 0.568$) across forest plots.

Analyses

Species richness and diversity – For each plot, we calculated forest-wide species richness (the total number of species in a forest plot), forest-wide rarefied species richness (rarefied to the number of individuals in the forest plot with the lowest abundance, i.e. Yosemite with 7,083 live individuals), forest-wide species diversity (Shannon diversity index), mean species richness per 20×20 m quadrat, mean rarefied species richness per 20×20 m quadrat (rarefied to 20 individuals per quadrat because 95% of all quadrats across plots contained ≥20 individuals; observed species richness was used for those quadrats with < 20 individuals), and mean local species diversity (Shannon diversity index) per 20×20 m quadrat using the package 'vegan' in R *(35, 36)*. These data are shown for each plot in Table S1. We also calculated rarefied species richness per forest plot based on area (instead of numbers of individuals; species richness was rarefied to a standardized area of 4 ha). However, this area-based rarefied species richness was nearly perfectly correlated with individual-based rarefied species richness ($r_p = 0.998$; $p < 0.001$), so only individual-based rarefied richness was used in analyses. Simple linear regression tests showed that forest-wide species richness ($r^2 = 0.663$, $P < 0.001$), rarefied richness ($r^2 = 0.680$, $P < 0.001$), and diversity ($r^2 = 0.631$, $P < 0.001$) were all greatest in the tropics and decreased with increasing distance from the equator.

Conspecific and heterospecific density dependence with the Ricker model – We measured the effects of CNDD and HNDD on sapling recruitment at two quadrat sizes: 10×10-m and 20×20-m. We chose these quadrat sizes because effects of conspecific density can decay strongly beyond distances of 10–20 m from a given adult tree in both tropical and temperate forests *(26, 37)*. We measured CNDD and HNDD in 10×10 m and 20×20 m quadrats, rather than in 10 or 20 m radii around individual trees, because individuals occur in multiple overlapping circles around trees, and such individual-based approaches involve pseudo-replication. In contrast, quadrats do not overlap, and thus individuals were only included once in analyses at a given spatial scale (10×10 m or 20×20 m). We estimated the effect of conspecific adult densities (i.e. CNDD) and heterospecific adult and sapling densities (i.e. HNDD) on sapling recruitment for each tree species with the Ricker model *(38, 39)*. The Ricker model is a common function used to measure density dependence *(40)* that allows for overcompensating density dependence (i.e. recruitment that peaks at intermediate adult densities), a process thought to play an important role in the maintenance of diversity *(41)*. It also performs well at accurately and precisely predicting known values of CNDD in simulation tests that incorporate multiple potential forms of error *(39)*. The Ricker model with negative binomial error takes the following form:

$$\hat{S}_i = A_i e^{(r + CNDD \times A_i + HNDDadult \times a_i + HNDDsap \times s_i)} \quad (1)$$

$$S_i \sim \text{NegBin}(\hat{S}_i, \gamma)$$

Where $\hat{S}_i$ is the expected number of saplings of the focal species in quadrat *i*, A_i is the observed number of conspecific adults of the focal species in quadrat *i*, *r* is the per-capita recruitment rate for the focal species at low conspecific adult densities, *CNDD* is the per-capita effect of conspecific adult density on sapling recruitment of the focal species, *HNDDadult* is the per-capita effect of heterospecific adult density on sapling recruitment of the focal species, a_i is the observed number of heterospecific adults in quadrat *i*, *HNDDsap* is the per-capita effect of heterospecific sapling density on sapling recruitment of the focal species, s_i is the observed number of heterospecific saplings in quadrat *i*, S_i is the observed number of saplings of the focal species in quadrat *i*, and γ is the negative binomial overdispersion parameter for the focal species. Lower (i.e. more negative) values of *CNDD* and *HNDD* indicate stronger conspecific negative density dependence and heterospecific negative density dependence, respectively (Fig. S8). Ricker models were estimated using R (package 'gnm') *(35, 42)*, and R code for implementing this model is included in the **R scripts** section below (R script 1).

The Ricker model assumes that if there are no conspecific adults in a quadrat, then there should also be no saplings. This assumption is met in most cases (e.g. 96% and 92% of quadrats with no conspecific adults also had no conspecific saplings at the 10×10 m and 20×20 m scales, respectively). However, several quadrats contain saplings but do not contain conspecific adults, likely reflecting seeds that dispersed across quadrats. Thus, the per-capita influence of conspecific adults on these quadrats is not truly zero, but somewhere between zero and one. This data is useful to include when estimating conspecific density dependence, as these samples reflect successful establishment and survival of saplings in the absence of the generally negative influence of a neighboring conspecific adult (e.g. negative effects of specialized pathogens or insect herbivores that thrive near a conspecific adult tree). To ensure that this data was not excluded from our estimates of density dependence, we assumed that these plots did not have a true zero value for per-capita influence of conspecific adults (at least one seed, and likely more,

must have arrived from a conspecific parent tree in another area). Instead, we assigned quadrats that contained conspecific saplings but no conspecific adults a minimal non-zero conspecific adult abundance of 0.1 to reflect a greater than zero but less than one per-capita influence of conspecific adults (i.e. seed dispersal) in that quadrat (see *Simulation tests* section below for further discussion and evaluation of this offset value). Results were qualitatively similar if saplings present in quadrats without conspecific adults were excluded, but we present results that include these data.

We used numerical densities for adults and sapling densities as used in previous studies *(4, 14)*, but conspecific adult densities were nonetheless correlated with conspecific basal areas in each forest plot (mean r_p across 24 plots = 0.55, mean P across 24 plots < 0.00001). Likewise, densities of heterospecific adults were correlated with their basal area in each forest plot (mean r across 24 plots = 0.54, mean P across 24 plots < 0.00001).

We did not examine the influence of conspecific sapling density on conspecific sapling recruitment because these are the same variable and perfectly correlated, violating basic assumptions of regression models *(40)*. Negative effects from conspecific adults were originally hypothesized to cause CNDD *(2, 3)*. However, conspecific adult densities in this analysis reflect not only conspecific adult densities but also the associated densities of conspecific seeds, seedlings, and saplings with which existing conspecific saplings interacted with while recruiting. Indeed, a previous analysis of one of the forest plots in this study (Tyson Research Center, Missouri, USA) found strong correlations between conspecific adult and seed densities *(14)*.

Model residuals were visually checked to assure adequate model fit to the data. Model residuals were not correlated with conspecific adult densities at the 10×10 m scale (mean r_p across species = -0.103) nor at the 20×20 m scale (mean r_p across species = -0.082). Spatial proximity of quadrats within a forest plot may have yielded spatial auto-correlation in our models for CNDD. To assess this possibility, we calculated mean Mantel correlations between model residuals for each species and geographic distance matrices for each plot using the 'mantel.test' function in R package 'ade4' *(35, 43)*. These analyses indicated very low spatial auto-correlation between model residuals and spatial distance (Table S10).

To assess the strength of density dependence in each forest plot, we calculated both median and mean values of *r*, *CNDD*, *HNDDadult*, and *HNDDsap* across species in each forest plot. Mean values for each forest plot were weighted by the inverse standard error of individual species estimates (1/SE of the estimate). Median and mean values of all variables were highly correlated (r > 0.80), and results using median and mean values of CNDD and HNDD were qualitatively similar, so only results using median values are shown. Before calculating median and mean CNDD for each plot, we first removed the rarest species (i.e. those with adults or saplings occupying fewer than 10 quadrats). CNDD estimates (relationships between conspecific adult and sapling densities) for species whose adults and saplings occupy fewer than 10 quadrats are unreliable due to small sample sizes and can unduly influence the median and mean estimates of CNDD across species for each plot, especially in plots with relatively few species. We also removed those species with substantial error in their estimates of CNDD, which indicates the model was unable to estimate CNDD for these species. Specifically, we removed species with an estimated standard error (SE) of CNDD greater than 100 (all remaining species had an estimated CNDD SE below 6, with a mean SE = 0.18 and a median SE = 0.09). However, the proportion of species removed from each plot due to low sample size or model inability to estimate CNDD did not change with increasing distance from the equator at the 10×10 m scale (r_p = -0.251, P = 0.237) or the 20×20 m scale (r_p = 0.107, P = 0.618). In addition,

results were qualitatively similar using data from all species in a hierarchical model (see *Conspecific and heterospecific density dependence with the offset-power model* below). Median values of *r*, or per-capita recruitment at low conspecific densities (r_p = 0.617; P = 0.001), CNDD (r_p = 0.917, P < 0.001), HNDD from heterospecific adults (r_p = 0.710, P < 0.001), and HNDD from heterospecific saplings (r_p = 0.818, P < 0.001) for each forest plot from the Ricker model were all correlated across spatial scales (10×10 m scale and 20×20 m scale).

Conspecific and heterospecific density dependence with the offset-power model – To evaluate the extent to which our results might be influenced by the functional form used to measure density dependence and to allow comparability of our results with previous work, we repeated the measurements of *r*, CNDD, and HNDD with a power model used in previous studies of density dependence *(4, 14)*. We used a log-transformed version of the power function to facilitate the use of a linear-hierarchical model that can estimate mean density dependence across all species in a forest plot. For each forest plot, we used the following hierarchical model to estimate the mean strength of CNDD and heterospecific density dependence (HNDD):

$$\log(S_{ij}+1) = r_j + CNDD_j \times \log\left(A_{ij}+1\right) + HNDDadult_j \times a_{ij} + HNDDsap_j \times s_{ij} + \varepsilon_{ij}$$
$$\varepsilon_{ij} \sim \mathrm{N}(0, \sigma^2) \qquad (2)$$

Where S_{ij} is the observed number of saplings of a focal species *j* in quadrat *i*, r_j is the per-capita recruitment rate for species *j* at low conspecific adult densities, $CNDD_j$ is the per-capita effect of conspecific adult density on sapling recruitment for species *j*, A_{ij} is the observed number of conspecific adults of species *j* in quadrat *i*, $HNDDadult_j$ is the per-capita effect of heterospecific adult density on sapling recruitment for species *j*, a_{ij} is the observed number of heterospecific adults (i.e. not species *j*) in quadrat *i*, $HNDDsap_j$ is the per-capita effect of heterospecific sapling density on sapling recruitment of species *j*, s_{ij} is the observed number of heterospecific saplings (i.e. not species *j*) in quadrat *i*, and ε_{ij} is normally-distributed error. We began with a full random effects structure (i.e. random species-specific effects for r_j, $CNDD_j$, $HNDDadult_j$, and $HNDDsap_j$), and then removed random effects that were either correlated ($r \geq 0.7$) with the random effects of conceptual interest (r_j, $CNDD_j$) or whose standard deviation was estimated to be at or near zero ($SD \leq 0.1$). This approach avoids over-parameterization of models while retaining the random terms of interest *(44, 45)*. However, relationships between CNDD, species richness, and diversity were qualitatively similar if all random effects were included in the model. These models were run in R (package 'lme4'), and R code for implementing this model using 'lme4' is included in the **R scripts** section below (R script 2) *(35, 46)*. For this hierarchical model, conspecific adult and sapling densities were log-transformed to estimate the proportional (and not additive) change in sapling densities with increasing conspecific adult densities *(4, 14)*. An offset of one was added to conspecific adult and sapling densities prior to log-transformation because the logarithm of zero is undefined, and hereafter we refer to this model as an offset-power model *(4, 14)*. Values of $CNDD_j$ increasingly less than 1 (Tables S11, S12) represent a proportional decline in sapling densities with increasing adult densities and, thus, stronger CNDD *(4, 14)*. Estimates of CNDD were correlated between the offset-power and Ricker models (10×10-m scale: r_p = 0.857, P < 0.001; 20×20-m scale: r_p = 0.789, P < 0.001) across forest plots, and all relationships between CNDD and species richness and diversity were qualitatively similar using either the Ricker (Figs. S1, S2) or offset-power model (Figs. S5, S6). Residuals from the offset-power models were not associated with conspecific adult densities at

the 10×10 m scale (mean r_p across species = -0.009) nor at the 20×20 m scale (mean r_p across species = -0.013) nor were they spatially-autocorrelated (Table S13).

Relationships between CNDD and measures of species diversity – We examined hypothesized relationships between the strength of CNDD and measures of local and forest-wide species richness and diversity across plots. Because relationships were non-linear and to account for differences in potential biases in estimates of CNDD across forest plots (see *Model evaluation with dispersal effects and process and measurement error* section below), we used non-parametric Spearman-rank correlations (r_s). Before calculating median or mean CNDD for each plot, we first removed the rarest species (i.e. those with adults or saplings occupying fewer than 10 quadrats). CNDD estimates for species whose adults and saplings occupy fewer than 10 quadrats are unreliable due to small sample sizes and can unduly influence the mean estimate of CNDD across species for each plot, especially in plots with relatively few species. In addition, the presence of many rare species, which have limited ranges of conspecific adult densities, in tropical forests may bias our estimates of CNDD lower (i.e. stronger). Therefore, we also estimated the strength of CNDD for each forest plot after removing any species with adults or saplings occupying fewer than 30 or 50 quadrats at both spatial scales (10×10 m and 20×20 m scales). The relationships between CNDD and diversity were qualitatively similar for all analyses (Tables S5, S6, S14, S15). Qualitatively similar relationships were also found if we removed species with adults and sapling occupying fewer than 1%, 2%, and 4% of quadrats in a forest plot (these percentages removed approximately the same number of species from the analysis as the thresholds in Tables S5, S6, S14, S15). We were able to include data from all species in the hierarchical offset-power model because the hierarchical model uses data from all species to help estimate parameters for those species with very small sample sizes (those with adults or saplings occupying fewer than 10 quadrats). Relationships between CNDD and species richness and diversity were qualitatively similar if all data were included (Tables S14, S15). In addition, relationships between CNDD and species richness and diversity were qualitatively similar across spatial scales (Figs. S1, S2, S5, S6).

Differences in CNDD between eastern and western hemispheres may have influenced our results. While we attempted to access data from as many CTFS-ForestGEO plots as possible, the distribution of CTFS-ForestGEO plots around the world heavily represents temperate North America and the old-world tropics. Specifically, 78.6% of all tropical forest plots in the network are in the old-world tropics (Asia, Africa, and Oceania), and 66.7% of temperate forest plots are in North America. To assess the possibility that observed differences in CNDD across latitudes are due to a difference between eastern and western hemispheres, we performed a simple multiple-linear regression model with CNDD as the response, latitude as a continuous predictor variable, and eastern-western hemisphere as a binary variable. The two Hawaiian plots were included in the old world given the greater degree of historical contact (and potential for dispersal and gene flow) between the Hawaiian Islands and Polynesia. This analysis showed that the strength of CNDD measured with the Ricker model significantly decreased with latitude (at the 10×10 m scale: $F_{1,21} = 16.16$, $P < 0.001$; at the 20×20 m scale: $F_{1,21} = 25.28$, $P < 0.001$) but did not differ between eastern and western hemispheres (at the 10×10 m scale: $F_{1,21} = 0.01$, $P = 0.910$; at the 20×20 m scale: $F_{1,21} = 0.90$, $P = 0.354$). Likewise, the strength of CNDD measured with the offset-power model significantly decreased with latitude (at the 10×10 m scale: $F_{1,21} = 9.89$, $P = 0.004$; at the 20×20 m scale: $F_{1,21} = 6.64$, $P = 0.018$) but did not differ between eastern and western hemispheres (at the 10×10 m scale: $F_{1,21} = 0.04$, $P = 0.838$; at the 20×20 m scale:

$F_{1,21}$ = 0.41, P = 0.531). Thus, it does not appear that differences in CNDD between eastern and western hemispheres influenced our results, but this remains an area for future research given differences in biogeographic history between these two hemispheres.

Negative effects of conspecific densities on recruitment are expected to maintain diversity when they are stronger relative to negative effects from heterospecific densities (i.e. negative frequency dependence). The difference between estimates of CNDD and HNDD from the Ricker function reflect the strength of negative frequency dependence (the mathematical derivation of negative frequency dependence from CNDD and HNDD estimates of the Ricker model are described in Appendix S2 of reference *17*). Negative effects from heterospecifics were relatively weak compared to CNDD across forest plots (Tables S3, S4). Nonetheless, we assessed whether stronger negative frequency dependence was associated with higher species richness and diversity by examining whether the difference between CNDD and HNDD changed systematically with species richness or diversity across forest plots. Heterospecific density dependence from saplings was generally positive (likely indicating that certain areas of each forest plot were favorable to sapling recruitment regardless of species; Tables S3, S4). Heterospecific adults did have negative effects on sapling recruitment in most plots, and was estimated as the negative influence of each additional heterospecific adult on sapling recruitment (i.e. analogous to how we estimated CNDD, which was the negative influence of each additional conspecific adult on sapling recruitment). Using progressively restrictive datasets as described for Tables S5, S6 above, species richness and diversity increased with the strength of negative frequency dependence across tropical and temperate forest plots similar to relationships between CNDD and species richness/diversity (this is because HNDD was relatively weak; Table S7). Because CNDD and negative frequency dependence were so closely related, we present results for CNDD in the manuscript. We also examined the relative strength of CNDD to HNDD by examining the ratio of CNDD to HNDD estimates from the offset-power model. For some plots, heterospecific density dependence from heterospecific adults was positive (i.e. no HNDD), and these plots were assigned the mean value of heterospecific density dependence (20×20-m scale mean = -0.003, 10×10-m scale mean = -0.001) so that no forest plots would have negative ratios of CNDD to HNDD. We then examined relationships between the log-ratio of CNDD to HNDD and all measures of species richness and diversity. In all cases, relationships between species richness/diversity metrics and the CNDD:HNDD ratio were qualitatively similar to relationships between species richness/diversity and CNDD alone (Table S16).

Neither the mean number of conspecific adults (r_p = 0.354, P = 0.089) nor saplings (r_p = 0.342, P = 0.102) per 10×10 m quadrat changed systematically with latitude. Likewise, neither the mean number of conspecific adults (r_p = 0.353, P = 0.091) nor saplings (r_p = 0.324, P = 0.123) per 20×20-m quadrat changed systematically with latitude. Nonetheless, we estimated CNDD over a standardized range of conspecific adult densities (0-10 conspecific adults per quadrat) to verify that differences in the range of conspecific adult densities across forest plots did not spuriously influence the observed relationships between CNDD and species richness and diversity. We removed all species whose maximum number of conspecific adults per quadrat was less than three and truncated the remaining species to a maximum conspecific adult density of 10 adults per quadrat. Thus, all species had at least one quadrat with an abundance of three conspecific adults and no quadrats with abundances greater than 10 conspecific adults. Using this limited range of conspecific adult densities, we then estimated the median strength of CNDD and negative frequency dependence for each forest plot (using the Ricker model) and regressed these values with our measures of species richness and diversity. In all cases, species richness

and diversity increased with the strength of CNDD calculated with this truncation analysis (Tables S5 to S7). Thus, after estimating CNDD using a limited and standardized range of conspecific adult densities across all forest plots, our results do not qualitatively change, indicating that they are not spuriously driven by differences in the densities of species across plots.

CNDD and species abundance – We assessed the relationship between species abundance and the strength of CNDD across species within each forest plot with linear regression models. We used size-weighted abundance (basal area, m^2/ha) to measure species commonness/rarity instead of numerical abundance due to differences in size-age distributions across species *(9)*. Nonetheless, numerical abundance and basal area were correlated across all species in all forest plots ($r_p = 0.77$, $P < 0.00001$). Basal areas of species were log-transformed prior to analyses due to right-skewed distributions *(9)*. We calculated the intercept and slope of the relationship between species abundance and the strength of CNDD in each forest plot. We calculated these by weighting the estimate of CNDD for each species by the inverse of the standard error of the estimate (i.e. more weight to species with more accurate estimates of CNDD). We then used a simple linear model to test for a change in the slope between CNDD and species abundance with latitude across forest plots. Intercepts and slopes between species abundance and the strength of CNDD for each forest plot are shown in Table S8 for the Ricker model and Table S17 for the offset-power model. We also calculated the median strength of CNDD for rare species (species with basal area < 0.1 m^2/ha, or approximately 10 10-cm diameter trees per ha), and used a simple linear model to test if CNDD of rare species changed with latitude across forest plots.

CNDD was stronger for rare than for common species in the tropics and either equivalent for rare and common or stronger for common species in the temperate zone if CNDD was measured with the Ricker model at the 10×10-m or 20×20-m scale (Fig. 2), or with the offset-power model at the 10×10-m or 20×20-m scale (Fig. S7). Results were also qualitatively similar if we analyzed all data with the hierarchical offset-power model (10×10-m scale: $r_p = -0.660$, $P < 0.001$; 20×20-m scale: $r_p = -0.688$, $P < 0.001$) or removed the rarest species from each plot (occupying fewer than 10 quadrats) whose estimates of CNDD may be unreliable due to small sample sizes (Figs. 2, S7). In addition, systematic changes in the species-abundance distribution across latitudes may have influenced the observed shifts in the relationship between species abundance and CNDD across latitudes. However, the observed relationship between species abundance and CNDD across latitudes was qualitatively similar when we analyzed a standardized range of conspecific adult densities (i.e. the truncation analysis described above; 10×10-m scale: $r_p = -0.438$, $P = 0.032$; 20×20-m scale: $r_p = -0.487$, $P = 0.016$), suggesting that our results are robust to changes in species abundances across latitudes.

Differences in the relationship between species abundance and CNDD across eastern and western hemispheres might have also influenced the observed relationship with latitude. We evaluated this possibility by performing a simple multiple-linear regression model with the slope between species abundance and CNDD for each forest plot as the response, latitude as a continuous predictor variable, and eastern-western hemisphere as a binary predictor variable. This analysis showed that the slope between species abundance and CNDD estimated with the Ricker model significantly decreased with latitude ($F_{1,21} = 9.77$, $P = 0.005$) but did not differ between eastern and western hemispheres ($F_{1,21} = 1.15$, $P = 0.296$) at the 20×20 m scale. The slope between species abundance and CNDD estimated with the Ricker model did not significantly decrease with latitude ($F_{1,21} = 0.54$, $P = 0.471$) after accounting for differences

between eastern and western hemispheres ($F_{1,21}$ = 8.23, P = 0.009) at the 10×10 m scale. However, the median strength of CNDD for rare species (species with basal area less than 0.1 m^2/ha; compare to Fig. 2C) estimated with the Ricker model decreased with latitude at both the 10×10 m scale ($F_{1,21}$ = 11.15, P = 0.003) and the 20×20 m scale ($F_{1,21}$ = 6.55, P = 0.018) and did not differ between eastern and western hemispheres at either spatial scale (at the 10×10 m scale: $F_{1,21}$ = 0.94, P = 0.344; at the 20×20 m scale: $F_{1,21}$ = 1.50, P = 0.235). Moreover, the slope between species abundance and CNDD estimated with the offset-power model significantly decreased with latitude at both spatial scales (at the 10×10 m scale: $F_{1,21}$ = 9.45, P = 0.006; at the 20×20 m scale: $F_{1,21}$ = 12.54, P = 0.018) after accounting for differences between eastern and western hemispheres (at the 10×10 m scale: $F_{1,21}$ = 14.89, P = 0.001; at the 20×20 m scale: $F_{1,21}$ = 9.41, P = 0.006). Thus, most available evidence suggests that observed changes in CNDD for rare and common species across latitudes were not influenced by differences in CNDD between eastern and western hemispheres.

Simulation tests

We used simulations to evaluate the robustness of our CNDD estimates. First, to assess the robustness of CNDD estimates to differences in total number of individuals and species across forest plots, we used a neutral model to simulate communities that assemble in the absence of density dependence. Second, we assessed the ability of our models to recover known values of CNDD from simulated data that incorporate process and measurement error as well as dispersal. Detailed descriptions of these simulation tests follow.

Neutral model – To evaluate if our measurements of CNDD were spuriously biased stronger in tropical plots because of greater total number of individuals or species, we used a spatially- and temporally-explicit neutral model to simulate the expected measurement of CNDD for each plot in the absence of density dependence. In this neutral model, the observed total number of individuals and species were retained for each plot, but spatial patterns were determined by recruitment, mortality, and dispersal limitation that were all neutral with respect to species identity. We carried out this analysis at the 20×20 m scale because estimates of density dependence were highly correlated across spatial scales. For each plot, we began with a species-abundance distribution expected under neutral processes (calculated using function 'pvolkov' from R package 'sads') that contained the observed total number of species and individuals from each forest plot *(35, 47)*. For all forest plots, this neutral species-abundance distribution closely approximated the observed species-abundance distribution. At the beginning of each iteration of this model, we classified all individuals as 1 cm dbh saplings, and distributed them randomly among a given plot's 20×20 m quadrats. Each iteration of the model was then run for 400 time steps. Each time step, 6.0% of smaller saplings (1−5 cm dbh), 4.0% of larger saplings (5−10 cm dbh), and 2.0% of adults (>10 cm dbh) were randomly selected for mortality. Older age classes experienced lower mortality rates because mortality rates are known to decline with size and age in woody-plant species *(48)*, and these mortality rates were used across all plots so that they would be neutral with respect to species identity across a wide range of forests. Of those individuals that died, a random 90% were replaced by a 1 cm dbh individual of another species in the same quadrat (i.e. a local recruit), and the remaining 10% were replaced by a 1 cm dbh individual from the original neutral species-abundance distribution (i.e. an immigrant recruit from the meta-community). All individuals that survived a time step grew 0.25 cm dbh. At the end of 400 time steps, we used the same methods described above for the Ricker and offset-

power functions to measure the expected CNDD and heterospecific density effects from the neutral model. We ran each iteration of the model for 400 time steps because the measurement of CNDD tended to asymptote at or before this point (Fig. S9). Each 400-time-step simulation was iterated 50 times for each plot, producing 50 expected estimates of CNDD and heterospecific density effects given neutral dynamics and no density dependence. Because we randomized the locations of the initial 1 cm saplings at the beginning of each of these 50 iterations, each iteration began with a different spatial distribution of species and individuals. However, each of the 50 iterations for a given forest plot converged on similar expected CNDD and heterospecific density effect estimates within 400 time steps (i.e. small SD of expected values; Tables S9, S18, Fig. S9). Nearly all forest plots had low measured values of CNDD in the absence of density dependence (Tables S9, S18), suggesting that differences in total abundance and number of species across plots did not spuriously influence our measurements of CNDD.

We used these neutral-model iterations to calculate standardized effect sizes for CNDD and heterospecific density effects of adults and saplings using the following formulae:

$$CNDD_{SES} = \frac{(CNDD - \mu_{CNDDnull})}{\sigma_{CNDDnull}} \quad (3)$$

$$HNDD_{SES} = \frac{(HNDD - \mu_{HNDDnull})}{\sigma_{HNDDnull}} \quad (4)$$

Where $CNDD_{SES}$ and $HNDD_{SES}$ are the standardized CNDD and heterospecific density effect sizes, respectively (note that separate standardized effect sizes were calculated for the effects of heterospecific saplings and adults); *CNDD* and *HNDD* are the observed CNDD and heterospecific density effects for a plot, respectively; $\mu_{CNDDneutral}$ and $\mu_{HDDneutral}$ are the mean expected values for CNDD and heterospecific density effects for a plot, respectively; and $\sigma_{CNDDneutral}$ and $\sigma_{HDDneutral}$ are the standard deviations of expected values for CNDD and heterospecific density effects for a plot, respectively (Tables S9, S18, Figs. S3, S10). A positive standardized effect size (> 2) for CNDD or a heterospecific density effect indicates that the observed value was more positive than expected from a neutral model (positive density dependence), and a negative standardized effect size (< -2) for CNDD or a heterospecific density effect indicates that the observed value was more negative than expected from a neutral model (negative density dependence). At the end of each 400-time-step model, we also calculated the expected correlation between species abundance and the strength of CNDD across species as described for observed data above. We used these expected correlations to calculate a standardized effect size for the correlation between species abundance and CNDD for each plot using an identical formula to equation 3 above (Tables S9, S18). A positive standardized effect size (> 2) for the correlation between species abundance and CNDD indicates the observed value was more positive than expected from a neutral model (CNDD stronger for rare species), and a negative standardized effect size (< -2) for the correlation between species-relative abundance and CNDD indicates the observed value was more negative than expected from a neutral model (CNDD stronger for common species). These standardized effect sizes still decreased with latitude (Fig. S4), and indicated that CNDD was stronger for rare species in tropical latitudes and stronger for common species in temperate latitudes.

Model evaluation with dispersal effects and process and measurement error – We used stem-mapped censuses of forest plots, in which the number of adults and saplings in each quadrat have been accurately assessed, to estimate CNDD. However, demographic stochasticity in sapling recruitment is a likely source of process error influencing sapling density *(27)*. In addition, while conspecific adult densities in these forest plots can correlate with seed rain densities *(14)*, conspecific adult abundances in quadrats likely do not perfectly reflect the abundance of seeds dispersing into those quadrats. This may introduce error in our measurement of the number of conspecific adults that influence recruitment in each quadrat *(27)*. Yet, the number of adults in a quadrat does accurately measure the number of adults that seedlings establishing in a quadrat will interact with as they recruit into saplings, and adults can have substantial negative effects on conspecific seedlings growing in their neighborhoods *(12)*. Nevertheless, we assessed the robustness of the Ricker and offset-power models to the presence of both process error (error in the number of saplings resulting from demographic stochasticity) and measurement error (error in the number of adults resulting from seed dispersal across quadrats) *(27)*. We also assessed the robustness of these models to the possibility that some proportion of seeds (d) may disperse outside the forest plot all together. Finally, we assessed the robustness of these models to the values of offsets used in each.

We simulated conspecific adult tree abundances with a negative binomial distribution (a typical distribution for count data), and used known values of CNDD and per-capita recruitment at low conspecific densities (r) to calculate expected sapling abundances with both the Ricker and power equations. We then removed a proportion (d) of expected saplings from each quadrat to simulate dispersal of offspring outside the forest plot. We introduced process error (negative-binomially distributed) into sapling abundances and measurement error (poisson distributed) into adult abundances. Finally, we measured the strength of CNDD with both the Ricker and offset-power models and assessed the degree to which these models accurately estimated the known value of CNDD (i.e. recovered the "truth"). We iterated this process 100 times for every unique combination of: (1) 15 evenly-spaced values of CNDD (Ricker model: CNDD = -2.00 – 0.05; offset-power model: CNDD = 0.1 – 1.15); (2) six evenly-spaced values of r (Ricker model: r = -1.20 – 1.40; offset-power model: r = -1.20 – 0.40); (3) six values of mean conspecific adult trees per quadrat, based on the minimum, 1st quartile (or 25th percentile), median (or 50th percentile), 3rd quartile (or 75th percentile), and 90th percentile of mean conspecific adults per quadrat across forest plots (reflecting a range of abundances from rare to common species); (4) five values of error (the negative-binomial overdispersion parameter θ = 0.1, 0.5, 1.0, 1.5, and 2.0); (5) three values of dispersal (d = 0.1, 0.2, and 0.3); and (6) three values of each model's offset (see below). These parameter values were chosen to evaluate model biases across a range of biologically reasonable parameter values. The range of values chosen for known CNDD and r produce estimates of CNDD similar to the range of values estimated in our analyses of actual data above. Values chosen for mean conspecific adult densities match the distribution of mean conspecific adult densities across forest plots in the data. Values chosen for θ result in simulated data with a range of proportions of quadrats with saplings but no conspecific adults that is similar to the range of these proportions in the data. Values chosen for dispersal (d) reflect moderate (10%) to high (30%) dispersal of seeds outside of the forest plot, given that these are large (4 – 50 ha; mean = 27.5 ha) square or rectangular forest plots where most seeds likely fall within the plot boundaries (*49*). For the Ricker model, offsets were minimal non-zero values of conspecific adult densities assigned to quadrats with saplings but no conspecific adults (simulated values = 0.001, 0.01, and 0.1). For the offset-power model, offsets were added to values of conspecific

adult and sapling densities before log-transformation (eq. 2; simulated values = 0.01, 0.1, and 1.0). The above parameters yielded 24,300 unique combinations for simulation, or 8,100 unique combinations per offset value. R code for these simulations are included in the **R script**s section below (R script 3).

We examined correlations between known and estimated values of CNDD from each model across all parameters separately for each offset value. Correlations between known values of CNDD and values estimated by our methods (with the offset value used in the data analyses described above, i.e., 0.1 for the Ricker model) demonstrate the ability of the Ricker model to precisely measure trends in CNDD ($r_p = 0.887$, $P < 0.0001$) across a wide range of values of per-capita recruitment at low densities ($r_{recruit}$) as well as forest plots that differ in mean abundance, the presence of considerable process and measurement error, and magnitudes of dispersal of seeds outside the forest plot (Fig. S11A). The offset-power model (with the offset value used in the data analyses described above, i.e., 1.0) was also able to recover known trends in CNDD given the wide range of parameters over which CNDD was simulated ($r_p = 0.429$, $P < 0.0001$; Fig. S11). The Ricker model used in our analyses had some negative bias at stronger values of known CNDD (i.e. estimated values were lower than known values as known CNDD became stronger; Fig. S11A), whereas the offset-power model used in our analyses had some negative bias at weaker values of known CNDD (i.e. estimated values were lower than known values as known CNDD became weaker; Fig. S11B). Qualitatively similar results from two models with opposite biases (Figs. 1, 2, S1, S2, S3, S4, S5) combined with the ability of both models to recover known trends in CNDD (Fig. S11) suggest that our results are robust to potential biases arising from differences in densities, measurement and process error and dispersal among forest plots. Nonetheless, we used non-parametric Spearman-rank correlation tests to test for changes in CNDD across latitudes in order to accommodate potential biases in our estimates of CNDD.

We also examined correlations between the mean number of conspecific trees per quadrat (mean abundance) and CNDD bias (estimated CNDD values minus known CNDD values) to assess whether systematic changes in CNDD bias with species abundance might influence our results (i.e. Figs. 2, S7). However, the small amount of variation in CNDD bias associated with abundance for both models (Ricker: $r^2 = 0.022$; offset-power: $r^2 = 0.005$) combined with opposing directions of the relationship between bias and abundance across the two models (Fig. S12) indicate that our result of stronger CNDD for rare species in the tropics (found with both models; see Figs. 2, S7) appears robust to the potential for systematic changes in CNDD bias with species abundance. We also found stronger CNDD for rare species in the tropics when restricting our analysis to species within a standardized range of abundances (i.e. the truncation analysis described in *CNDD and species abundance* above).

For both the Ricker and offset-power models, lowering the value of the offset term reduced the ability of each model to precisely measure known trends in CNDD (i.e. reduced the correlation between estimated CNDD values and known CNDD values in a linear regression; Ricker model: r_p for offset of 0.01 = 0.689, r_p for offset of 0.001 = 0.552; offset-power model: r_p for offset of 0.1 = 0.318, r_p for offset of 0.01 = 0.255). While the Ricker model with a 0.01 offset term was unable to estimate trends in CNDD as precisely as the Ricker model with a 0.1 offset term (i.e. estimated CNDD values were less correlated with known CNDD values due to higher variance), it had nearly no bias at all values of known CNDD (i.e. mean estimates were close to known values). Importantly, relationships between CNDD and species richness and diversity metrics were qualitatively similar regardless of whether an offset term of 0.1, 0.01, or 0.001 was used for the Ricker model (Table S19). In general, our analyses and these simulations

highlight the challenges in estimating CNDD from observational data. We recommend that future studies estimating CNDD from observational data carefully consider the methods and models used to estimate CNDD as well as use simulations to assess whether those methods can precisely and accurately recover known values of CNDD.

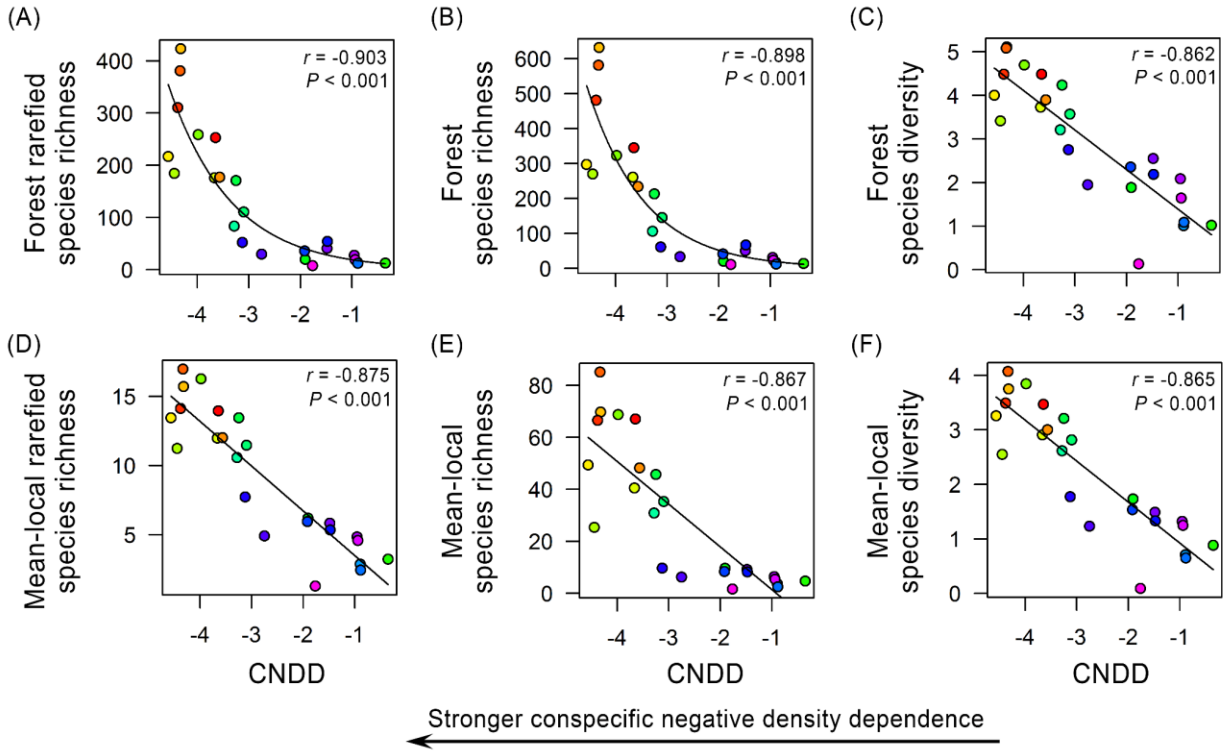

Fig. S1. Species richness and diversity increased with conspecific negative density dependence (CNDD) measured with the Ricker model at the 10×10 m scale across tropical and temperate forests. (A) Rarefied species richness, (B) observed (non-rarefied) species richness, and (C) Shannon diversity indices measured at the forest-wide scale all increased with the strength of CNDD (lower values indicate stronger CNDD). (D) Rarefied species richness, (E) observed (non-rarefied) species richness, and (F) Shannon diversity indices measured at the mean-local scale (averaged across 20×20 m quadrats) also increased with the strength of CNDD. Plots are colored by increasing distance from the equator (as in Fig. 1). In all panels, each point is a forest plot (N = 24 forest plots). Lines are best fits from poisson (A, B) or linear (C – F) regression, and correlation coefficients (r) are from Spearman-rank tests.

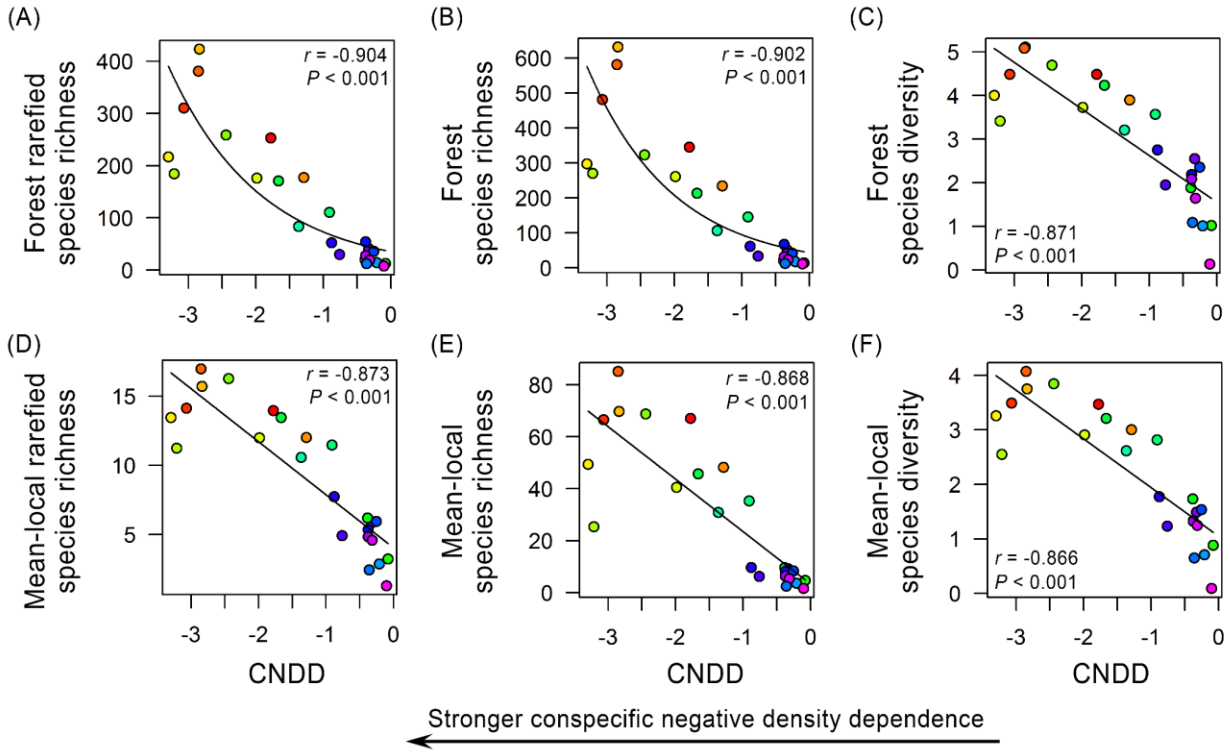

Fig. S2. Species richness and diversity increased with conspecific negative density dependence (CNDD) measured with the Ricker model at the 20×20 m scale across tropical and temperate forests. (A) Rarefied species richness, (B) observed (non-rarefied) species richness, and (C) Shannon diversity indices measured at the forest-wide scale all increased with the strength of CNDD (lower values indicate stronger CNDD). (D) Rarefied species richness, (E) observed (non-rarefied) species richness, and (F) Shannon diversity indices measured at the mean-local scale (averaged across 20×20 m quadrats) also increased with the strength of CNDD. Plots are colored by increasing distance from the equator (as in Fig. 1). In all panels, each point is a forest plot (N = 24 forest plots). Lines are best fits from poisson (A, B) or linear (C – F) regression, and correlation coefficients (r) are from Spearman-rank tests.

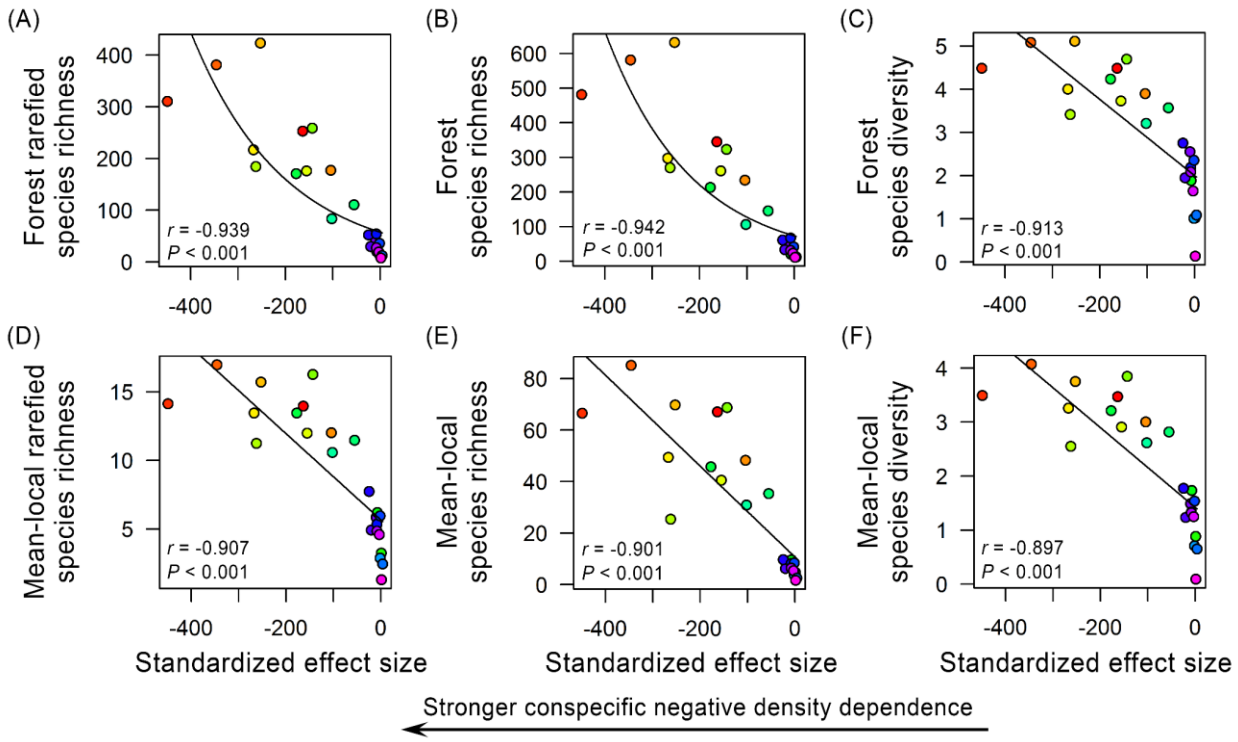

Fig. S3. Species richness and diversity increased with conspecific negative density dependence (CNDD) measured with the Ricker model after controlling for potentially spurious influences of changes in number of species and individuals across forest plots. Standardized effect sizes of CNDD are the observed value of CNDD for each forest plot minus the value expected given neutral assembly (i.e. no density dependence) of a community with the same number of species and individuals. At the forest plot scale, (A) rarefied species richness, (B) observed (non-rarefied) species richness, and (C) Shannon diversity indices all increased with CNDD standardized effect sizes (lower values indicate stronger CNDD). At the mean-local (20×20 m quadrats) scale, (D) rarefied species richness, (E) observed (non-rarefied) species richness, and (F) Shannon diversity indices also increased with CNDD standardized effect sizes. This analysis was conducted at the 20×20-m scale because estimates from the Ricker model were correlated across spatial scales (see materials and methods). Plots are colored by increasing distance from the equator (as in Fig. 1). In all panels, each point is a forest plot (N = 24 forest plots). Lines are best fits from poisson (A, B) or linear (C – F) regression, and correlation coefficients (r) are from Spearman-rank tests.

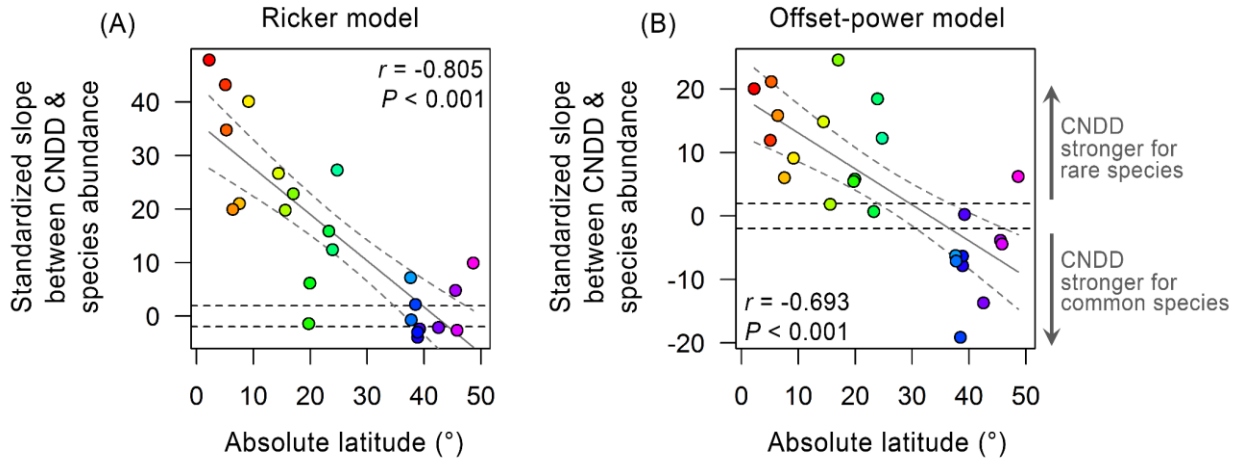

Fig. S4. Latitudinal shift in the strength of conspecific negative density dependence (CNDD) among common and rare species after controlling for potentially spurious influences of changes in number of species and individuals across forest plots. After controlling for potentially spurious influences of different numbers of species and individuals across forests on measurements of the relationship between species abundance and CNDD across forest plots (N = 24 forest plots), CNDD was still stronger for rare than for common species at tropical latitudes and equally strong or stronger for common than for rare species at temperate latitudes. CNDD was calculated using both (A) the Ricker model and (B) the offset-power model. Because units are in SD, any values below -2 or above 2 (dashed lines) indicate that the observed value was significantly outside the range of expected values. Results are shown at the 20×20 m scale because estimates of density dependence were highly correlated across spatial scales. Test statistics are Pearson correlation coefficients (r) from linear regression models.

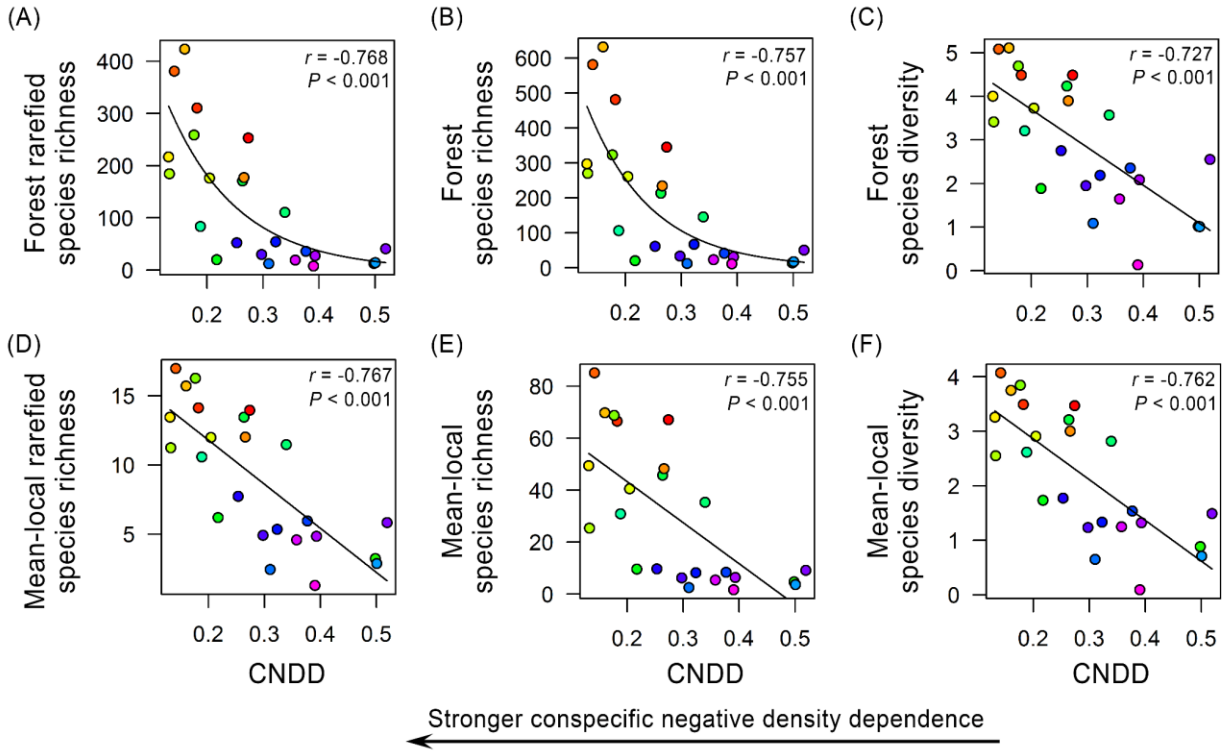

Fig. S5. Species richness and diversity increased with conspecific negative density dependence (CNDD) measured with the offset-power model at the 10×10 m scale across tropical and temperate forests. (A) Rarefied species richness, (B) observed (non-rarefied) species richness, and (C) Shannon diversity indices measured at the forest-wide scale all increased with the strength of CNDD (lower values indicate stronger CNDD). (D) Rarefied species richness, (E) observed (non-rarefied) species richness, and (F) Shannon diversity indices measured at the mean-local scale (averaged across 20×20 m quadrats) also increased with the strength of CNDD. Plots are colored by increasing distance from the equator (as in Fig. 1). In all panels, each point is a forest plot (N = 24 forest plots). Lines are best fits from poisson (A, B) or linear (C – F) regression, and correlation coefficients (r) are from Spearman-rank tests.

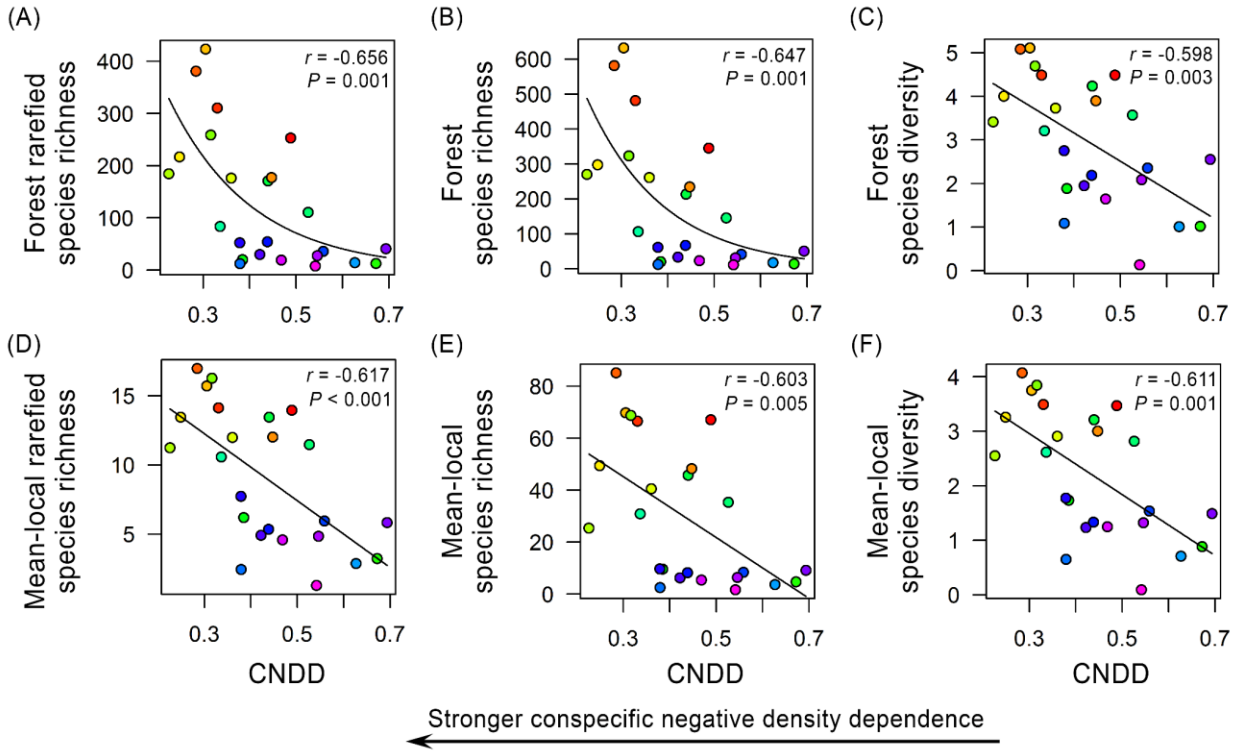

Fig. S6. Species richness and diversity increased with conspecific negative density dependence (CNDD) measured with the offset-power model at the 20×20 m scale across tropical and temperate forests. (A) Rarefied species richness, (B) observed (non-rarefied) species richness, and (C) Shannon diversity indices measured at the forest-wide scale all increased with the strength of CNDD (lower values indicate stronger CNDD). (D) Rarefied species richness, (E) observed (non-rarefied) species richness, and (F) Shannon diversity indices measured at the mean-local scale (averaged across 20×20 m quadrats) also increased with the strength of CNDD. Plots are colored by increasing distance from the equator (as in Fig. 1). In all panels, each point is a forest plot (N = 24 forest plots). Lines are best fits from poisson (A, B) or linear (C – F) regression, and correlation coefficients (r) are from Spearman-rank tests.

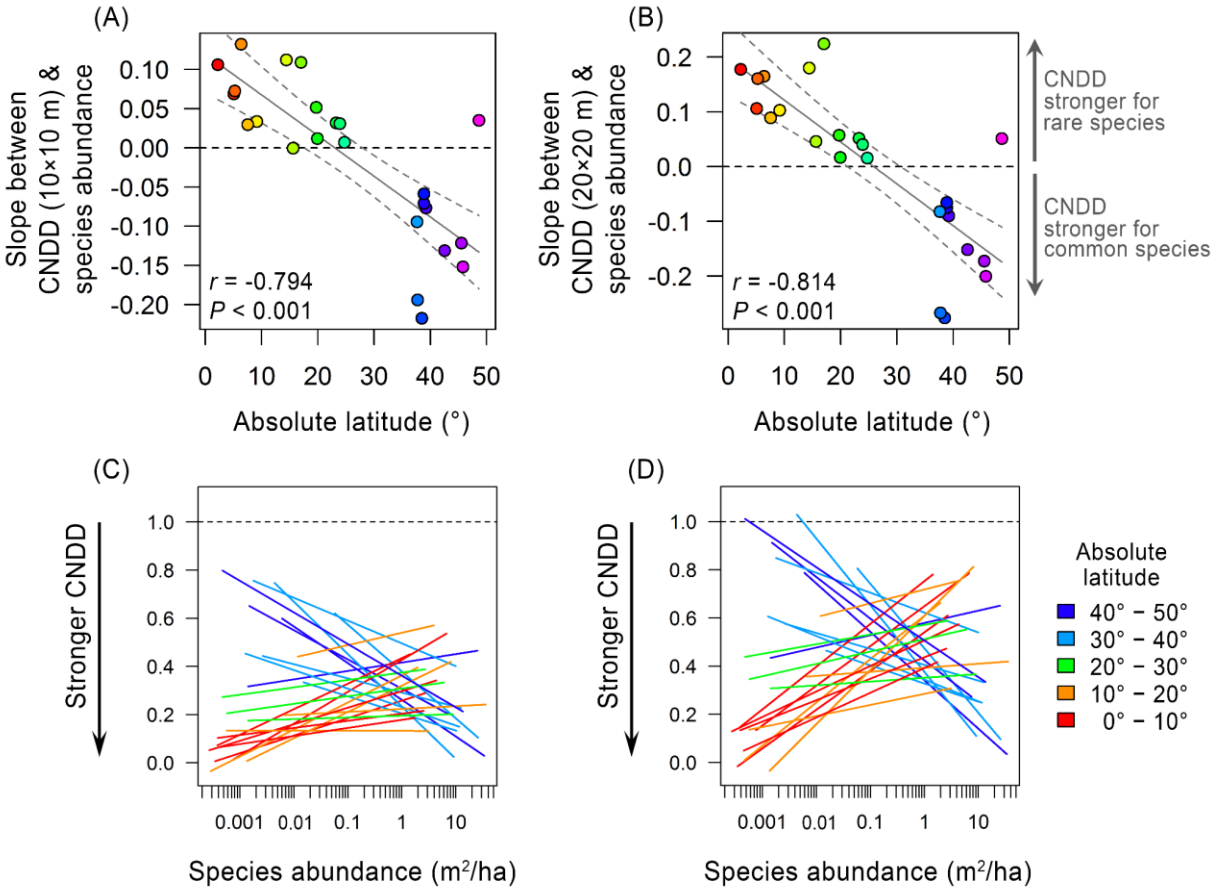

Fig. S7. Latitudinal shifts in the strength of conspecific negative density dependence (CNDD) measured with the offset-power model among common and rare species. Slopes between species abundance (measured by basal area, m^2/ha) and CNDD measured at the (A) 10×10 m scale and the (B) 20×20 m scale across species within each forest plot (N = 24 forest plots). Absolute value of latitude reflects increasing distance from the equator. Because lower values of CNDD reflect stronger CNDD, positive slopes indicate stronger CNDD for rare than for common species and negative slopes indicate stronger CNDD for common than for rare species. Plots are colored according to Fig. 1. Best-fit relationships between the strength of CNDD and species abundance (m^2/ha) within each forest plot with CNDD measured at the (C) 10×10 m scale and the (D) 20×20 m scale. Colors in (C) and (D) represent the latitudinal band a forest plot occupies, from tropical (red) to temperate (blue) latitudes. The point at which conspecific negative density dependence switches to conspecific positive negative density dependence (i.e. the point at which increased densities of conspecifics do not proportionally increase or decrease sapling densities) is shown as a dashed line. Species abundance is shown on a log scale, with rare species on the left and common species on the right. Slopes and intercepts in (C) and (D) are presented for each forest plot in Table S17. Qualitatively similar results were found using another functional form (Ricker model) to measure CNDD (Fig. 2; see materials and methods). Test statistics are Pearson correlation coefficients (r) from linear regression models.

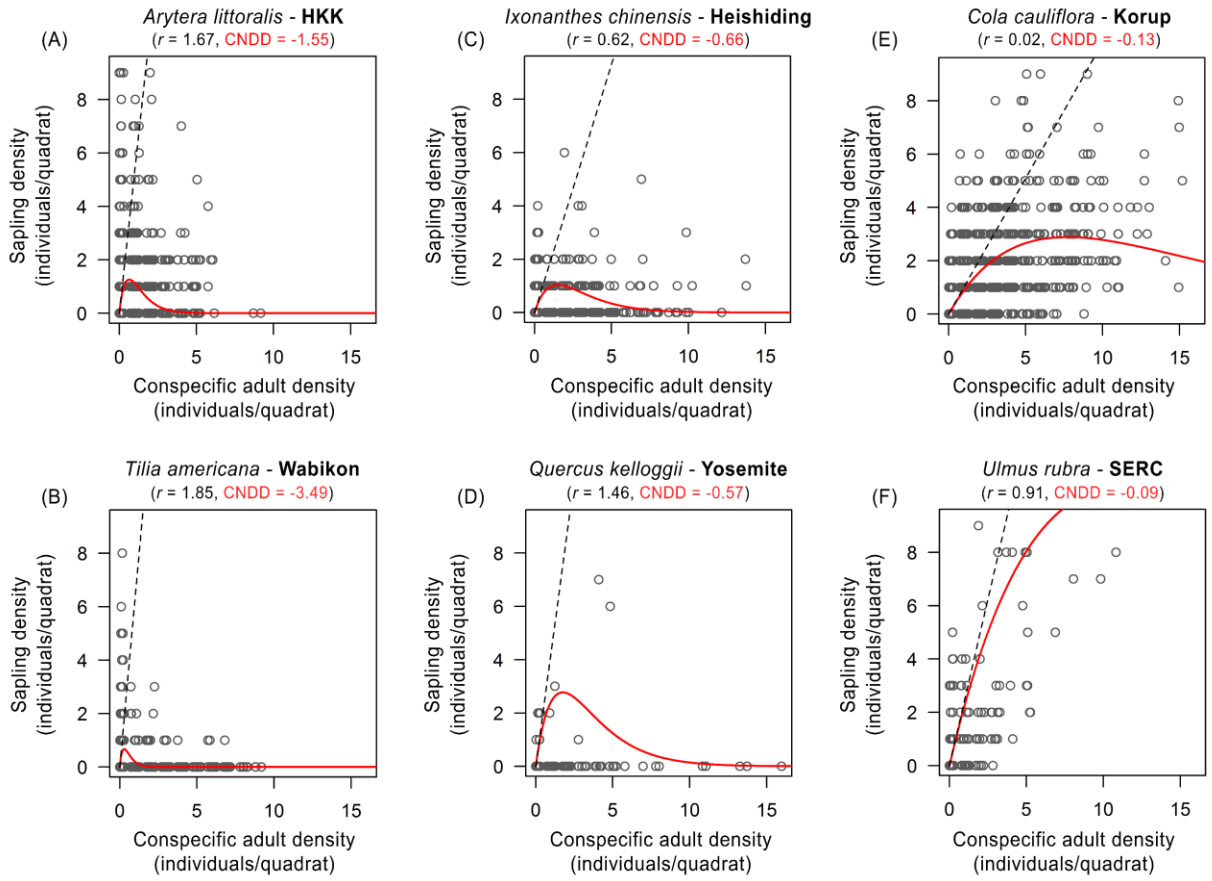

Fig. S8. Example calculations of conspecific negative density dependence (CNDD) with the Ricker model. All panels show sapling densities (individuals per 20×20 m quadrat) against conspecific adult densities (individuals per 20×20 m quadrat) across quadrats within six of the 24 forest plots analyzed. In each panel, the red curve is the best-fit recruitment curve from the Ricker model reflecting per-capita recruitment at low densities (r) and the strength of CNDD (eq. 1). Each black dashed line has a slope equal to the estimated per-capita recruitment rate at low density (*r*) for visualization. The strength of CNDD is reflected in the rate at which per-capita recruitment (red curve) decreases (from a maximum rate at low density, or *r*) as a function of increasing conspecific adult density. (A) *Arytera littoralis* at Huai Kha Khaeng (HKK; *N* = 1,250 quadrats) and (B) *Tilia americana* at Wabikon Lake (*N* = 625 quadrats) had relatively strong CNDD; (C) *Ixonanthes chinensis* at Heishiding (*N* = 1,250 quadrats) and (D) *Quercus kelloggii* at Yosemite (*N* = 262 quadrats) had intermediate CNDD; and (E) *Cola cauliflora* at Korup (*N* = 1,250 quadrats) and (F) *Ulmus rubra* at the Smithsonian Environmental Research Center (SERC; *N* = 400 quadrats) had relatively weak CNDD.

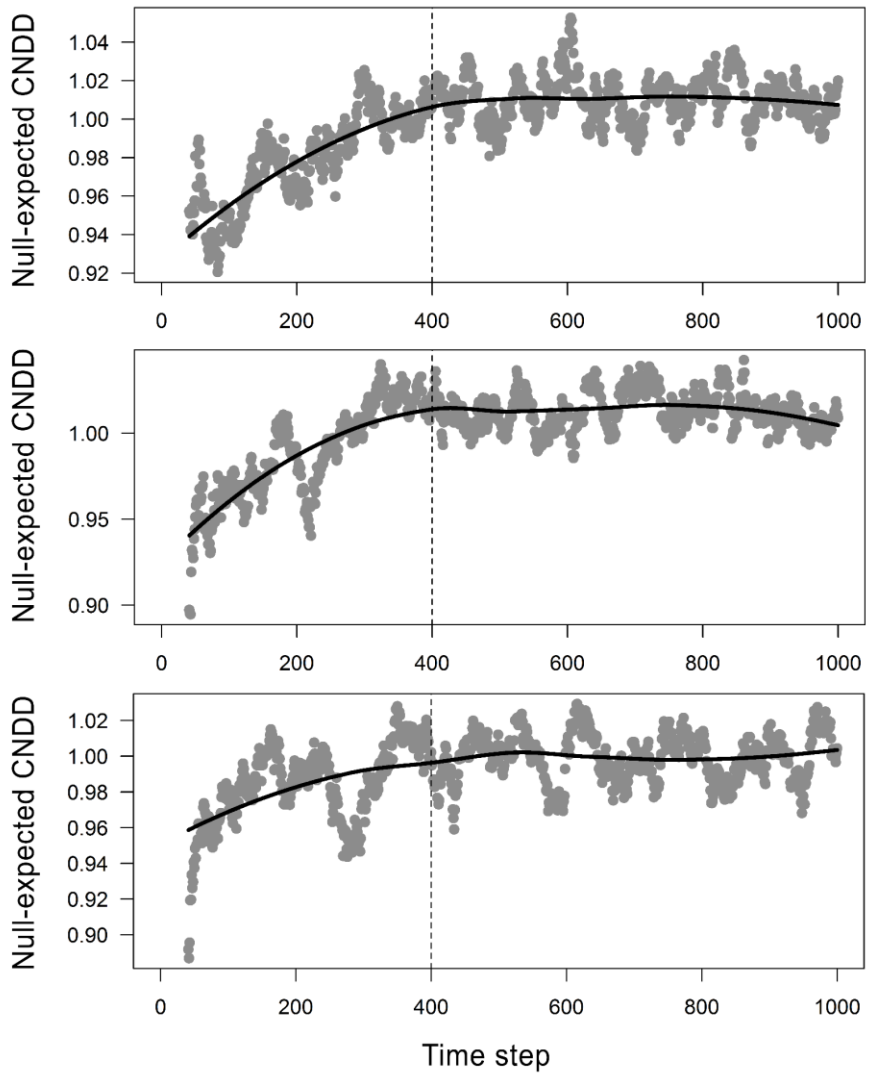

Fig. S9. Example iterations of a neutral model for the expected value of conspecific negative density dependence (CNDD) given neutral dynamics and no density dependence. To account for potential biases in our measurements of CNDD due to differences in total number of species or individuals across forest plots, neutral models were run to produce spatial relationships between conspecific adults and saplings that result from neutral dynamics and an absence density dependence. All models began with a neutral species-abundance distribution of 1 cm saplings with the observed number of species and number of individuals in a given forest plot. At time step 0, these 1 cm dbh saplings were randomly distributed among a plot's 20×20 quadrats. Each time step, a random portion of the community died, and were replaced either by a local recruit (i.e. 1 cm individual of a species in the same 20×20 quadrat) or immigrant from the meta-community (i.e. 1 cm individual from the initial species-abundance distribution). Those individuals that survived a time step grew 0.25 cm dbh. At the end of 400 time steps, CNDD was calculated using identical methods to those used to calculate observed CNDD for each plot (CNDD is measured with the offset-power model in this example), and the model was iterated 50 times (400 time steps each) for each plot. These example model iterations (run out to 1,000 time steps) demonstrate that the measurement of CNDD asymptotes at or before 400 time steps, thus 400 time steps was chosen as the duration for each iteration.

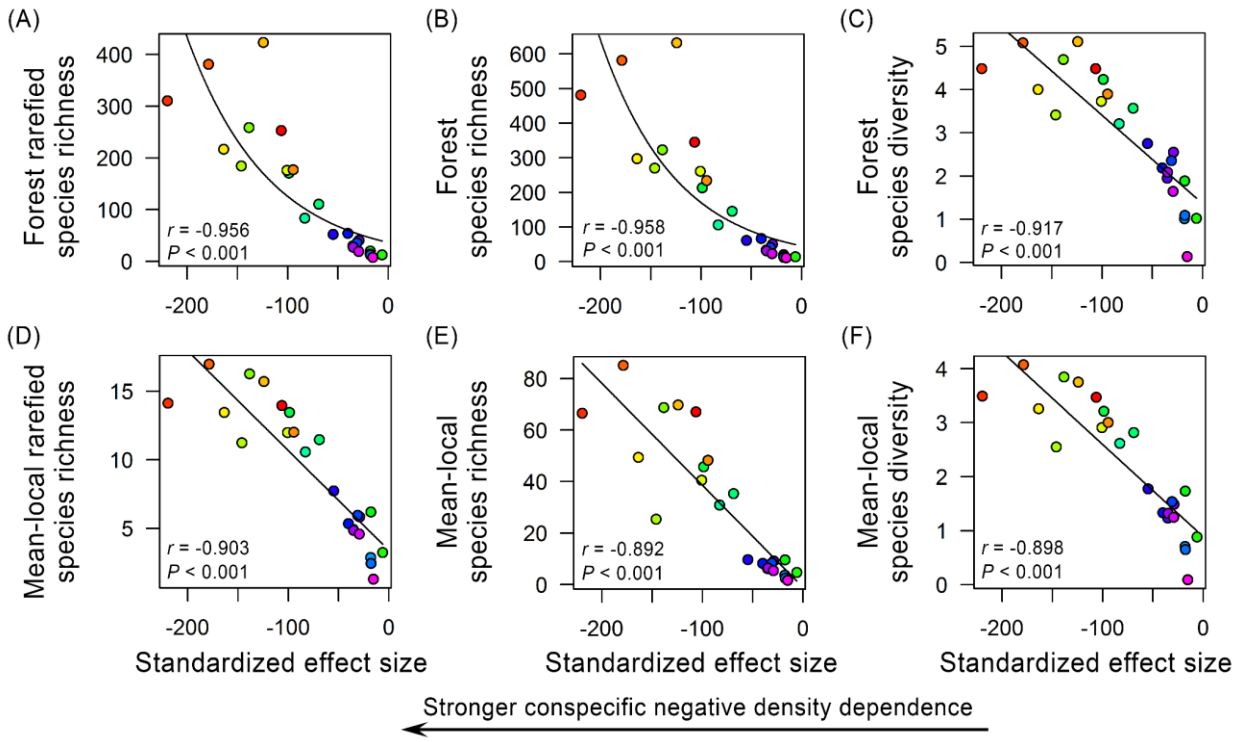

Fig. S10. S**pecies richness and diversity increased with conspecific negative density dependence (CNDD) measured with the offset-power model after controlling for potentially spurious influences of changes in number of species and individuals across forest plots.** Standardized effect sizes of CNDD are the observed value of CNDD for each forest plot minus the value expected given neutral assembly (i.e. no density dependence) of a community with the same number of species and individuals. At the forest plot scale, (A) rarefied species richness, (B) observed (non-rarefied) species richness, and (C) Shannon diversity indices all increased with CNDD standardized effect sizes (lower values indicate stronger CNDD). At the mean-local (20×20 m quadrats) scale, (D) rarefied species richness, (E) observed (non-rarefied) species richness, and (F) Shannon diversity indices also increased with CNDD standardized effect sizes. This analysis was conducted at the 20×20-m scale because estimates from the offset-power model were correlated across spatial scales (see materials and methods). Plots are colored by increasing distance from the equator (as in Fig. 1). In all panels, each point is a forest plot (N = 24 forest plots). Lines are best fits from poisson (A, B) or linear (C – F) regression, and correlation coefficients (r) are from Spearman-rank tests.

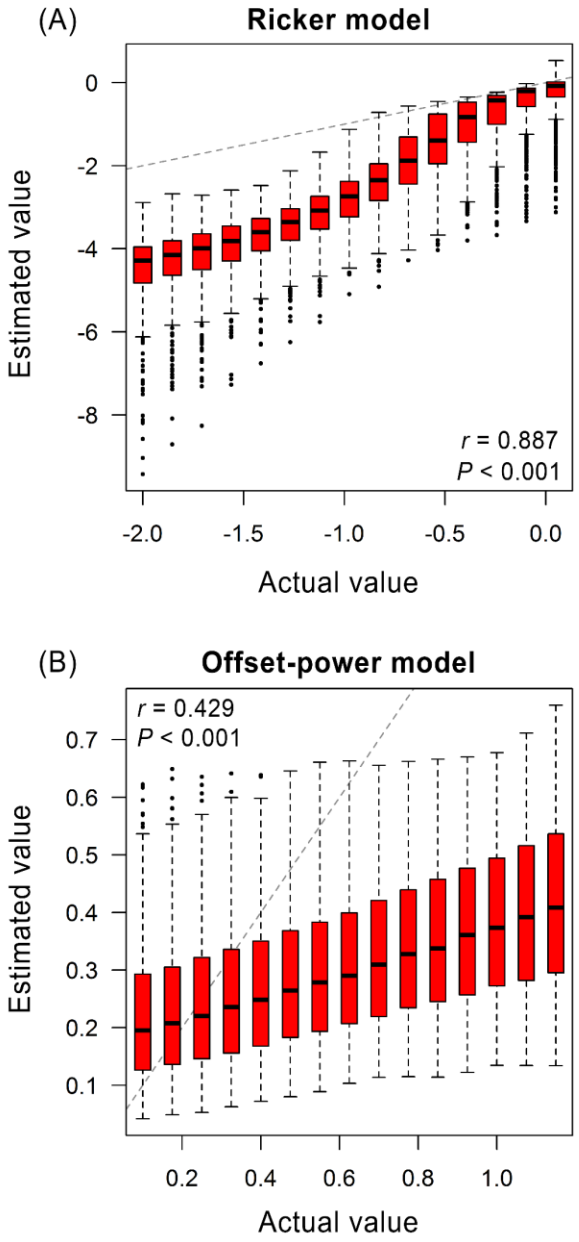

Fig. S11. Relationships between known values of conspecific negative density dependence (CNDD) and values estimated by our models across an array of parameter values, error, and dispersal rates. Data were simulated using different values of per-capita recruitment at low densities (r), the negative-binomial overdispersion parameter (θ), mean trees per quadrat, and dispersal (d) to test the robustness of our CNDD models to different ranges of error, tree densities, and dispersal rates. Plots show correlations between known values of CNDD and estimates from the (A) Ricker model and the (B) offset-power model across all parameters considered (N = 8,100 parameter combinations; shown as boxplots for ease of visualization). Pearson correlation coefficients and statistical tests are shown along with the identity line (dashed line). Ricker model was simulated using an offset of 0.1 for quadrats with saplings but no conspecific adults, and the offset-power model used an offset of 1 to add to sapling and adult densities prior to log-transformation (see materials and methods for details).

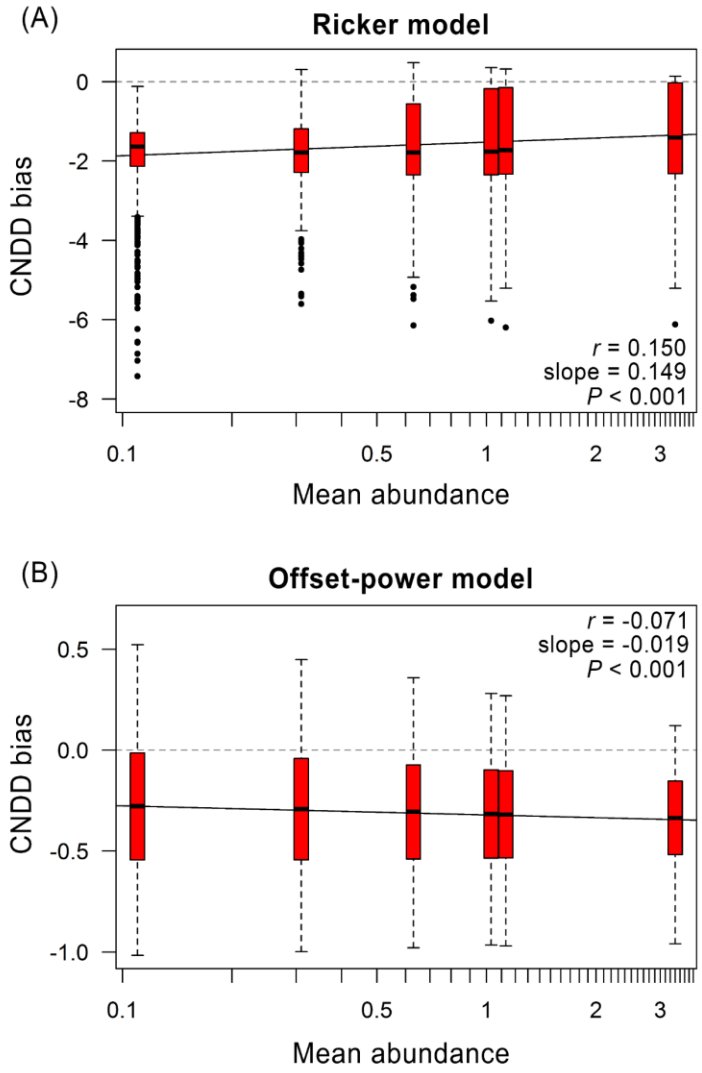

Fig. S12. Relationships between bias in conspecific negative density dependence (CNDD) and mean abundance. Data were simulated using different values of per-capita recruitment at low densities (r), the negative-binomial overdispersion parameter (θ), mean trees per quadrat, and dispersal (d) to test the robustness of our CNDD models to different ranges of error, tree densities, and dispersal rates. Plots show correlations between mean trees per quadrat (mean abundance) and CNDD bias (estimated CNDD values minus known CNDD values) for the (A) Ricker model and the (B) offset-power model across all parameters considered (N = 8,100 parameter combinations; shown as boxplots for ease of visualization). Pearson correlation coefficients, slopes, and regression lines fit through all 8,100 parameter combinations (solid lines) are shown. The small amount of variation in CNDD bias associated with abundance for both models (Ricker: r^2 = 0.022; offset-power: r^2 = 0.005) combined with opposing directions of the relationship between bias and abundance across the two models indicate that our result of stronger CNDD for rare species in the tropics (found with both models; see Figs. 2, S7) appears robust to the potential for systematic changes in CNDD bias with species abundance. We also found stronger CNDD for rare species in the tropics after restricting our analysis to species within a standardized range of abundances (i.e. the truncation analysis described in materials and methods).

Table S1. Summary statistics for the 24 Smithsonian Center for Tropical Forest Science-Forest Global Earth Observatory (CTFS-ForestGEO) plots used in this analysis. Richness was rarefied to 7,083 individuals at the forest-plot scale and 20 individuals at the local (20×20 m quadrat) scale. Shannon diversity indices are reported at each spatial scale. Values reflect live individuals.

Forest plot	Latitude	Longitude	Plot size (ha)	Total individuals in plot	Plot species richness	Plot rarefied richness	Plot Shannon diversity	Mean-local richness	Mean-local rarefied richness	Mean-local Shannon diversity
Rabi, Gabon	-2.22	9.92	25	173,556	345	253.1	4.48	67.1	13.9	3.47
Korup, Cameroon	5.07	8.85	50	314,388	481	310.3	4.49	66.5	14.1	3.49
Wanang, Papua New Guinea	-5.25	145.27	50	253,609	581	381	5.08	85.1	17.0	4.07
Sinharaja, Sri Lanka	6.4	80.4	25	181,238	234	177.1	3.89	48.2	12.0	3.00
Khao Chong, Thailand	7.54	99.8	24	96,473	632	423.4	5.11	69.7	15.7	3.75
Barro Colorado Island, Panama (BCI)	9.15	-79.85	50	207,258	297	216.7	4.00	49.4	13.4	3.26
Mo Singto, Thailand	14.43	101.35	30.48	128,557	261	176.1	3.73	40.5	12.0	2.91
Huai Kha Khaeng, Thailand	15.63	99.22	50	104,982	270	184.3	3.41	25.3	11.2	2.55
Palanan, Phillipines	17.04	122.39	16	74,426	323	258.7	4.69	68.7	16.3	3.85
Palamanui, Hawaii, USA	19.74	-155.99	4	12,387	14	12.6	1.02	4.7	3.2	0.88
Laupahoehoe, Hawaii, USA	19.93	-155.29	4	12,887	20	19.6	1.89	9.6	6.2	1.73
Heishiding, China	23.27	111.53	50	213,235	213	170.7	4.23	45.7	13.4	3.21
Lienhuachih, Taiwan	23.91	120.88	25	153,268	145	110.4	3.57	35.3	11.5	2.82
Fushan, Taiwan	24.76	121.56	25	114,651	106	83.3	3.21	30.8	10.6	2.62
Utah Cedar Breaks, USA	37.66	-112.86	13.04	22,277	17	14.2	1.01	3.6	2.9	0.71
Yosemite National Park, USA	37.77	-119.82	25.6	7,083	12	12	1.09	2.5	2.4	0.65
Tyson Research Center, USA	38.52	-90.56	20.16	30,249	41	35.6	2.35	8.4	5.9	1.53
Smithsonian Conservation Biology Institute (SCBI), USA	38.89	-78.15	20.88	21,770	61	52.3	2.75	9.7	7.7	1.77
Smithsonian Environmental Research Center (SERC), USA	38.89	-76.56	16	24,065	67	53.9	2.19	8.2	5.3	1.33
Lilly Dickey Woods, USA	39.24	-86.22	25	26,443	33	29.7	1.95	6.2	4.9	1.23
Harvard Forest, USA	42.54	-72.18	35	77,006	50	40.8	2.55	9.1	5.8	1.49
Wabikon Lake, USA	45.55	-88.8	25.6	37,401	31	27.5	2.09	6.3	4.8	1.32
Wind River, USA	45.82	-121.96	25.6	26,056	23	19	1.64	5.4	4.6	1.25
Zofin, Czech Republic	48.66	14.71	25	58,491	11	7.6	0.13	1.6	1.3	0.09

Table S2. Brief description of vegetation type and climate zone for Smithsonian CTFS-ForestGEO forest plots. Dominant vegetation type and Köppen climate zone provided *(33)*. Forest plots are arranged in order of increasing distance from the equator (absolute value of latitude).

Forest plot	Dominant vegetation type(s)	Köppen climate zone
Rabi, Gabon	Broadleaf evergreen	Tropical, wet and dry seasons
Korup, Cameroon	Broadleaf evergreen	Tropical, monsoon
Wanang, Papua New Guinea	Broadleaf evergreen	Tropical, with significant precipitation year-round
Sinharaja, Sri Lanka	Broadleaf evergreen	Tropical, with significant precipitation year-round
Khao Chong, Thailand	Broadleaf evergreen	Tropical, monsoon
Barro Colorado Island, Panama	Broadleaf drought deciduous, Broadleaf evergreen	Tropical, monsoon
Mo Singto, Thailand	Broadleaf evergreen, Broadleaf drought deciduous	Tropical, wet and dry seasons
Huai Kha Khaeng, Thailand	Broadleaf evergreen, Broadleaf drought deciduous	Tropical, wet and dry seasons
Palanan, Phillipines	Broadleaf evergreen	Tropical, with significant precipitation year-round
Palamanui, Hawaii, USA	Broadleaf evergreen	Oceanic, with significant precipitation year-round
Laupahoehoe, Hawaii, USA	Broadleaf evergreen	Oceanic, with significant precipitation year-round
Heishiding, China	Broadleaf evergreen	Humid subtropical/mid-latitude, with significant precipitation year-round
Lienhuachih, Taiwan	Broadleaf evergreen	Oceanic, with dry winters
Fushan, Taiwan	Broadleaf evergreen	Humid subtropical/mid-latitude, with significant precipitation year-round
Utah Cedar Breaks, USA	Needleleaf evergreen, Broadleaf cold deciduous	Dry-summer subtropical/mid-latitude, with dry summers
Yosemite National Park, USA	Needleleaf evergreen	Dry-summer subtropical/mid-latitude, with dry summers
Tyson Research Center, USA	Broadleaf cold deciduous	Humid subtropical/mid-latitude, with significant precipitation year-round
Smithsonian Conservation Biology Institute (SCBI), USA	Broadleaf cold deciduous	Humid subtropical/mid-latitude, with significant precipitation year-round
Smithsonian Environmental Research Center (SERC), USA	Broadleaf cold deciduous	Humid subtropical/mid-latitude, with significant precipitation year-round
Lilly Dickey Woods, USA	Broadleaf cold deciduous	Humid subtropical/mid-latitude, with significant precipitation year-round
Harvard Forest, USA	Broadleaf cold deciduous	Humid continental, with significant precipitation year-round
Wabikon Lake, USA	Broadleaf cold deciduous	Humid continental, with significant precipitation year-round
Wind River, USA	Needleleaf evergreen	Dry-summer subtropical/mid-latitude, with dry summers
Zofin, Czech Republic	Broadleaf cold deciduous, Needleleaf evergreen	Oceanic, with significant precipitation year-round

Table S3. Median and weighted-mean estimates of conspecific negative density dependence (CNDD), density dependence from heterospecific adults (adult HNDD) and heterospecific saplings (sapling HNDD), and per-capita recruitment at low densities (*r*) measured at the 10×10 m scale (Ricker model). 95% confidence intervals (CI) are provided, and plots are ordered as in Table S1.

Forest plot	Median CNDD	Mean CNDD	Mean CNDD CI	Median adult HNDD	Mean adult HNDD	Mean adult HDD CI	Median sapling HNDD	Mean sapling HNDD	Mean sapling HNDD CI	Median *r*	Mean *r*	Mean *r* CI
Rabi	-3.64	-2.15	(-2.43,-1.86)	-0.003	-0.002	(-0.004,0.001)	0.002	0.002	(0.001,0.003)	2.7	2.6	(2.5,2.8)
Korup	-4.38	-2.92	(-3.21,-2.64)	-0.002	-0.003	(-0.005,-0.002)	0.002	0.002	(0.001,0.003)	2.8	2.8	(2.7,2.9)
Wanang	-4.33	-4.16	(-4.32,-4.00)	0.001	0.000	(-0.002,0.002)	0.003	0.003	(0.002,0.003)	2.7	2.8	(2.7,2.8)
Sinharaja	-3.56	-1.26	(-1.57,-0.95)	-0.001	0.000	(-0.001,0.001)	0.002	0.002	(0.001,0.003)	2.7	2.4	(2.3,2.6)
Khao Chong	-4.32	-3.91	(-4.10,-3.72)	-0.002	-0.003	(-0.005,-0.001)	0.003	0.003	(0.002,0.004)	2.8	2.8	(2.7,2.8)
BCI	-4.56	-3.70	(-4.01,-3.39)	-0.003	-0.002	(-0.004,0.000)	0.004	0.004	(0.003,0.005)	2.8	2.8	(2.7,2.9)
Mo Singto	-3.66	-2.15	(-2.56,-1.73)	-0.004	-0.004	(-0.007,-0.001)	0.005	0.005	(0.003,0.007)	2.7	2.6	(2.4,2.7)
Huai Kha Khaeng	-4.44	-3.09	(-3.56,-2.62)	-0.001	0.000	(-0.004,0.004)	0.005	0.006	(0.003,0.009)	2.8	2.7	(2.6,2.8)
Palanan	-3.98	-3.59	(-3.81,-3.38)	0.000	0.000	(-0.003,0.002)	0.004	0.004	(0.002,0.006)	2.7	2.7	(2.6,2.7)
Palamanui	-0.35	-0.14	(-0.40,0.11)	-0.003	-0.007	(-0.031,0.016)	0.008	0.006	(-0.010,0.021)	1.1	1.1	(0.4,1.9)
Laupahoehoe	-1.91	-1.01	(-1.86,-0.17)	0.007	0.007	(-0.006,0.020)	0.006	0.017	(0.005,0.029)	1.8	1.7	(0.5,2.8)
Heishiding	-3.25	-1.85	(-2.16,-1.53)	-0.003	-0.004	(-0.006,-0.002)	0.007	0.006	(0.005,0.007)	2.7	2.5	(2.4,2.6)
Lienhuachih	-3.10	-1.15	(-1.50,-0.81)	0.000	0.000	(-0.004,0.004)	0.005	0.005	(0.004,0.006)	2.5	2.2	(2.0,2.4)
Fushan	-3.28	-2.27	(-2.76,-1.78)	0.006	0.007	(0.000,0.014)	0.008	0.008	(0.006,0.010)	2.2	2.3	(2.1,2.6)
Utah	-0.89	-0.63	(-1.52,0.25)	-0.022	-0.020	(-0.058,0.018)	0.005	0.004	(-0.006,0.013)	1.6	2.2	(1.6,2.8)
Yosemite	-0.88	-0.72	(-1.22,-0.23)	-0.014	-0.027	(-0.169,0.115)	-0.100	-0.109	(-0.156,-0.061)	2.2	1.8	(0.9,2.6)
Tyson	-1.92	-0.53	(-1.04,-0.02)	-0.016	-0.018	(-0.029,-0.008)	-0.018	-0.008	(-0.024,0.007)	2.6	2.4	(2.0,2.8)
SCBI	-3.12	-0.87	(-1.47,-0.26)	-0.006	-0.011	(-0.026,0.003)	-0.005	-0.008	(-0.019,0.003)	2.8	2.6	(2.4,2.9)
SERC	-1.47	-0.92	(-1.52,-0.32)	-0.037	-0.044	(-0.068,-0.019)	0.007	0.015	(-0.001,0.031)	2.7	2.4	(1.9,2.8)
Lilly Dickey Woods	-2.75	-0.73	(-1.44,-0.01)	-0.004	-0.003	(-0.039,0.033)	0.008	0.021	(-0.002,0.044)	2.4	2.2	(1.6,2.8)
Harvard Forest	-1.48	-0.41	(-0.74,-0.08)	-0.023	-0.020	(-0.032,-0.009)	0.008	0.010	(0.004,0.016)	2.3	2.2	(1.8,2.5)
Wabikon Lake	-0.96	-0.48	(-0.95,-0.01)	0.020	0.021	(0.002,0.040)	-0.004	-0.001	(-0.012,0.009)	1.3	1.8	(1.2,2.5)
Wind River	-0.94	-0.76	(-1.70,0.18)	-0.012	-0.013	(-0.047,0.020)	0.007	0.001	(-0.026,0.027)	2.4	2.4	(1.9,3.0)
Zofin	-1.76	-0.21	(-0.99,0.57)	-0.044	-0.038	(-0.070,-0.006)	-0.031	-0.016	(-0.045,0.014)	3.1	2.2	(0.9,3.5)

Table S4. Median and weighted-mean estimates of conspecific negative density dependence (CNDD), density dependence from heterospecific adults (adult HNDD) and heterospecific saplings (sapling HNDD), and per-capita recruitment at low densities (*r*) measured at the 20×20 m scale (Ricker model). 95% confidence intervals (CI) are provided, and plots are ordered as in Table S1.

Forest Plot	Median CNDD	Mean CNDD	Mean CNDD CI	Median adult HNDD	Mean adult HNDD	Mean adult HDD CI	Median sapling HNDD	Mean sapling HNDD	Mean sapling HNDD CI	Median *r*	Mean *r*	Mean *r* CI
Rabi	-1.78	-0.64	(-0.84,-0.44)	-0.001	-0.001	(-0.002,0.001)	0.002	0.002	(0.001,0.003)	2.1	2.0	(1.8,2.2)
Korup	-3.07	-0.94	(-1.17,-0.70)	-0.001	-0.002	(-0.003,-0.001)	0.002	0.001	(0.001,0.002)	2.6	2.5	(2.3,2.6)
Wanang	-2.85	-1.94	(-2.16,-1.72)	0.001	0.001	(-0.000,0.002)	0.002	0.002	(0.001,0.002)	2.4	2.2	(2.1,2.4)
Sinharaja	-1.29	-0.19	(-0.36,-0.03)	0.000	-0.001	(-0.002,0.000)	0.001	0.002	(0.001,0.003)	2.0	1.7	(1.5,2.0)
Khao Chong	-2.84	-1.80	(-2.07,-1.54)	-0.002	-0.002	(-0.003,-0.000)	0.003	0.003	(0.002,0.004)	2.4	2.3	(2.2,2.5)
BCI	-3.30	-1.36	(-1.69,-1.04)	-0.003	-0.003	(-0.005,-0.002)	0.004	0.003	(0.002,0.004)	2.4	2.4	(2.2,2.6)
Mo Singto	-1.98	-0.75	(-1.04,-0.45)	-0.002	-0.002	(-0.003,-0.001)	0.003	0.003	(0.002,0.004)	2.4	2.1	(1.9,2.4)
Huai Kha Khaeng	-3.21	-1.02	(-1.37,-0.66)	-0.004	-0.002	(-0.005,0.001)	0.004	0.004	(0.002,0.006)	2.6	2.3	(2.1,2.5)
Palanan	-2.44	-1.44	(-1.70,-1.18)	0.000	0.000	(-0.001,0.002)	0.003	0.003	(0.002,0.003)	2.2	2.1	(1.9,2.3)
Palamanui	-0.08	-0.03	(-0.11,0.06)	-0.003	-0.003	(-0.015,0.009)	0.001	0.000	(-0.005,0.006)	0.8	0.9	(0.3,1.6)
Laupahoehoe	-0.38	-0.19	(-0.64,0.27)	0.002	0.002	(-0.007,0.010)	0.005	0.007	(0.002,0.013)	0.7	0.9	(-0.7,2.5)
Heishiding	-1.66	-0.46	(-0.64,-0.28)	-0.004	-0.004	(-0.005,-0.002)	0.004	0.004	(0.003,0.005)	2.1	1.9	(1.7,2.1)
Lienhuachih	-0.91	-0.34	(-0.54,-0.13)	-0.001	0.000	(-0.002,0.002)	0.003	0.003	(0.002,0.003)	1.1	1.5	(1.1,1.8)
Fushan	-1.37	-0.48	(-0.77,-0.18)	0.003	0.005	(0.002,0.009)	0.004	0.004	(0.003,0.005)	1.1	1.0	(0.6,1.5)
Utah	-0.21	-0.13	(-0.43,0.16)	-0.009	-0.004	(-0.017,0.008)	0.001	0.002	(-0.002,0.006)	1.1	1.6	(0.7,2.4)
Yosemite	-0.36	-0.22	(-0.37,-0.07)	0.012	0.005	(-0.059,0.069)	0.046	0.035	(0.009,0.060)	-0.3	0.4	(-0.9,1.6)
Tyson	-0.25	-0.40	(-0.77,-0.02)	-0.004	-0.005	(-0.014,0.003)	-0.010	-0.004	(-0.013,0.005)	1.2	1.4	(0.9,2.0)
SCBI	-0.88	-0.30	(-0.62,0.02)	-0.011	-0.011	(-0.021,-0.002)	0.001	-0.001	(-0.008,0.005)	1.6	1.7	(1.2,2.2)
SERC	-0.37	-0.18	(-0.35,-0.00)	-0.032	-0.035	(-0.047,-0.024)	0.011	0.011	(0.005,0.018)	1.9	1.6	(0.9,2.2)
Lilly Dickey Woods	-0.76	-0.19	(-0.53,0.15)	-0.003	-0.007	(-0.025,0.010)	0.014	0.014	(0.005,0.022)	1.7	1.6	(0.8,2.4)
Harvard Forest	-0.33	-0.11	(-0.27,0.05)	-0.008	-0.008	(-0.013,-0.004)	0.005	0.006	(0.002,0.009)	1.3	1.5	(0.9,2.0)
Wabikon Lake	-0.37	-0.17	(-0.50,0.17)	0.005	0.003	(-0.002,0.009)	0.004	0.005	(-0.000,0.010)	1.5	1.3	(0.4,2.3)
Wind River	-0.32	-0.22	(-0.61,0.18)	-0.002	-0.003	(-0.013,0.008)	0.000	0.003	(-0.002,0.008)	1.9	1.8	(1.0,2.6)
Zofin	-0.10	-0.02	(-0.25,0.21)	-0.014	-0.015	(-0.038,0.009)	-0.012	-0.004	(-0.018,0.011)	1.8	1.3	(0.2,2.4)

Table S5. Relationships between the strength of conspecific negative density dependence (CNDD) and species richness and diversity across forest plots. Relationships between the median value of CNDD in a forest plot (measured at the 10×10 m quadrat scale with the Ricker model) and species richness may have been influenced by the inclusion of rare species (i.e. with small sample sizes). To ensure this was not the case, the strength of CNDD was measured using progressively-restrictive datasets, each one excluding a greater proportion of rare species than the prior one. These measurements were then regressed against forest-wide rarefied richness (rarefied to 7,083 individuals), forest-wide Shannon diversity indices, mean-local (20×20 m quadrat) rarefied richness (rarefied to 20 individuals), and mean-local Shannon diversity indices. Spearman-rank correlation coefficients (r_s) for relationships of species richness and diversity metrics with CNDD and associated *P*-values are presented for each test (N = 24 forest plots). Relationships were highly significant in all cases. In this manuscript, we report results excluding species with adults or saplings in fewer than 10 quadrats because relationships between conspecific adult and sapling densities across quadrats (i.e. measurements of CNDD) are not reliable for species with such low sample sizes. Qualitatively similar relationships were found if we removed species with adults and sapling occupying fewer than 1%, 2%, and 4% of quadrats in a forest plot (these percentages removed approximately the same number of species from the analysis as noted for the quadrat thresholds in this table). We also show results from the truncation analysis, where species with a maximum conspecific adult density lower than three adults per quadrat were removed, and all remaining data was truncated at a conspecific adult density of 10 adults per quadrat.

Dataset (Ricker model at the 10×10 m scale)	Total number of species	CNDD & forest rarefied richness		CNDD & forest Shannon diversity		CNDD & mean-local rarefied richness		CNDD & mean-local Shannon diversity	
		r_s	*P*	r_s	*P*	r_s	*P*	r_s	*P*
Species with both adults and saplings present in ≥ 10 quadrats each	1,919	-0.903	< 0.0001	-0.862	< 0.0001	-0.875	< 0.0001	-0.865	< 0.0001
Species with both adults and saplings present in ≥ 30 quadrats each	1,549	-0.918	< 0.0001	-0.887	< 0.0001	-0.898	< 0.0001	-0.885	< 0.0001
Species with both adults and saplings present in ≥ 50 quadrats each	1,276	-0.886	< 0.0001	-0.859	< 0.0001	-0.858	< 0.0001	-0.839	< 0.0001
Truncation analysis	1,084	-0.868	< 0.0001	-0.856	< 0.0001	-0.860	< 0.0001	-0.857	< 0.0001

Table S6. Relationships between the strength of conspecific negative density dependence (CNDD) and species richness and diversity across forest plots. Relationships between the median value of CNDD in a forest plot (measured at the 20×20 m quadrat scale with the Ricker model) and species richness may have been influenced by the inclusion of rare species (i.e. with small sample sizes). To ensure this was not the case, the strength of CNDD was measured using progressively-restrictive datasets, each one excluding a greater proportion of rare species than the prior one. These measurements were then regressed against forest-wide rarefied richness (rarefied to 7,083 individuals), forest-wide Shannon diversity indices, mean-local (20×20 m quadrat) rarefied richness (rarefied to 20 individuals), and mean-local Shannon diversity indices. Spearman-rank correlation coefficients (r_s) for relationships of species richness and diversity metrics with CNDD and associated *P*-values are presented for each test (N = 24 forest plots). Relationships were highly significant in all cases. In this manuscript, we report results excluding species with adults or saplings in fewer than 10 quadrats because relationships between conspecific adult and sapling densities across quadrats (i.e. measurements of CNDD) are not reliable for species with such low sample sizes. Qualitatively similar relationships were found if we removed species with adults and sapling occupying fewer than 1%, 2%, and 4% of quadrats in a forest plot (these percentages removed approximately the same number of species from the analysis as noted for the quadrat thresholds in this table). We also show results from the truncation analysis, where species with a maximum conspecific adult density lower than three adults per quadrat were removed, and all remaining data was truncated at a conspecific adult density of 10 adults per quadrat.

Dataset (Ricker model at the 20×20 m scale)	Total number of species	CNDD & forest rarefied richness		CNDD & forest Shannon diversity		CNDD & mean-local rarefied richness		CNDD & mean-local Shannon diversity	
		r_s	*P*	r_s	*P*	r_s	*P*	r_s	*P*
Species with both adults and saplings present in ≥ 10 quadrats each	1,443	-0.904	< 0.0001	-0.871	< 0.0001	-0.873	< 0.0001	-0.866	< 0.0001
Species with both adults and saplings present in ≥ 30 quadrats each	1,126	-0.892	< 0.0001	-0.856	< 0.0001	-0.859	< 0.0001	-0.836	< 0.0001
Species with both adults and saplings present in ≥ 50 quadrats each	887	-0.855	< 0.0001	-0.827	< 0.0001	-0.804	< 0.0001	-0.778	< 0.0001
Truncation analysis	1,058	-0.929	< 0.0001	-0.917	< 0.0001	-0.910	< 0.0001	-0.903	< 0.0001

Table S7. Relationships between the strength of negative frequency dependence (NFD) and species richness and diversity across forest plots. Relationships between the median value of NFD in a forest plot (measured at the 10×10 m and the 20×20 m quadrat scales with the Ricker model) and species richness and diversity. Spearman-rank correlation coefficients (r_s) and associated *P*-values are shown for each test (N = 24 forest plots). Median NFD was calculated as the median value of CNDD minus the median value of HNDD for heterospecific adults (see materials and methods). See Tables S5 and S6 for descriptions of species richness and diversity metrics. We also show results from the truncation analysis, where species with a maximum conspecific adult density lower than three adults per quadrat were removed, and all remaining data truncated at a conspecific adult density of 10 adults per quadrat.

Dataset (Ricker model at the 10×10 m scale)	Total number of species	NFD & forest rarefied richness		NFD & forest Shannon diversity		NFD & mean-local rarefied richness		NFD & mean-local Shannon diversity	
		r_s	*P*	r_s	*P*	r_s	*P*	r_s	*P*
Species with both adults and saplings present in ≥ 10 quadrats each	1,919	-0.900	< 0.0001	-0.858	< 0.0001	-0.876	< 0.0001	-0.866	< 0.0001
Species with both adults and saplings present in ≥ 30 quadrats each	1,549	-0.920	< 0.0001	-0.888	< 0.0001	-0.899	< 0.0001	-0.887	< 0.0001
Species with both adults and saplings present in ≥ 50 quadrats each	1,276	-0.881	< 0.0001	-0.851	< 0.0001	-0.853	< 0.0001	-0.834	< 0.0001
Truncation analysis	1,084	-0.869	< 0.0001	-0.857	< 0.0001	-0.861	< 0.0001	-0.859	< 0.0001

Dataset (Ricker model at the 20×20 m scale)	Total number of species	NFD & forest rarefied richness		NFD & forest Shannon diversity		NFD & mean-local rarefied richness		NFD & mean-local Shannon diversity	
		r_s	*P*	r_s	*P*	r_s	*P*	r_s	*P*
Species with both adults and saplings present in ≥ 10 quadrats each	1,443	-0.896	< 0.0001	-0.867	< 0.0001	-0.868	< 0.0001	-0.861	< 0.0001
Species with both adults and saplings present in ≥ 30 quadrats each	1,126	-0.889	< 0.0001	-0.854	< 0.0001	-0.851	< 0.0001	-0.828	< 0.0001
Species with both adults and saplings present in ≥ 50 quadrats each	887	-0.853	< 0.0001	-0.830	< 0.0001	-0.808	< 0.0001	-0.783	< 0.0001
Truncation analysis	1,058	-0.931	< 0.0001	-0.923	< 0.0001	-0.917	< 0.0001	-0.911	< 0.0001

Table S8. Relationships between species abundance and the strength of conspecific negative density dependence (CNDD) across species within each forest plot. Results are shown for estimates of density dependence using the Ricker model. Intercepts and slopes for species abundance predicting the strength of CNDD are shown with 95% confidence intervals (CI). Plots are ordered as in Table S1.

Forest plot	Relationship between species abundance in a forest plot and CNDD							
	CNDD measured at the 10×10 m scale				CNDD measured at the 20×20 m scale			
	Intercept	*Int. CI*	*Slope*	*Slope CI*	*Intercept*	*Int. CI*	*Slope*	*Slope CI*
Rabi	-1.02	(-1.51,-0.52)	0.38	(0.24,0.53)	0.24	(-0.15,0.63)	0.33	(0.20,0.46)
Korup	-1.29	(-1.83,-0.75)	0.47	(0.33,0.60)	0.21	(-0.20,0.62)	0.41	(0.28,0.54)
Wanang	-3.33	(-3.72,-2.93)	0.22	(0.12,0.31)	-0.67	(-1.12,-0.23)	0.38	(0.26,0.50)
Sinharaja	-0.37	(-0.68,-0.07)	0.59	(0.46,0.71)	-0.02	(-0.18,0.14)	0.23	(0.13,0.33)
Khao Chong	-3.48	(-3.92,-3.04)	0.13	(0.01,0.25)	-0.85	(-1.42,-0.29)	0.29	(0.14,0.45)
BCI	-2.91	(-3.50,-2.32)	0.26	(0.09,0.42)	-0.44	(-0.91,0.02)	0.41	(0.25,0.58)
Mo Singto	-0.79	(-1.44,-0.13)	0.49	(0.30,0.69)	0.10	(-0.48,0.68)	0.30	(0.12,0.48)
Huai Kha Khaeng	-1.84	(-2.55,-1.13)	0.46	(0.25,0.67)	-0.47	(-0.90,-0.04)	0.31	(0.15,0.46)
Palanan	-2.79	(-3.23,-2.34)	0.26	(0.13,0.39)	-0.55	(-0.95,-0.16)	0.36	(0.23,0.49)
Palamanui	-0.11	(-0.43,0.22)	0.06	(-0.20,0.31)	-0.02	(-0.13,0.10)	0.02	(-0.08,0.12)
Laupahoehoe	-1.33	(-1.80,-0.85)	0.39	(0.24,0.55)	-0.58	(-1.09,-0.06)	0.21	(0.02,0.40)
Heishiding	-0.76	(-1.29,-0.24)	0.35	(0.21,0.49)	-0.05	(-0.31,0.21)	0.18	(0.09,0.26)
Lienhuachih	-0.32	(-0.72,0.09)	0.48	(0.32,0.64)	-0.04	(-0.35,0.28)	0.16	(0.03,0.29)
Fushan	-1.36	(-1.88,-0.84)	0.56	(0.36,0.76)	-0.21	(-0.48,0.07)	0.34	(0.19,0.50)
Utah	-0.92	(-1.72,-0.13)	0.31	(0.01,0.61)	-0.46	(-0.79,-0.14)	0.20	(0.05,0.34)
Yosemite	-0.77	(-1.33,-0.21)	0.06	(-0.14,0.27)	-0.29	(-0.44,-0.14)	0.05	(-0.01,0.10)
Tyson	-1.18	(-2.59,0.23)	-0.24	(-0.74,0.25)	-0.28	(-0.71,0.15)	0.10	(-0.08,0.29)
SCBI	-1.56	(-3.26,0.14)	-0.29	(-0.94,0.37)	-0.40	(-1.03,0.22)	-0.05	(-0.31,0.21)
SERC	-0.78	(-1.59,0.02)	0.08	(-0.22,0.38)	-0.20	(-0.39,-0.01)	-0.02	(-0.09,0.04)
Lilly Dickey Woods	-0.69	(-1.85,0.46)	0.01	(-0.39,0.42)	-0.20	(-0.68,0.27)	-0.01	(-0.21,0.19)
Harvard Forest	-0.18	(-0.82,0.47)	0.08	(-0.11,0.28)	-0.10	(-0.43,0.24)	0.00	(-0.11,0.12)
Wabikon Lake	-0.32	(-0.82,0.18)	0.17	(-0.05,0.38)	-0.16	(-0.48,0.17)	0.14	(-0.07,0.35)
Wind River	-1.17	(-2.62,0.28)	-0.13	(-0.46,0.21)	-0.24	(-0.78,0.31)	-0.01	(-0.14,0.12)
Zofin	-1.12	(-1.19,-1.04)	0.33	(0.31,0.36)	-0.77	(-1.05,-0.48)	0.24	(0.15,0.32)

Table S9. Expected values for CNDD and HNDD (measured with Ricker model) given neutral dynamics and no density dependence, and standardized effect sizes (SES). Means and SD of expected values for CNDD, adult HNDD, sapling HNDD, and the slope between CNDD and species abundance within each forest plot from neutral models. See materials and methods for details.

Forest plot	Neutral CNDD	Neutral CNDD SD	CNDD SES	Neutral Adult HNDD	Neutral Adult HNDD SD	Adult HNDD SES	Neutral Sapling HNDD	Neutral Sapling HNDD SD	Sapling HNDD SES	Neutral CNDD-abund slope	Neutral CNDD-abund slope SD	CNDD-abund slope SES
Rabi, Gabon	-0.146	0.010	-163.8	-0.007	0.00	4.2	-0.008	0.001	9.7	0.036	0.006	47.9
Korup, Cameroon	-0.152	0.006	-448.9	-0.009	0.00	8.5	-0.008	0.001	12.2	0.035	0.009	43.2
Wanang, Papua New Guinea	-0.169	0.008	-345.8	-0.010	0.00	10.7	-0.010	0.001	14.8	0.037	0.010	34.7
Sinharaja, Sri Lanka	-0.134	0.011	-104.1	-0.008	0.00	6.7	-0.007	0.001	9.2	0.038	0.010	19.9
Khao Chong, Thailand	-0.192	0.010	-252.6	-0.013	0.00	5.5	-0.013	0.002	9.1	0.048	0.012	21.0
Barro Colorado Island, Panama	-0.166	0.012	-267.3	-0.012	0.00	7.7	-0.012	0.001	13.7	0.034	0.009	40.1
Mo Singto, Thailand	-0.166	0.012	-155.2	-0.012	0.00	6.2	-0.012	0.001	11.7	0.040	0.010	26.7
Huai Kha Khaeng, Thailand	-0.217	0.011	-262.2	-0.024	0.00	8.0	-0.023	0.002	13.9	0.045	0.013	19.8
Palanan, Phillipines	-0.170	0.016	-143.4	-0.011	0.00	4.4	-0.011	0.002	7.5	0.045	0.014	22.8
Palamanui, Hawaii, USA	-0.120	0.035	1.2	-0.012	0.01	1.5	-0.015	0.004	3.6	0.050	0.022	-1.4
Laupahoehoe, Hawaii, USA	-0.118	0.036	-7.3	-0.014	0.01	2.5	-0.014	0.004	4.3	0.054	0.025	6.1
Heishiding, China	-0.157	0.008	-177.4	-0.012	0.00	5.0	-0.012	0.001	15.4	0.037	0.009	15.9
Lienhuachih, Taiwan	-0.134	0.014	-55.4	-0.009	0.00	5.3	-0.008	0.001	11.4	0.039	0.010	12.4
Fushan, Taiwan	-0.139	0.012	-102.2	-0.011	0.00	7.6	-0.011	0.001	11.0	0.040	0.011	27.3
Utah Cedar Breaks, USA	-0.172	0.027	-1.3	-0.024	0.01	3.0	-0.024	0.004	5.8	0.053	0.020	7.2
Yosemite National Park, USA	-0.590	0.060	3.9	-0.078	0.02	5.2	-0.093	0.015	9.0	0.085	0.055	-0.7
Tyson Research Center, USA	-0.220	0.025	-1.3	-0.030	0.01	4.7	-0.029	0.004	5.0	0.055	0.022	2.2
Smithsonian Conservation Biology Institute (SCBI), USA	-0.279	0.025	-24.4	-0.040	0.01	4.3	-0.040	0.005	7.6	0.055	0.027	-4.0
Smithsonian Environmental Research Center (SERC), USA	-0.224	0.019	-7.9	-0.030	0.01	-0.4	-0.030	0.006	6.9	0.054	0.026	-3.0
Lilly Dickey Woods, USA	-0.256	0.025	-19.9	-0.039	0.01	6.7	-0.038	0.005	10.7	0.054	0.026	-2.4
Harvard Forest, USA	-0.177	0.016	-9.5	-0.021	0.00	5.1	-0.020	0.002	12.4	0.044	0.019	-2.1
Wabikon Lake, USA	-0.205	0.021	-7.9	-0.030	0.00	8.3	-0.028	0.004	9.0	0.049	0.019	4.8
Wind River, USA	-0.254	0.021	-3.0	-0.039	0.01	6.1	-0.039	0.005	8.4	0.054	0.023	-2.7
Zofin, Czech Republic	-0.141	0.028	1.3	-0.017	0.00	0.8	-0.019	0.004	1.7	0.045	0.019	9.9

Table S10. Mean Mantel correlation coefficients testing for spatial auto-correlation in CNDD model residuals for each forest plot (Ricker model). Mantel tests assessed for relationships between model residuals of each species and spatial distance within each forest plot. Results are shown for models estimating CNDD at the 20×20-m scale, but correlations were similar for models estimating CNDD at the 10×10-m scale. Mean Mantel correlation coefficients (r_m) across species are shown, along with the SD of these coefficients and their mean *P*-value for each forest plot.

Forest plot	Mean r_m	SD r_m	Mean *P*
Rabi, Gabon	0.003	0.048	0.474
Korup, Cameroon	0.001	0.030	0.501
Wanang, Papua New Guinea	0.005	0.035	0.470
Sinharaja, Sri Lanka	0.009	0.048	0.478
Khao Chong, Thailand	0.013	0.042	0.400
Barro Colorado Island, Panama	0.009	0.034	0.412
Mo Singto, Thailand	0.014	0.037	0.364
Huai Kha Khaeng, Thailand	-0.009	0.030	0.636
Palanan, Phillipines	0.009	0.037	0.414
Palamanui, Hawaii, USA	-0.014	0.089	0.533
Laupahoehoe, Hawaii, USA	0.033	0.036	0.275
Heishiding, China	0.008	0.053	0.470
Lienhuachih, Taiwan	0.011	0.055	0.481
Fushan, Taiwan	-0.008	0.046	0.553
Utah Cedar Breaks, USA	-0.015	0.037	0.700
Yosemite National Park, USA	0.032	0.012	0.110
Tyson Research Center, USA	0.016	0.053	0.394
Smithsonian Conservation Biology Institute (SCBI), USA	-0.025	0.056	0.675
Smithsonian Environmental Research Center (SERC), USA	0.039	0.060	0.314
Lilly Dickey Woods, USA	0.015	0.057	0.392
Harvard Forest, USA	0.010	0.053	0.362
Wabikon Lake, USA	0.019	0.050	0.440
Wind River, USA	0.006	0.043	0.416
Zofin, Czech Republic	-0.030	0.005	0.965

Table S11. Mean estimates of conspecific negative density dependence (CNDD), density dependence from heterospecific adults (adult HNDD) and heterospecific saplings (sapling HNDD), and per-capita recruitment at low densities (*r*) measured at the 10×10 m scale (hierarchical offset-power model). 95% confidence intervals (CI) are provided, and plots are ordered as in Table S1.

Forest plot	CNDD	CNDD CI	Adult HNDD	Adult HDD CI	Sapling HNDD	Sapling HNDD CI	*r*	*r* CI
Rabi, Gabon	0.27	(0.24,0.31)	-0.0003	(-0.0007,-0.0001)	0.0045	(0.0041,0.0048)	0.027	(0.027,0.028)
Korup, Cameroon	0.18	(0.15,0.22)	0.0006	(0.0004,0.0008)	0.0035	(0.0033,0.0037)	0.020	(0.020,0.020)
Wanang, Papua New Guinea	0.14	(0.12,0.15)	0.0006	(0.0005,0.0008)	0.0047	(0.0046,0.0049)	0.019	(0.018,0.019)
Sinharaja, Sri Lanka	0.27	(0.22,0.31)	-0.0011	(-0.0016,-0.0006)	0.0056	(0.0051,0.0061)	0.025	(0.025,0.026)
Khao Chong, Thailand	0.15	(0.13,0.18)	0.0006	(0.0004,0.0009)	0.0051	(0.0049,0.0053)	0.017	(0.017,0.017)
Barro Colorado Island, Panama	0.13	(0.10,0.16)	-0.0010	(-0.0012,-0.0008)	0.0036	(0.0033,0.0038)	0.021	(0.021,0.021)
Mo Singto, Thailand	0.20	(0.16,0.25)	-0.0019	(-0.0023,-0.0016)	0.0058	(0.0054,0.0061)	0.026	(0.025,0.026)
Huai Kha Khaeng, Thailand	0.13	(0.10,0.17)	-0.0013	(-0.0015,-0.0010)	0.0038	(0.0035,0.0040)	0.015	(0.014,0.015)
Palanan, Phillipines	0.18	(0.15,0.21)	0.0011	(0.0006,0.0015)	0.0054	(0.0049,0.0058)	0.028	(0.027,0.028)
Palamanui, Hawaii, USA	0.50	(0.24,0.75)	-0.0095	(-0.0210,0.0020)	0.0157	(0.0043,0.0271)	0.162	(0.007,0.317)
Laupahoehoe, Hawaii, USA	0.22	(0.07,0.36)	0.0239	(0.0168,0.0310)	0.0319	(0.0252,0.0386)	0.139	(0.035,0.243)
Heishiding, China	0.26	(0.22,0.30)	-0.0011	(-0.0014,-0.0008)	0.0084	(0.0081,0.0087)	0.025	(0.025,0.026)
Lienhuachih, Taiwan	0.34	(0.28,0.39)	0.0015	(0.0006,0.0024)	0.0197	(0.0188,0.0205)	0.047	(0.034,0.060)
Fushan, Taiwan	0.19	(0.14,0.23)	0.0105	(0.0096,0.0114)	0.0254	(0.0245,0.0263)	0.067	(0.038,0.097)
Utah Cedar Breaks, USA	0.50	(0.18,0.82)	-0.0079	(-0.0132,-0.0026)	-0.0038	(-0.0090,0.0015)	0.051	(0.046,0.056)
Yosemite National Park, USA	0.31	(0.02,0.60)	-0.0137	(-0.0211,-0.0063)	-0.0251	(-0.0323,-0.0180)	0.058	(0.049,0.066)
Tyson Research Center, USA	0.38	(0.22,0.54)	-0.0040	(-0.0056,-0.0024)	-0.0058	(-0.0074,-0.0043)	0.028	(0.027,0.029)
Smithsonian Conservation Biology Institute (SCBI), USA	0.25	(0.14,0.36)	-0.0017	(-0.0028,-0.0006)	-0.0039	(-0.0050,-0.0028)	0.020	(0.019,0.021)
Smithsonian Environmental Research Center (SERC), USA	0.32	(0.16,0.48)	-0.0117	(-0.0135,-0.0100)	0.0008	(-0.0009,0.0026)	0.030	(0.028,0.032)
Lilly Dickey Woods, USA	0.30	(0.16,0.43)	-0.0070	(-0.0085,-0.0054)	0.0033	(0.0017,0.0048)	0.048	(0.003,0.092)
Harvard Forest, USA	0.52	(0.37,0.67)	-0.0065	(-0.0075,-0.0056)	0.0137	(0.0128,0.0147)	0.026	(0.025,0.027)
Wabikon Lake, USA	0.39	(0.22,0.56)	0.0135	(0.0115,0.0155)	-0.0057	(-0.0077,-0.0037)	0.056	(0.003,0.110)
Wind River, USA	0.36	(0.16,0.55)	-0.0077	(-0.0101,-0.0053)	0.0050	(0.0027,0.0074)	0.099	(0.025,0.174)
Zofin, Czech Republic	0.39	(0.29,0.49)	-0.0036	(-0.0092,0.0020)	-0.0075	(-0.0128,-0.0023)	0.122	(-0.064,0.307)

Table S12. Mean estimates of conspecific negative density dependence (CNDD), density dependence from heterospecific adults (adult HNDD) and heterospecific saplings (sapling HNDD), and per-capita recruitment at low densities (*r*) measured at the 20×20 m scale (hierarchical offset-power model). 95% confidence intervals (CI) are provided, and plots are ordered as in Table S1.

Forest plot	CNDD	CNDD CI	Adult HNDD	Adult HDD CI	Sapling HNDD	Sapling HNDD CI	*r*	*r* CI
Rabi, Gabon	0.49	(0.44,0.54)	-0.0018	(-0.0029,-0.0007)	0.0118	(0.0107,0.0129)	0.061	(0.060,0.062)
Korup, Cameroon	0.33	(0.28,0.38)	-0.0009	(-0.0017,-0.0001)	0.0097	(0.0089,0.0104)	0.046	(0.046,0.047)
Wanang, Papua New Guinea	0.28	(0.25,0.31)	-0.0010	(-0.0016,-0.0004)	0.0124	(0.0118,0.0130)	0.049	(0.048,0.049)
Sinharaja, Sri Lanka	0.45	(0.39,0.50)	-0.0064	(-0.0082,-0.0047)	0.0142	(0.0124,0.0160)	0.058	(0.057,0.060)
Khao Chong, Thailand	0.30	(0.26,0.33)	0.0009	(-0.0000,0.0018)	0.0135	(0.0126,0.0144)	0.049	(0.048,0.050)
Barro Colorado Island, Panama	0.24	(0.20,0.29)	-0.0025	(-0.0032,-0.0018)	0.0090	(0.0083,0.0097)	0.051	(0.050,0.051)
Mo Singto, Thailand	0.36	(0.29,0.43)	-0.0068	(-0.0080,-0.0056)	0.0116	(0.0104,0.0128)	0.061	(0.060,0.062)
Huai Kha Khaeng, Thailand	0.23	(0.17,0.28)	-0.0052	(-0.0062,-0.0043)	0.0113	(0.0104,0.0123)	0.037	(0.036,0.038)
Palanan, Phillipines	0.32	(0.27,0.36)	-0.0004	(-0.0019,0.0011)	0.0145	(0.0130,0.0161)	0.073	(0.071,0.074)
Palamanui, Hawaii, USA	0.67	(0.40,0.95)	-0.0128	(-0.0390,0.0134)	-0.0002	(-0.0264,0.0261)	0.194	(-0.045,0.432)
Laupahoehoe, Hawaii, USA	0.39	(0.15,0.62)	0.0363	(0.0174,0.0553)	0.0490	(0.0318,0.0663)	0.240	(0.052,0.428)
Heishiding, China	0.44	(0.39,0.49)	-0.0062	(-0.0072,-0.0052)	0.0196	(0.0186,0.0206)	0.062	(0.061,0.063)
Lienhuachih, Taiwan	0.53	(0.47,0.59)	-0.0089	(-0.0120,-0.0059)	0.0464	(0.0434,0.0494)	0.100	(0.076,0.124)
Fushan, Taiwan	0.34	(0.28,0.39)	0.0174	(0.0145,0.0202)	0.0520	(0.0492,0.0549)	0.145	(0.095,0.195)
Utah Cedar Breaks, USA	0.63	(0.32,0.93)	0.0062	(-0.0071,0.0195)	0.0106	(-0.0026,0.0239)	0.065	(0.053,0.077)
Yosemite National Park, USA	0.38	(0.01,0.75)	-0.0066	(-0.0185,0.0052)	0.0108	(-0.0000,0.0217)	0.051	(0.036,0.065)
Tyson Research Center, USA	0.56	(0.38,0.74)	-0.0061	(-0.0113,-0.0010)	-0.0068	(-0.0120,-0.0017)	0.041	(0.037,0.045)
Smithsonian Conservation Biology Institute (SCBI), USA	0.38	(0.25,0.51)	-0.0042	(-0.0078,-0.0006)	-0.0057	(-0.0093,-0.0021)	0.040	(0.037,0.043)
Smithsonian Environmental Research Center (SERC), USA	0.44	(0.25,0.62)	-0.0258	(-0.0309,-0.0207)	0.0132	(0.0082,0.0182)	0.053	(0.047,0.058)
Lilly Dickey Woods, USA	0.42	(0.26,0.59)	-0.0214	(-0.0261,-0.0167)	0.0202	(0.0156,0.0249)	0.085	(0.015,0.154)
Harvard Forest, USA	0.69	(0.53,0.86)	-0.0134	(-0.0162,-0.0107)	0.0316	(0.0289,0.0344)	0.041	(0.038,0.043)
Wabikon Lake, USA	0.55	(0.35,0.74)	0.0280	(0.0213,0.0346)	-0.0053	(-0.0119,0.0014)	0.109	(0.013,0.205)
Wind River, USA	0.47	(0.23,0.71)	-0.0121	(-0.0186,-0.0056)	0.0131	(0.0070,0.0193)	0.223	(0.064,0.382)
Zofin, Czech Republic	0.54	(0.40,0.68)	-0.0074	(-0.0204,0.0056)	-0.0102	(-0.0222,0.0018)	0.094	(-0.031,0.219)

Table S13. Mean Mantel correlation coefficients testing for spatial auto-correlation in CNDD model residuals for each forest plot (offset-power model). Mantel tests assessed for relationships between model residuals of each species and spatial distance within each forest plot. Results are shown for models estimating CNDD at the 20×20-m scale, but correlations were similar for models estimating CNDD at the 10×10-m scale. Mean Mantel correlation coefficients (r_m) across species are shown, along with the SD of these coefficients and their mean *P*-value for each forest plot.

Forest plot	Mean r_m	SD r_m	Mean *P*
Rabi, Gabon	0.008	0.049	0.429
Korup, Cameroon	0.012	0.046	0.425
Wanang, Papua New Guinea	0.010	0.040	0.410
Sinharaja, Sri Lanka	0.017	0.049	0.407
Khao Chong, Thailand	0.029	0.049	0.309
Barro Colorado Island, Panama	0.016	0.037	0.372
Mo Singto, Thailand	0.021	0.039	0.319
Huai Kha Khaeng, Thailand	-0.010	0.037	0.624
Palanan, Phillipines	0.011	0.039	0.393
Palamanui, Hawaii, USA	0.005	0.072	0.478
Laupahoehoe, Hawaii, USA	0.028	0.040	0.318
Heishiding, China	0.016	0.057	0.418
Lienhuachih, Taiwan	0.023	0.053	0.387
Fushan, Taiwan	-0.004	0.049	0.597
Utah Cedar Breaks, USA	0.010	0.046	0.463
Yosemite National Park, USA	0.026	0.017	0.170
Tyson Research Center, USA	0.022	0.060	0.340
Smithsonian Conservation Biology Institute (SCBI), USA	0.047	0.060	0.240
Smithsonian Environmental Research Center (SERC), USA	0.012	0.081	0.447
Lilly Dickey Woods, USA	0.018	0.058	0.382
Harvard Forest, USA	0.010	0.056	0.407
Wabikon Lake, USA	0.022	0.068	0.443
Wind River, USA	0.005	0.034	0.382
Zofin, Czech Republic	-0.015	0.014	0.728

Table S14. Relationships between the strength of conspecific negative density dependence (CNDD) and species richness and diversity across forest plots. Relationships between the mean value of CNDD in a forest plot (measured at the 10×10 m quadrat scale with the offset-power model) and species richness may have been influenced by the inclusion of rare species (i.e. with small sample sizes). To ensure this was not the case, the strength of CNDD was measured using progressively-restrictive datasets, each one excluding a greater proportion of rare species than the prior one. Because a hierarchical model was used for these estimates, we could also use all data to measure the strength of CNDD because species with small samples sizes would not greatly affect the mean for a forest plot. These measurements were then regressed against forest-wide rarefied richness (rarefied to 7,083 individuals), forest-wide Shannon diversity indices, mean-local (20×20 m quadrat) rarefied richness (rarefied to 20 individuals), and mean-local Shannon diversity indices. Spearman-rank correlation coefficients (r_s) for relationships of species richness and diversity metrics with CNDD and associated *P*-values are presented for each test (N = 24 forest plots). Relationships were highly significant in all cases. In this manuscript, we report results excluding species with adults or saplings in fewer than 10 quadrats because relationships between conspecific adult and sapling densities across quadrats (i.e. measurements of CNDD) are not reliable for species with such low sample sizes. Qualitatively similar relationships were found if we removed species with adults and sapling occupying fewer than 1%, 2%, and 4% of quadrats in a forest plot (these percentages removed approximately the same number of species from the analysis as noted for the quadrat thresholds in this table).

Dataset (offset-power model at the 10×10 m scale)	Total number of species	CNDD & forest rarefied richness		CNDD & forest Shannon diversity		CNDD & mean-local rarefied richness		CNDD & mean-local Shannon diversity	
		r_s	*P*	r_s	*P*	r_s	*P*	r_s	*P*
All data	3,185	-0.710	0.0002	-0.643	0.0009	-0.694	0.0002	-0.678	0.0004
Species with both adults and saplings present in ≥ 10 quadrats each	2,196	-0.768	< 0.0001	-0.727	< 0.0001	-0.767	< 0.0001	-0.762	< 0.0001
Species with both adults and saplings present in ≥ 30 quadrats each	1,659	-0.800	< 0.0001	-0.761	< 0.0001	-0.795	< 0.0001	-0.798	< 0.0001
Species with both adults and saplings present in ≥ 50 quadrats each	1,352	-0.636	0.0011	-0.614	0.0018	-0.634	0.0011	-0.631	0.0012

Table S15. Relationships between the strength of conspecific negative density dependence (CNDD) and species richness and diversity across forest plots. Relationships between the mean value of CNDD in a forest plot (measured at the 20×20 m quadrat scale with the offset-power model) and species richness may have been influenced by the inclusion of rare species (i.e. with small sample sizes). To ensure this was not the case, the strength of CNDD was measured using progressively-restrictive datasets, each one excluding a greater proportion of rare species than the prior one. Because a hierarchical model was used for these estimates, we could also use all data to measure the strength of CNDD because species with small samples sizes would not greatly affect the mean for a forest plot. These measurements were then regressed against forest-wide rarefied richness (rarefied to 7,083 individuals), forest-wide Shannon diversity indices, mean-local (20×20 m quadrat) rarefied richness (rarefied to 20 individuals), and mean-local Shannon diversity indices. Spearman-rank correlation coefficients (r_s) for relationships of species richness and diversity metrics with CNDD and associated *P*-values are presented for each test (N = 24 forest plots). Relationships were highly significant in most cases. In this manuscript, we report results excluding species with adults or saplings in fewer than 10 quadrats because relationships between conspecific adult and sapling densities across quadrats (i.e. measurements of CNDD) are not reliable for species with such low sample sizes. Qualitatively similar relationships were found if we removed species with adults and sapling occupying fewer than 1%, 2%, and 4% of quadrats in a forest plot (these percentages removed approximately the same number of species from the analysis as noted for the quadrat thresholds in this table).

Dataset (offset-power model at the 20×20 m scale)	Total number of species	CNDD & forest rarefied richness		CNDD & forest Shannon diversity		CNDD & mean-local rarefied richness		CNDD & mean-local Shannon diversity	
		r_s	*P*	r_s	*P*	r_s	*P*	r_s	*P*
All data	3,185	-0.515	0.0110	-0.443	0.0315	-0.486	0.0171	-0.477	0.0197
Species with both adults and saplings present in ≥ 10 quadrats each	2,173	-0.656	0.0007	-0.598	0.0024	-0.617	0.0017	-0.611	0.0019
Species with both adults and saplings present in ≥ 30 quadrats each	1,611	-0.650	0.0008	-0.611	0.0019	-0.637	0.0011	-0.645	0.0009
Species with both adults and saplings present in ≥ 50 quadrats each	1,276	-0.475	0.0202	-0.458	0.0255	-0.454	0.0270	-0.457	0.0258

Table S16. Relationships between species richness or diversity and the ratio of conspecific negative density dependence (CNDD) to heterospecific density dependence (HNDD) across forest plots. Relationships between the ratio of CNDD to HNDD in a forest plot (measured at the 10×10 m and the 20×20 m quadrat scales with the offset-power model) and species richness and diversity. Spearman-rank correlation coefficients (r_s) and associated *P*-values are shown for each test (N = 24 forest plots). See Tables S14 and S15 for descriptions of species richness and diversity metrics.

Species richness or diversity metric	Offset-power model			
	10×10-m scale		20×20-m scale	
	r_s	*P*	r_s	*P*
Forest rarefied richness	0.806	< 0.001	0.610	0.002
Forest observed richness	0.795	< 0.001	0.598	0.002
Forest Shannon diversity	0.807	< 0.001	0.612	0.002
Local rarefied richness	0.852	< 0.001	0.654	0.001
Local observed richness	0.871	< 0.001	0.664	0.001
Local Shannon diversity	0.866	< 0.001	0.678	0.000

Table S17. Relationships between species abundance and the strength of conspecific negative density dependence (CNDD) across species within each forest plot. Results are shown for estimates of density dependence using the offset-power model. Intercepts and slopes for species abundance predicting the strength of CNDD are shown with 95% confidence intervals (CI). Plots are ordered as in Table S1.

Forest plot	Relationship between species abundance in a forest plot and CNDD							
	CNDD measured at the 10×10 m scale				CNDD measured at the 20×20 m scale			
	Intercept	*Int. CI*	*Slope*	*Slope CI*	*Intercept*	*Int. CI*	*Slope*	*Slope CI*
Rabi	0.43	(0.36,0.51)	0.11	(0.06,0.15)	0.75	(0.66,0.85)	0.18	(0.12,0.24)
Korup	0.30	(0.22,0.37)	0.07	(0.03,0.11)	0.51	(0.40,0.61)	0.11	(0.05,0.16)
Wanang	0.24	(0.20,0.28)	0.07	(0.04,0.09)	0.53	(0.46,0.59)	0.16	(0.12,0.19)
Sinharaja	0.43	(0.36,0.50)	0.13	(0.08,0.18)	0.65	(0.56,0.74)	0.16	(0.10,0.23)
Khao Chong	0.22	(0.17,0.27)	0.04	(0.01,0.07)	0.45	(0.38,0.53)	0.10	(0.06,0.15)
BCI	0.18	(0.12,0.24)	0.04	(-0.00,0.08)	0.39	(0.30,0.49)	0.11	(0.05,0.17)
Mo Singto	0.36	(0.27,0.45)	0.11	(0.06,0.17)	0.61	(0.49,0.73)	0.18	(0.10,0.26)
Huai Kha Khaeng	0.13	(0.07,0.20)	0.00	(-0.04,0.04)	0.28	(0.19,0.38)	0.05	(-0.02,0.11)
Palanan	0.32	(0.26,0.38)	0.11	(0.07,0.15)	0.61	(0.53,0.69)	0.22	(0.17,0.28)
Palamanui	0.54	(0.14,0.94)	0.05	(-0.29,0.39)	0.72	(0.29,1.15)	0.06	(-0.30,0.42)
Laupahoehoe	0.22	(0.07,0.38)	0.01	(-0.10,0.12)	0.39	(0.14,0.65)	0.02	(-0.17,0.20)
Heishiding	0.31	(0.23,0.38)	0.03	(-0.01,0.08)	0.51	(0.41,0.61)	0.05	(-0.01,0.11)
Lienhuachih	0.37	(0.29,0.46)	0.03	(-0.03,0.09)	0.57	(0.48,0.66)	0.04	(-0.02,0.10)
Fushan	0.19	(0.13,0.26)	0.01	(-0.04,0.05)	0.35	(0.28,0.43)	0.02	(-0.04,0.07)
Utah	0.50	(0.14,0.85)	-0.09	(-0.40,0.21)	0.62	(0.30,0.95)	-0.08	(-0.36,0.20)
Yosemite	0.38	(0.06,0.70)	-0.19	(-0.50,0.11)	0.47	(0.09,0.86)	-0.27	(-0.63,0.10)
Tyson	0.23	(0.05,0.42)	-0.22	(-0.39,-0.04)	0.38	(0.18,0.57)	-0.28	(-0.46,-0.09)
SCBI	0.20	(0.05,0.36)	-0.07	(-0.22,0.08)	0.33	(0.15,0.50)	-0.08	(-0.25,0.10)
SERC	0.29	(0.10,0.48)	-0.06	(-0.23,0.11)	0.41	(0.19,0.62)	-0.07	(-0.26,0.12)
Lilly Dickey Woods	0.23	(0.06,0.40)	-0.08	(-0.20,0.04)	0.34	(0.13,0.55)	-0.09	(-0.24,0.06)
Harvard Forest	0.36	(0.15,0.57)	-0.13	(-0.26,-0.01)	0.51	(0.28,0.73)	-0.15	(-0.28,-0.02)
Wabikon Lake	0.31	(0.11,0.50)	-0.12	(-0.27,0.03)	0.42	(0.22,0.63)	-0.17	(-0.33,-0.02)
Wind River	0.26	(0.08,0.44)	-0.15	(-0.28,-0.02)	0.34	(0.13,0.55)	-0.2	(-0.35,-0.05)
Zofin	0.42	(0.32,0.52)	0.03	(-0.01,0.08)	0.58	(0.44,0.72)	0.05	(-0.02,0.12)

Table S18. Expected values for CNDD and HNDD (measured with offset-power model) given neutral dynamics and no density dependence, and standardized effect sizes (SES). Means and SD of expected values for CNDD, adult HNDD, sapling HNDD, and the slope between CNDD and species abundance within each forest plot from neutral models. See materials and methods for details.

Forest plot	Neutral CNDD	Neutral CNDD SD	CNDD SES	Neutral Adult HNDD	Neutral Adult HNDD SD	Adult HNDD SES	Neutral Sapling HNDD	Neutral Sapling HNDD SD	Sapling HNDD SES	Neutral CNDD-abund slope	Neutral CNDD-abund slope SD	CNDD-abund slope SES
Rabi, Gabon	1.027	0.005	-106.3	-0.006	0.001	4.4	-0.008	0.001	25.7	0.044	0.007	20.1
Korup, Cameroon	1.031	0.003	-219.6	-0.004	0.000	11.1	-0.005	0.000	51.5	0.036	0.006	11.9
Wanang, Papua New Guinea	1.033	0.004	-178.8	-0.003	0.000	8.5	-0.005	0.000	64.5	0.030	0.006	21.1
Sinharaja, Sri Lanka	1.025	0.006	-94.4	-0.007	0.001	0.8	-0.009	0.001	23.9	0.054	0.007	15.8
Khao Chong, Thailand	1.028	0.006	-124.2	-0.004	0.001	8.2	-0.006	0.000	42.6	0.028	0.010	6.0
Barro Colorado Island, Panama	1.027	0.005	-163.7	-0.005	0.000	7.4	-0.007	0.000	35.9	0.038	0.007	9.1
Mo Singto, Thailand	1.026	0.007	-100.7	-0.006	0.001	-1.3	-0.008	0.001	33.5	0.042	0.009	14.8
Huai Kha Khaeng, Thailand	1.025	0.005	-146.0	-0.005	0.000	-0.4	-0.007	0.000	47.7	0.029	0.009	1.8
Palanan, Phillipines	1.022	0.005	-138.5	-0.007	0.001	6.6	-0.009	0.001	25.0	0.042	0.007	24.6
Palamanui, Hawaii, USA	0.832	0.026	-6.1	-0.028	0.010	1.6	-0.052	0.012	4.3	-0.205	0.048	5.4
Laupahoehoe, Hawaii, USA	0.850	0.026	-17.7	-0.027	0.009	7.2	-0.043	0.011	8.5	-0.208	0.039	5.8
Heishiding, China	1.026	0.006	-98.8	-0.006	0.000	-0.1	-0.008	0.001	54.1	0.045	0.009	0.7
Lienhuachih, Taiwan	0.980	0.007	-69.0	-0.008	0.001	-0.5	-0.012	0.001	57.7	-0.080	0.007	18.4
Fushan, Taiwan	0.976	0.008	-83.0	-0.010	0.001	22.3	-0.013	0.001	64.2	-0.083	0.008	12.3
Utah Cedar Breaks, USA	0.980	0.020	-17.9	-0.025	0.004	7.9	-0.038	0.006	7.9	0.055	0.022	-6.2
Yosemite National Park, USA	0.873	0.028	-17.6	-0.026	0.003	6.7	-0.037	0.004	12.2	0.049	0.045	-7.1
Tyson Research Center, USA	0.991	0.014	-30.9	-0.016	0.002	4.3	-0.023	0.002	6.8	0.063	0.018	-19.1
Smithsonian Conservation Biology Institute (SCBI), USA	0.991	0.011	-54.8	-0.013	0.002	5.3	-0.018	0.002	6.9	0.047	0.016	-7.9
Smithsonian Environmental Research Center (SERC), USA	0.998	0.014	-40.2	-0.013	0.002	-7.6	-0.018	0.003	12.0	0.048	0.018	-6.3
Lilly Dickey Woods, USA	0.946	0.015	-35.2	-0.017	0.002	-2.1	-0.024	0.003	17.4	-0.094	0.015	0.2
Harvard Forest, USA	1.008	0.011	-29.0	-0.013	0.002	-0.2	-0.019	0.001	36.4	0.061	0.016	-13.7
Wabikon Lake, USA	0.939	0.011	-34.9	-0.017	0.002	27.6	-0.024	0.003	7.5	-0.113	0.016	-3.8
Wind River, USA	0.922	0.015	-29.4	-0.020	0.002	3.2	-0.028	0.002	20.0	-0.111	0.020	-4.4
Zofin, Czech Republic	0.818	0.018	-15.3	-0.030	0.005	4.8	-0.050	0.006	7.1	-0.199	0.040	6.2

Table S19. Relationships between the strength of conspecific negative density dependence (CNDD) and species richness and diversity across forest plots with different offset values for the Ricker model. Analyses are identical to those presented in Figs. S1 and S2 above, except 0.01 and 0.001 were used as offset values in the Ricker model. These values were used in place of zero when a quadrat contained saplings of a focal species but no conspecific adults (see materials and methods for details). Spearman-rank correlation coefficients (r_s) and associated *P*-values are shown for each test (N = 24 forest plots). See Tables S5 and S6 for descriptions of species richness and diversity metrics.

Species richness/diversity metric	Relationship between CNDD and species richness/diversity							
	10×10 m scale				20×20 m scale			
	Offset = 0.010		Offset = 0.001		Offset = 0.010		Offset = 0.001	
	r_s	*P*	r_s	*P*	r_s	*P*	r_s	*P*
Forest rarefied species richness	-0.883	< 0.001	-0.904	< 0.001	-0.922	< 0.001	-0.745	< 0.001
Forest observed species richness	-0.878	< 0.001	-0.903	< 0.001	-0.925	< 0.001	-0.739	< 0.001
Forest Shannon species diversity	-0.851	< 0.001	-0.877	< 0.001	-0.889	< 0.001	-0.703	< 0.001
Mean-local rarefied species richness	-0.860	< 0.001	-0.886	< 0.001	-0.865	< 0.001	-0.704	< 0.001
Mean-local observed species richness	-0.850	< 0.001	-0.879	< 0.001	-0.852	< 0.001	-0.698	< 0.001
Mean-local Shannon species diversity	-0.851	< 0.001	-0.880	< 0.001	-0.854	< 0.001	-0.691	< 0.001

Table S20. Plot-specific acknowledgments for the Smithsonian CTFS-ForestGEO plots.

Plot	Acknowledgements	Census	References
Barro Colorado Island	The BCI forest dynamics research project was founded by S.P. Hubbell and R.B. Foster and is now managed by R. Condit, S. Lao, and R. Perez under the Center for Tropical Forest Science and the Smithsonian Tropical Research Institute in Panama. Numerous organizations have provided funding, principally the U.S. National Science Foundation, and hundreds of field workers have contributed.	7	49, 50, 51
Fushan	Taiwan Forestry Bureau, Taiwan Forestry Research Institute, Tunghai University (Taiwan), Institute of Ecology and Evolutionary Biology, National Taiwan University, and the Center for Tropical Forest Science of the Smithsonian Tropical Research Institute. (USA).	2	52
Harvard Forest	Funding for the Harvard ForestGEO Forest Dynamics plot was provided by the Center for Tropical Forest Science and Smithsonian Institute's Forest Global Earth Observatory (CTFS-ForestGEO), the National Science Foundation's LTER program (DEB 06-20443 and DEB 12-37491) and Harvard University. Thanks to many field technicians who helped census the plot and Jason Aylward for field supervision, data screening and database management. Thanks to John Wisnewski and the woods crew for providing materials, supplies, and invaluable field assistance with plot logistics and to David Foster for his support and assistance with plot design, location, and integration with other long-term studies at HF.	1	
Heishiding	We thank Sun Yat-sen University in Guangzhou, China for funding the Heishiding research forest plot.	1	23
Huai Kha Khaeng and Khao Chong	We thank many people helped to create the permanent research plots in Huai Kha Khaeng and Khao Chong. The administrative staff of Huai Kha Khaeng Wildlife Sanctuary and Khao Chong Botanical Garden helped with logistic problems of the plots in many occasions. Over the past two decades the Huai Kha Khaeng 50-hectare plot and the Khao Chong 24-hectare plot projects have been financially and administratively supported by many institutions and agencies. Direct financial support for the plot has been provided by the people of Thailand through the Royal Forest Department (1991-2003) and the National Parks Wildlife and Plant Conservation Department since 2003, the Arnold Arboretum of Harvard University, the Smithsonian Tropical Research Institute, and the National Institute for Environmental Studies, Japan, as well as grants from the US National Science Foundation (grant #DEB-0075334 to P.S. Ashton and S.J. Davies), US-AID (with the administrative assistance of WWF-USA), and the Rockefeller Foundation. Administrative support has been provided by the Arnold Arboretum, the Harvard Institute for International Development, the Royal Forest Department, and the National Parks Wildlife and Plant Conservation Department. In addition, general support for the CTFS program has come from the Arnold Arboretum of Harvard University, the Smithsonian Tropical Research Institute, the John D. and Catherine T. MacArthur Foundation, Conservation, Food and	4	53, 54, 55

	Health, Inc., and the Merck Foundation. All of these organizations are gratefully acknowledged for their support.		
Khao Chong	See above: Huai Kha Khaeng and Khao Chong.	3	53, 54, 55
Korup	The 50-ha is a collaborative project of the University of Buea, Cameroon, and the World Wide Fund for Nature, Cameroon Program in partnership with the Center for Tropical Forest Science of the Smithsonian Tropical Research Institute. Funding for the first census was provided by the International Cooperative Biodiversity Group (a consortium of the NIH, the NSF, and the USDA), with supplemental funding by the Central Africa Regional Program for the Environment (a program of USAID). Funding for the second census was provided by the Frank Levinson Family Foundation. Permission to conduct the field program in Cameroon is provided by the Ministry of Environment and Forests and the Ministry of Scientific Research and Innovation.	2	56, 57, 58
Laupahoehoe and Palamanui	The Hawai‘i Permanent Plot Network thanks the USFS Institute of Pacific Islands Forestry (IPIF) and the Hawai‘i Division of Forestry and Wildlife/Department of Land and Natural Resources for permission to conduct research within the Hawai‘i Experimental Tropical Forest; the Palāmanui Group, especially Roger Harris, for access to the lowland dry forest site. We thank the Smithsonian Tropical Research Institute Center for Tropical Forest Science. This work is possible because of support provided by NSF EPSCoR (Grant Numbers EPS- 0554657 and EPS-0903833), the USDA Forest Service, the Pacific Southwest Research Station of the USFS, the University of Hawaii, and the University of California at Los Angeles. I/We thank the USDA Forest Service and State of Hawaii Department of Land and Natural Resources Division of Forestry and Wildlife for access to the Hawaii Experimental Tropical Forest.	2	59, 60
Lienhuachih	Taiwan Forestry Research Institute, Taiwan Forestry Bureau, Taiwan Academy of Ecology, Tunghai University (Taiwan), and the Center for Tropical Forest Science of the Smithsonian Tropical Research Institute.	1	61
Lilly Dickey	Funding for the Lilly Dickey Woods Forest Dynamics Plot was provided by the Indiana Academy of Sciences, Indiana University Research and Teaching Preserve, and the Smithsonian Institution's Center for Tropical Forest Science.	1	37
Mo Singto	Thai National Park, Wildlife and Plant Conservation Department; Thai Ministry of Natural Resources and Environment; National Center for Genetic Engineering and Biotechnology (Thailand); National Science and Technology Development Agency (Thailand).	3	62
Palamanui	See above: Laupahoehoe and Palamanui	2	59, 60
Palanan	Isabela State University (Philippines), Conservation International, PLAN, Arnold Arboretum of Harvard University (USA).	4	63
Rabi	The Rabi 25-ha is a collaborative project of the National Center for Scientific and Technical Research (CENAREST) in Gabon, the Center for Conservation Education and Sustainability (CCES) of the Smithsonian Conservation Biology Institute (SCBI) and the Center for Tropical Forest Science - Forest	1	34

	Global Earth Observatories (CTFS-ForestGEO) of the Smithsonian Tropical Research Institute. Funding for the first census was provided by Shell Gabon, CTFS-ForestGEO, and SCBI. Permission to conduct the field program in Gabon is provided by CENAREST. The plot is located in a conservation area of a forest concession of the Compagnie des Bois du Gabon (CBG).		
SCBI	Funding for the Smithsonian Conservation Biology Institute (SCBI) Large Forest Dynamics Plot (LFDP) was provided by the Smithsonian Institution, the National Zoological Park, and the HSBC Climate Partnership. The SCBI LFDP is part of the Smithsonian Institution Forest Global Earth Observatory, a worldwide network of large, long-term forest dynamics plots.	1	64
SERC	Smithsonian Environmental Research Center, Earthwatch Institute	2	65
Sinharaja	The 25-ha Long-Term Ecological Research Project at Sinharaja World Heritage Site is a collaborative project of the University of Peradeniya, the Center for Tropical Forest Science of the Smithsonian Tropical Research Institute and the Arnold Arboretum of Harvard University, USA, with supplementary funding received from the John D. and Catherine T. Macarthur Foundation, the National Institute for Environmental Science, Japan, and the Helmholtz Centre for Environmental Research-UFZ, Germany, for past censuses. The PIs gratefully acknowledge the Forest Department and the Post-Graduate Institute of Science at the University of Peradeniya, Sri Lanka for supporting this project, and the local field and lab staff who tirelessly contributed in the repeated censuses of this plot.	3	66
Tyson	The Tyson Research Center Forest Dynamics Plot (TRCP) is supported by Washington University in St. Louis' Tyson Research Center. Funding was provided by the International Center for Advanced Renewable Energy and Sustainability (I-CARES) at Washington University in St. Louis, the National Science Foundation (DEB 1557094), and the Tyson Research Center. We thank the Tyson Research Center staff for providing logistical support, and the more than 100 high school students, undergraduate students, and researchers that have contributed to the project. The TRCP is part of the Center for Tropical Forest Science-Forest Global Earth Observatory (CTFS-ForestGEO), a global network of large-scale forest dynamics plots.	1	14, 67
Utah	Utah State University (USA), the US National Park Service, and all the volunteers listed at http://www.ufdp.org.	1	68
Wabikon Lake	The Wabikon Lake Forest Dynamics Plot, located in the Chequamegon-Nicolet National Forest of northern Wisconsin, is part of the Smithsonian Institution's CTFS-ForestGEO network. Tree censuses at the site have been supported by The 1923 Fund, the Smithsonian Tropical Research Institute, and the Cofrin Center for Biodiversity at the University of Wisconsin-Green Bay. More than 50 scientists and student assistants contributed to the first two plot censuses. We are particularly grateful for the leadership of Gary Fewless, Steve Dhein, Kathryn Corio, Juniper Sundance, Cindy Burtley, Curt Rollman, Mike Stiefvater, Kim McKeefry, and U.S. Forest Service collaborators Linda Parker and Steve Janke.	2	

Wanang	The 50-ha Wanang Forest Dynamics Plot is a collaborative project of the New Guinea Binatang Research Center, the Center for Tropical Forest Science of the Smithsonian Tropical Research Institute, the Forest Research Institute of Papua New Guinea, the Czech Academy of Sciences (grant GACR 16-18022S) and the University of Minnesota supported by NSF DEB- 1027297 and NIH ICBG 5UO1TW006671. We acknowledge the government of Papua New Guinea and the customary landowners of Wanang for supporting and maintaining the plot.	1	69
Wind River	We acknowledge Ken Bible, Todd Wilson, the Gifford Pinchot National Forest, the USDA Forest Service Pacific Northwest Research Station, Utah State University, University of Washington, University of Montana, Washington State University, and the volunteers listed at http://www.wfdp.org.	1	70, 71
Yosemite	The Yosemite Forest Dynamics Plot is a collaborative project of Utah State University, the University of Montana, the University of Washington, and Washington State University. Funding was provided by the Center for Tropical Forest Science of the Smithsonian Tropical Research Institute, Utah State University, and the University of Washington. We thank Yosemite National Park for providing logistical support, and the students, volunteers and staff individually listed at http://yfdp.org.	1	72
Zofin	The Zofin Forest Dynamics Plot is part of the Smithsonian Institution Forest Global Earth Observatory, a worldwide network of large, long-term forest dynamics plots. We acknowledge the Department of Forest Ecology of the Silva Tarouca Research Institute for supporting and maintaining the long-term monitoring of the Zofin Forest Dynamics Plot under the GA CR grant No. P504/16-18022S.	1	73

R scripts

1) R script for non-linear Ricker model for each species

```
### R script to run nonlinear density dependence model (Ricker model)
### to calculate CNDD and HDD for each species in the CTFS-ForestGEO
### analysis.
###
### By: J. A. LaManna, updated 02-23-2017

# Load required packages
library(doBy)
library(gnm)

# 1. Load functions for analyses

Ricker <- function(x,Had,Hsap){
       list(predictors =   list(r = 1, CNDD = 1, HNDDad = 1, HNDDsap = 1),
       variables = list(substitute(x), substitute(Had), substitute(Hsap)),
      term = function(predictors, variables) {
          pred <- paste("(", variables[1],")*exp(", predictors[1],
                        ")*exp(", predictors[2], "*", variables[1],
                        ")*exp(", predictors[3], "*", variables[2],
                        ")*exp(", predictors[4], "*", variables[3],")+0.0001",
                        sep = "")
         })
}
class(Ricker ) <- "nonlin"


# fit model and plot fit line with nonlinear Ricker function
fit.ricker.cndd = function(data){
x=data$adult; y = data$sap; Hsap = data$Hsap; Had = data$Had
return(tryCatch(gnm(y~-1+Ricker(x,Had,Hsap),family = quasipoisson(link="identity")),
error=function(e) NULL))
}


# 2. Definition of variables
# sap = number of saplings of a focal species in a quadrat or subquadrat
# adult = number of conspecific adults of a focal species in a quadrat or subquadrat
# hsap = number of heterospecific saplings in in a quadrat or subquadrat
# hadult = number of heterospecific adults in in a quadrat or subquadrat


# 2. Code to prepare data (include non-zero sapling abundances in subquadrats or
#    quadrats with zero adults by adding 0.1, these data are otherwise ignored
#    by the Ricker model)

adult2=adult
adult2[which(adult==0 & sap>0)]=adult2[which(adult==0 & sap>0)]+0.1
data=data.frame("adult"=adult2, "sap"=sap, "Had"=hadult, "Hsap"=hsap)

# 3. Code to run the model for all species in a forest plot

fit=fit.ricker.cndd(data)
```

2) R script to calculate CNDD and HDD with lme4

```
### R script to run linear mixed-effects model (offset-power model)
### to calculate CNDD and HDD for each forest plot in the CTFS-ForestGEO
### analysis.
###
### By: J. A. LaManna, updated 02-23-2017

# Load required packages
library(lme4)

# 1. Definition of variables
# sap = number of saplings of a focal species in a quadrat or subquadrat
# adult = number of conspecific adults of a focal species in a quadrat or subquadrat
# hsap = number of heterospecific saplings in in a quadrat or subquadrat
# hadult = number of heterospecific adults in in a quadrat or subquadrat
# spp = unique identifier for each species


# 2. Code to prepare data

lgsap = log10(1 + sap)
lgadult = log10(1 + adult)
hsap = scale(hsap, center = T, scale = T)
hadult = scale(hsadult, center = T, scale = T)


# 3. Code to run model with full random-effects structure

model=lmer(lgsap~lgadult+hsap+hadult+(lgadult+hsap+hadult|spp),REML=F)
summary(model)

# 4. Code to run model with random-effects for intercept and CNDD only

model=lmer(lgsap~lgadult+hsap+hadult+(lgadult|spp),REML=F)
summary(model)
```

3) R script for simulation of data with process and measurement error, functions to fit the data, and automated simulation tests for model bias across parameter space

```
### R script to simulate data with known value of CNDD, process
### error (demographic stochasticity, measurement error
### (seeds dispersing across quadrats), and dispersal of seeds outside
### the forest plot for CTFS-ForestGEO analysis.
###
### By: J. A. LaManna, updated 04-12-2017

# Load required packages
library(doBy)
library(reshape)
library(VGAM)
library(emdbook)
library(nlme)
library(ggplot2)
library(RColorBrewer)
library(mvtnorm)
library(doBy)
library(ggplot2)
library(pscl)
library(MASS)
library(boot)

##############################################################################################
##########
# I. Functions
##############################################################################################
##########
### Functions to simulate data with known CNDD
# n = number of quadrats in simulated forest plot
# meanTrees = number of mean adult trees per quadrat
# lambda = per capita recruitment rate (in absence of density dependence)
# trueCNDD = conspecific density dependence (value=1 means no CNDD)
# theta = negative binomial overdispersion parameter
# d = proportion of seeds dispersing outside of the simulated forest plot

# Simple Models

sim.data.simple.power = function(n, meanTrees, lambda, trueCNDD){
consppTrees = rpois(n, meanTrees)
recruits = (lambda)*(consppTrees^trueCNDD) # power law function
data=data.frame(consppTrees,recruits)}

sim.data.simple.ricker = function(n, meanTrees, lambda, trueCNDD){
consppTrees = rpois(n, meanTrees)
recruits = (lambda*consppTrees)*exp(-trueCNDD*consppTrees) # Ricker population model
data=data.frame(consppTrees,recruits)}


# Error Models

# Add measurement error on observed trees per quadrat
sim.data.error.power = function(n, meanTrees, lambda, trueCNDD, theta){
trueTrees = rnbinom(n,size = theta, mu=meanTrees)
truerecruits = (lambda)*(trueTrees^trueCNDD) # power law function
consppTrees = rpois(n,lambda=trueTrees)
recruits = rnbinom(n,size = theta, mu=truerecruits)
data=data.frame(trueTrees,truerecruits,consppTrees,recruits)}
```

```
# same thing but add measurement error on observed trees per quadrat
sim.data.error.ricker = function(n, meanTrees, lambda, trueCNDD, theta){
trueTrees = rnbinom(n,size = theta, mu=meanTrees)
truerecruits = (lambda*trueTrees)*exp(-trueCNDD*trueTrees) # Ricker population model
consppTrees = rpois(n,lambda=trueTrees)
recruits = rnbinom(n,size = theta, mu=truerecruits)
data=data.frame(trueTrees,truerecruits,consppTrees,recruits)}


# Dispersal and error models

# same as error version but some fraction (d) of recruits globally dispersed
sim.data.dispersal.power = function(n, meanTrees, lambda, trueCNDD, theta, d){
trueTrees = rnbinom(n,size = theta, mu=meanTrees)
totRecruits = (lambda)*(trueTrees^trueCNDD) # power law function
localRecruits = totRecruits*(1-d)
recruits=localRecruits + sum(totRecruits)*d/n
recruits = rnbinom(n,size = theta, mu=recruits)
consppTrees = rpois(n,lambda=trueTrees)
data=data.frame(trueTrees,totRecruits,consppTrees,recruits)}

# same as error version but some fraction (d) of recruits globally dispersed
sim.data.dispersal.ricker = function(n, meanTrees, lambda, trueCNDD, theta, d){
trueTrees = rnbinom(n,size = theta, mu=meanTrees)
totRecruits = (lambda*trueTrees)*exp(-trueCNDD*trueTrees) # logistic growth function
localRecruits = totRecruits*(1-d)
recruits=localRecruits + sum(totRecruits)*d/n
recruits = rnbinom(n,size = theta, mu=recruits)
consppTrees = rpois(n,lambda=trueTrees)
data=data.frame(trueTrees,totRecruits,consppTrees,recruits)}


##############################################################################
##########
### Fit Functions

# fit model with log-transformed power function and plot fit line (on real scale)
fit.logpower.cndd = function(data, offset){
x = log(data$consppTrees + offset); y = log(data$recruits + offset)
x2 = data$consppTrees; y2 = data$recruits
plot(x2,jitter(y2),xlab="conspp
trees",ylab="recruits",xlim=c(min(x2),max(x2)),ylim=c(min(y2),max(y2)))
abline(0,1,lty="dashed")
fit = lm(y~x)
test=seq(min(x2),max(x2),length=300)
beta=coef(fit)[2]
int=coef(fit)[1]
sap.pred <- exp(int+(log(offset+test)*beta))-offset
lines(test,sap.pred,col="black")
title(paste0("True CNDD = ",trueCNDD,"; Fit CNDD = ",round(coef(fit)[2],2)))
return(summary(fit))}


# fit model and plot fit line with nonlinear Ricker function
fit.ricker.cndd = function(data, offset){
x=data$consppTrees; y = data$recruits
x[which(x==0 & y>0)]=x[which(x==0 & y>0)] + offset    #Incorporate non-zero values on
y-axis
plot(x,jitter(y),xlab="conspp
trees",ylab="recruits",xlim=c(min(x),max(x)),ylim=c(min(y),max(y)))
abline(0,1,lty="dashed")
fit.power3 <- function(p, X, Y){
       CNDD <- (p[1])
```

```
       lambda    <- exp(p[2])
       y.pred <- (lambda*X)*exp(-CNDD*X)
       RSS    <- sum((Y-y.pred)*(Y-y.pred))/length(X)
       return(RSS)}
p <- c(CNDD = 0.9, lambda = log(0.04))
tmp <- optim(p, fit.power3, method="Nelder-Mead", X=x, Y=y,
control=list(maxit=20000,trace=0));
best.pow.optim <- c(tmp$par[1],exp(tmp$par[2]))
CNDD=best.pow.optim[1]
lambda=best.pow.optim[2]
test=seq(min(x),max(x),length=300)
sap.pred <- (lambda*test)*exp(-CNDD*test)
lines(test,sap.pred,col="black")
title(paste0("True CNDD = ",trueCNDD,"; Fit CNDD = ",round(CNDD,2)))
return(best.pow.optim)}


##############################################################################################
##########
# II. Simple: no observation or measurement error, no dispersal
##############################################################################################
##########

# Simple Power Simulation
n = 1000
meanTrees = 2
trueCNDD = 0.1      # True conspecific negative density-dependence (1 = no CNDD; lower
values = stronger CNDD)
lambda = 0.9
data = sim.data.simple.power(n = n, meanTrees = meanTrees, lambda = lambda, trueCNDD =
trueCNDD)
fit.logpower.cndd(data,offset=1)


# Simple Ricker Simulation
n = 1000
meanTrees = 2
trueCNDD = 0.1      # True conspecific negative density-dependence (0 = no CNDD;
higher values = stronger CNDD)
lambda = 0.9
data = sim.data.simple.ricker(n,meanTrees,lambda=lambda,trueCNDD=trueCNDD)
fit.ricker.cndd(data,offset=0.1)


##############################################################################################
##########
# III. Add observation and measurement error
##############################################################################################
##########
# assume recruits observed with NO observation error but
# that number of trees in quadrat is not a perfect measure
# of either seeds landing in quadrat (due to dispersal across
# plot boundaries) or number of trees influencing seedling
# success (edge effects)

meanTrees = 2 # Mean number of adult trees per quadrat
n = 1000            # Number of quadrats
trueCNDD = 0.1      # True conspecific negative density-dependence (1 = no CNDD; lower
values = stronger CNDD)
lambda = 1.00 # Density-independent population growth rate
theta = 1           # Error
data = sim.data.error.power(n = n, meanTrees = meanTrees, lambda = lambda, trueCNDD =
trueCNDD, theta = theta)
```

```
fit.logpower.cndd(data,offset=1)


meanTrees = 2
n = 1000
trueCNDD = 0.10     # True conspecific negative density-dependence (0 = no CNDD;
higher values = stronger CNDD)
lambda = 1.00
theta = 1
data = sim.data.error.ricker(n = n, meanTrees = meanTrees, lambda = lambda, trueCNDD =
trueCNDD, theta = theta)
fit.ricker.cndd(data,offset=0.1)


##############################################################################
##########
# IV. Add dispersal and observation and measurement error
##############################################################################
##########
# Measurement error, 90% of recruits stay put, 10% are globally dispersed

meanTrees = 2 # Mean number of adult trees per quadrat
n = 1000            # Number of quadrats
trueCNDD = 0.1      # True conspecific negative density-dependence (1 = no CNDD; lower
values = stronger CNDD)
lambda = 1.00 # Density-independent population growth rate
theta = 1           # Error
d = 0.10            # Dispersal Factor
data = sim.data.dispersal.power(n = n, meanTrees = meanTrees, lambda = lambda,
trueCNDD = trueCNDD, theta = theta, d = d)
fit.logpower.cndd(data,offset=1)


meanTrees = 2 # Mean number of adult trees per quadrat
n = 1000            # Number of quadrats
trueCNDD = 0.02     # True conspecific negative density-dependence (0 = no CNDD;
higher values = stronger CNDD, d = d)
lambda = 1.00
theta = 1
d = 0.10
data = sim.data.dispersal.ricker(n = n, meanTrees = meanTrees, lambda = lambda,
trueCNDD = trueCNDD, theta = theta, d = d)
fit.ricker.cndd(data,offset=0.1)


##############################################################################
##
##############################################################################
##
### Functional form simulations

# Simulate data for 100 iterations of each combination of CNDD
# and lambda.  Compare across different values of theta, n, meanTrees, and d.

##############################################################################
##
### Simulate data with power model as underlying function

set.seed(1254)
n = 1000            # Number of quadrats
its = 15            # number of breaks between extreme values of CNDD in parameter
space
k = 100             # number of iterations for each parameter combination
```

```
# meanTrees = Mean number of trees per quadrat
# d = proportion of seeds dispersing out of plot
# theta = Error (negative binomial scale parameter)

testCNDD = seq(0.1,1.15,length=its)
testlambda = seq(0.3,1.5,length=6)
testmeanTrees = c(0.11, 0.31, 0.63, 1.13, 1.03, 3.30)# Based on values in data (min,
25th percentile, median, mean, 75th percentile, and 90th percentile of mean adult
densities across plots)
testd = c(0.1, 0.2, 0.3)
testTheta = c(0.1, 0.5, 1.0, 1.5, 2.0)
testOffset = c(0.01, 0.1, 1)

offsetmatrix =
data.frame(matrix(c(NA),nrow=its*length(testlambda)*length(testmeanTrees)*length(testd
)*length(testTheta)*length(testOffset),ncol=8))
names(offsetmatrix) = c("knownCNDD", "knownLambda", "meanTrees", "d", "theta",
"offset", "estCNDD", "estLambda")
offsetmatrix$knownCNDD = rep(testCNDD, each = dim(offsetmatrix)[1]/length(testCNDD))
offsetmatrix$knownLambda = rep(testlambda, each =
dim(offsetmatrix)[1]/length(testCNDD)/length(testlambda))
offsetmatrix$meanTrees = rep(testmeanTrees, each =
dim(offsetmatrix)[1]/length(testCNDD)/length(testlambda)/length(testmeanTrees))
offsetmatrix$d = rep(testd, each =
dim(offsetmatrix)[1]/length(testCNDD)/length(testlambda)/length(testmeanTrees)/length(
testd))
offsetmatrix$theta = rep(testTheta, each =
dim(offsetmatrix)[1]/length(testCNDD)/length(testlambda)/length(testmeanTrees)/length(
testd)/length(testTheta))
offsetmatrix$offset = rep(testOffset, each =
dim(offsetmatrix)[1]/length(testCNDD)/length(testlambda)/length(testmeanTrees)/length(
testd)/length(testTheta)/length(testOffset))

begin.time = Sys.time()
for(i in 1:dim(offsetmatrix)[1]) {
trueCNDD = offsetmatrix$knownCNDD[i]
offsetfitCNDDlist=c()
offsetfitlambdalist=c()
for(z in 1:k) {
data = sim.data.dispersal.power(n=n, meanTrees=offsetmatrix$meanTrees[i],
lambda=offsetmatrix$knownLambda[i],
       trueCNDD=offsetmatrix$knownCNDD[i], theta=offsetmatrix$theta[i],
d=offsetmatrix$d[i])
offsetfit = fit.logpower.cndd(data,offset=offsetmatrix$offset[i])
offsetfitCNDDlist = append(offsetfitCNDDlist,offsetfit$coef[2,1])
offsetfitlambdalist = append(offsetfitlambdalist,exp(offsetfit$coef[1,1]))
}
offsetmatrix$estCNDD[i]=mean(offsetfitCNDDlist,na.rm=T)
offsetmatrix$estLambda[i]=mean(offsetfitlambdalist,na.rm=T)
}
end.time = Sys.time()
duration.offset = end.time - begin.time


##############################
### For Ricker model

set.seed(1254)
n = 1000            # Number of quadrats
its = 15            # number of breaks between extreme values of CNDD in parameter
space
k = 100             # number of iterations for each parameter combination
```

```
# meanTrees = Mean number of trees per quadrat
# d = proportion of seeds dispersing out of plot
# theta = Error (negative binomial scale parameter)

testCNDD = seq(-0.05,2.0,length=its)
testlambda = seq(0.3,4.0,length=6)
testmeanTrees = c(0.11, 0.31, 0.63, 1.13, 1.03, 3.30)# Based on values in data (min,
25th percentile, median, mean, 75th percentile, and 90th percentile of mean adult
densities across plots)
testd = c(0.1, 0.2, 0.3)
testTheta = c(0.1, 0.5, 1.0, 1.5, 2.0)
testOffset = c(0.001, 0.01, 0.1)

rickermatrix =
data.frame(matrix(c(NA),nrow=its*length(testlambda)*length(testmeanTrees)*length(testd
)*length(testTheta)*length(testOffset),ncol=8))
names(rickermatrix) = c("knownCNDD", "knownLambda", "meanTrees", "d", "theta",
"offset", "estCNDD", "estLambda")
rickermatrix$knownCNDD = rep(testCNDD, each = dim(rickermatrix)[1]/length(testCNDD))
rickermatrix$knownLambda = rep(testlambda, each =
dim(rickermatrix)[1]/length(testCNDD)/length(testlambda))
rickermatrix$meanTrees = rep(testmeanTrees, each =
dim(rickermatrix)[1]/length(testCNDD)/length(testlambda)/length(testmeanTrees))
rickermatrix$d = rep(testd, each =
dim(rickermatrix)[1]/length(testCNDD)/length(testlambda)/length(testmeanTrees)/length(
testd))
rickermatrix$theta = rep(testTheta, each =
dim(rickermatrix)[1]/length(testCNDD)/length(testlambda)/length(testmeanTrees)/length(
testd)/length(testTheta))
rickermatrix$offset = rep(testOffset, each =
dim(rickermatrix)[1]/length(testCNDD)/length(testlambda)/length(testmeanTrees)/length(
testd)/length(testTheta)/length(testOffset))

begin.time = Sys.time()
for(i in 1:dim(rickermatrix)[1]) {
trueCNDD = rickermatrix$knownCNDD[i]
rickerfitCNDDlist = c()
rickerfitlambdalist = c()
for(z in 1:k) {
data = sim.data.dispersal.ricker(n=n, meanTrees=rickermatrix$meanTrees[i],
lambda=rickermatrix$knownLambda[i],
       trueCNDD=rickermatrix$knownCNDD[i], theta=rickermatrix$theta[i],
d=rickermatrix$d[i])
rickerfit = fit.ricker.cndd(data,offset=rickermatrix$offset[i])
rickerfitCNDDlist = append(rickerfitCNDDlist, rickerfit[1])
rickerfitlambdalist = append(rickerfitlambdalist, rickerfit[2])
}
rickermatrix$estCNDD[i] = mean(rickerfitCNDDlist, na.rm = T)
rickermatrix$estLambda[i] = mean(rickerfitlambdalist, na.rm = T)
}
end.time = Sys.time()
duration.ricker = end.time - begin.time
```

References and Notes

1. G. G. Mittelbach, D. W. Schemske, H. V. Cornell, A. P. Allen, J. M. Brown, M. B. Bush, S. P. Harrison, A. H. Hurlbert, N. Knowlton, H. A. Lessios, C. M. McCain, A. R. McCune, L. A. McDade, M. A. McPeek, T. J. Near, T. D. Price, R. E. Ricklefs, K. Roy, D. F. Sax, D. Schluter, J. M. Sobel, M. Turelli, Evolution and the latitudinal diversity gradient: Speciation, extinction and biogeography. *Ecol. Lett.* **10**, 315–331 (2007). doi:10.1111/j.1461-0248.2007.01020.x Medline

2. D. H. Janzen, Herbivores and the number of tree species in tropical forests. *Am. Nat.* **104**, 501–528 (1970). doi:10.1086/282687

3. J. H. Connell, in *Dynamics of Populations*, P. J. den Boer, G. R. Gradwell, Eds. (Centre for Agricultural Publishing and Documentation, 1971), vol. 298, pp. 298–312.

4. K. E. Harms, S. J. Wright, O. Calderón, A. Hernández, E. A. Herre, Pervasive density-dependent recruitment enhances seedling diversity in a tropical forest. *Nature* **404**, 493–495 (2000). doi:10.1038/35006630 Medline

5. C. Wills, K. E. Harms, R. Condit, D. King, J. Thompson, F. He, H. C. Muller-Landau, P. Ashton, E. Losos, L. Comita, S. Hubbell, J. Lafrankie, S. Bunyavejchewin, H. S. Dattaraja, S. Davies, S. Esufali, R. Foster, N. Gunatilleke, S. Gunatilleke, P. Hall, A. Itoh, R. John, S. Kiratiprayoon, S. L. de Lao, M. Massa, C. Nath, M. N. Noor, A. R. Kassim, R. Sukumar, H. S. Suresh, I. F. Sun, S. Tan, T. Yamakura, J. Zimmerman, Nonrandom processes maintain diversity in tropical forests. *Science* **311**, 527–531 (2006). doi:10.1126/science.1117715 Medline

6. J. W. Terborgh, Toward a trophic theory of species diversity. *Proc. Natl. Acad. Sci. U.S.A.* **112**, 11415–11422 (2015). doi:10.1073/pnas.1501070112 Medline

7. Note that CNDD here refers to a per-neighbor or per-capita effect (the negative effect of an increase in the number of conspecific neighbors) that is species-specific and may be due to life-history differences among species. This is different from a community compensatory trend, where all species may have equivalent per-neighbor CNDD, but common species experience lower recruitment or survival on average because they encounter higher densities of conspecific neighbors.

8. A. Packer, K. Clay, Soil pathogens and spatial patterns of seedling mortality in a temperate tree. *Nature* **404**, 278–281 (2000). doi:10.1038/35005072 Medline

9. L. S. Comita, H. C. Muller-Landau, S. Aguilar, S. P. Hubbell, Asymmetric density dependence shapes species abundances in a tropical tree community. *Science* **329**, 330–332 (2010). doi:10.1126/science.1190772 Medline

10. S. A. Mangan, S. A. Schnitzer, E. A. Herre, K. M. L. Mack, M. C. Valencia, E. I. Sanchez, J. D. Bever, Negative plant-soil feedback predicts tree-species relative abundance in a tropical forest. *Nature* **466**, 752–755 (2010). doi:10.1038/nature09273 Medline

11. R. Bagchi, R. E. Gallery, S. Gripenberg, S. J. Gurr, L. Narayan, C. E. Addis, R. P. Freckleton, O. T. Lewis, Pathogens and insect herbivores drive rainforest plant diversity and composition. *Nature* **506**, 85–88 (2014). doi:10.1038/nature12911 Medline

12. L. S. Comita, S. A. Queenborough, S. J. Murphy, J. L. Eck, K. Xu, M. Krishnadas, N. Beckman, Y. Zhu, L. Gómez-Aparicio, Testing predictions of the Janzen-Connell hypothesis: A meta-analysis of experimental evidence for distance- and density-dependent seed and seedling survival. *J. Ecol.* **102**, 845–856 (2014). doi:10.1111/1365-2745.12232 Medline

13. D. J. Johnson, W. T. Beaulieu, J. D. Bever, K. Clay, Conspecific negative density dependence and forest diversity. *Science* **336**, 904–907 (2012). doi:10.1126/science.1220269 Medline

14. J. A. LaManna, M. L. Walton, B. L. Turner, J. A. Myers, Negative density dependence is stronger in resource-rich environments and diversifies communities when stronger for common but not rare species. *Ecol. Lett.* **19**, 657–667 (2016). doi:10.1111/ele.12603 Medline

15. R. E. Ricklefs, F. He, Region effects influence local tree species diversity. *Proc. Natl. Acad. Sci. U.S.A.* **113**, 674–679 (2016). doi:10.1073/pnas.1523683113 Medline

16. J. Terborgh, Enemies maintain hyperdiverse tropical forests. *Am. Nat.* **179**, 303–314 (2012). doi:10.1086/664183 Medline

17. G. Yenni, P. B. Adler, S. K. M. Ernest, Do persistent rare species experience stronger negative frequency dependence than common species? *Glob. Ecol. Biogeogr.* **26**, 513–523 (2017). doi:10.1111/geb.12566

18. G. Yenni, P. B. Adler, S. K. Ernest, Strong self-limitation promotes the persistence of rare species. *Ecology* **93**, 456–461 (2012). doi:10.1890/11-1087.1 Medline

19. A. Miranda, L. M. Carvalho, F. Dionisio, Lower within-community variance of negative density dependence increases forest diversity. *PLOS ONE* **10**, e0127260 (2015). doi:10.1371/journal.pone.0127260 Medline

20. R. D. Holt, Spatial heterogeneity, indirect interactions, and the coexistence of prey species. *Am. Nat.* **124**, 377–406 (1984). doi:10.1086/284280

21. R. A. Chisholm, H. C. Muller-Landau, A theoretical model linking interspecific variation in density dependence to species abundances. *Theor. Ecol.* **4**, 241–253 (2011). doi:10.1007/s12080-011-0119-z

22. K. M. Mack, J. D. Bever, Coexistence and relative abundance in plant communities are determined by feedbacks when the scale of feedback and dispersal is local. *J. Ecol.* **102**, 1195–1201 (2014). doi:10.1111/1365-2745.12269 Medline

23. Y. Liu, S. Fang, P. Chesson, F. He, The effect of soil-borne pathogens depends on the abundance of host tree species. *Nat. Commun.* **6**, 10017 (2015). doi:10.1038/ncomms10017 Medline

24. K. Zhu, C. W. Woodall, J. V. Monteiro, J. S. Clark, Prevalence and strength of density-dependent tree recruitment. *Ecology* **96**, 2319–2327 (2015). doi:10.1890/14-1780.1 Medline

25. See supplementary materials and methods.

26. S. P. Hubbell, J. A. Ahumada, R. Condit, R. B. Foster, Local neighborhood effects on long-term survival of individual trees in a neotropical forest. *Ecol. Res.* **16**, 859–875 (2001). doi:10.1046/j.1440-1703.2001.00445.x

27. R. P. Freckleton, A. R. Watkinson, R. E. Green, W. J. Sutherland, Census error and the detection of density dependence. *J. Anim. Ecol.* **75**, 837–851 (2006). doi:10.1111/j.1365-2656.2006.01121.x Medline

28. R. K. Kobe, C. F. Vriesendorp, Conspecific density dependence in seedlings varies with species shade tolerance in a wet tropical forest. *Ecol. Lett.* **14**, 503–510 (2011). doi:10.1111/j.1461-0248.2011.01612.x Medline

29. L. A. Dyer, M. S. Singer, J. T. Lill, J. O. Stireman, G. L. Gentry, R. J. Marquis, R. E. Ricklefs, H. F. Greeney, D. L. Wagner, H. C. Morais, I. R. Diniz, T. A. Kursar, P. D. Coley, Host specificity of Lepidoptera in tropical and temperate forests. *Nature* **448**, 696–699 (2007). doi:10.1038/nature05884 Medline

30. M. L. Forister, V. Novotny, A. K. Panorska, L. Baje, Y. Basset, P. T. Butterill, L. Cizek, P. D. Coley, F. Dem, I. R. Diniz, P. Drozd, M. Fox, A. E. Glassmire, R. Hazen, J. Hrcek, J. P. Jahner, O. Kaman, T. J. Kozubowski, T. A. Kursar, O. T. Lewis, J. Lill, R. J. Marquis, S. E. Miller, H. C. Morais, M. Murakami, H. Nickel, N. A. Pardikes, R. E. Ricklefs, M. S. Singer, A. M. Smilanich, J. O. Stireman, S. Villamarín-Cortez, S. Vodka, M. Volf, D. L. Wagner, T. Walla, G. D. Weiblen, L. A. Dyer, The global distribution of diet breadth in insect herbivores. *Proc. Natl. Acad. Sci. U.S.A.* **112**, 442–447 (2015). doi:10.1073/pnas.1423042112 Medline

31. F. R. Adler, H. C. Muller-Landau, When do localized natural enemies increase species richness? *Ecol. Lett.* **8**, 438–447 (2005). doi:10.1111/j.1461-0248.2005.00741.x

32. J. H. Marden, S. A. Mangan, M. P. Peterson, E. Wafula, H. W. Fescemyer, J. P. Der, C. W. dePamphilis, L. S. Comita, Ecological genomics of tropical trees: How local population size and allelic diversity of resistance genes relate to immune responses, cosusceptibility to pathogens, and negative density dependence. *Mol. Ecol.* **26**, 2498–2513 (2017). doi:10.1111/mec.13999 Medline

33. K. J. Anderson-Teixeira, S. J. Davies, A. C. Bennett, E. B. Gonzalez-Akre, H. C. Muller-Landau, S. J. Wright, K. Abu Salim, A. M. Almeyda Zambrano, A. Alonso, J. L. Baltzer, Y. Basset, N. A. Bourg, E. N. Broadbent, W. Y. Brockelman, S. Bunyavejchewin, D. F. R. P. Burslem, N. Butt, M. Cao, D. Cardenas, G. B. Chuyong, K. Clay, S. Cordell, H. S. Dattaraja, X. Deng, M. Detto, X. Du, A. Duque, D. L. Erikson, C. E. N. Ewango, G. A. Fischer, C. Fletcher, R. B. Foster, C. P. Giardina, G. S. Gilbert, N. Gunatilleke, S. Gunatilleke, Z. Hao, W. W. Hargrove, T. B. Hart, B. C. H. Hau, F. He, F. M. Hoffman, R. W. Howe, S. P. Hubbell, F. M. Inman-Narahari, P. A. Jansen, M. Jiang, D. J. Johnson, M. Kanzaki, A. R. Kassim, D. Kenfack, S. Kibet, M. F. Kinnaird, L. Korte, K. Kral, J. Kumar, A. J. Larson, Y. Li, X. Li, S. Liu, S. K. Y. Lum, J. A. Lutz, K. Ma, D. M. Maddalena, J.-R. Makana, Y. Malhi, T. Marthews, R. Mat Serudin, S. M. McMahon, W. J. McShea, H. R. Memiaghe, X. Mi, T. Mizuno, M. Morecroft, J. A. Myers, V. Novotny, A. A. de Oliveira, P. S. Ong, D. A. Orwig, R. Ostertag, J. den Ouden, G. G. Parker, R. P. Phillips, L. Sack, M. N. Sainge, W. Sang, K. Sri-Ngernyuang, R. Sukumar, I.-F. Sun, W. Sungpalee, H. S. Suresh, S. Tan, S. C. Thomas, D. W. Thomas, J. Thompson, B. L.

Turner, M. Uriarte, R. Valencia, M. I. Vallejo, A. Vicentini, T. Vrška, X. Wang, X. Wang, G. Weiblen, A. Wolf, H. Xu, S. Yap, J. Zimmerman, CTFS-ForestGEO: A worldwide network monitoring forests in an era of global change. *Global Change Biol.* **21**, 528–549 (2015). doi:10.1111/gcb.12712 Medline

34. H. R. Memiaghe, J. A. Lutz, L. Korte, A. Alonso, D. Kenfack, Ecological importance of small-diameter trees to the structure, diversity, and biomass of a tropical evergreen forest at Rabi, Gabon. *PLOS ONE* **11**, e0154988 (2016). doi:10.1371/journal.pone.0154988 Medline

35. R Core Team, R: A Language and Environment for Statistical Computing (R Foundation for Statistical Computing, Vienna, Austria, 2015); www.r-project.org/.

36. J. Oksanen *et al*., Vegan: Community Ecology Package. R package version 2.2-1 (2015).

37. D. J. Johnson, N. A. Bourg, R. Howe, W. J. McShea, A. Wolf, K. Clay, Conspecific negative density-dependent mortality and the structure of temperate forests. *Ecology* **95**, 2493–2503 (2014). doi:10.1890/13-2098.1

38. W. E. Ricker, Stock and recruitment. *J. Fish. Res. Board Can.* **11**, 559–623 (1954). doi:10.1139/f54-039

39. P. de Valpine, A. Hastings, Fitting population models incorporating process noise and observation error. *Ecol. Monogr.* **72**, 57–76 (2002). doi:10.1890/0012-9615(2002)072[0057:FPMIPN]2.0.CO;2

40. B. M. Bolker, *Ecological Models and Data in R* (Princeton Univ. Press, 2008).

41. R. P. Freckleton, O. T. Lewis, Pathogens, density dependence and the coexistence of tropical trees. *Proc. R. Soc. London Ser. B* **273**, 2909–2916 (2006). doi:10.1098/rspb.2006.3660 Medline

42. H. Turner, D. Firth, Generalized Nonlinear Models in R: An Overview of the gnm Package. R package version 1.0-8 (2015); http://cran.r-project.org/web/packages/gnm/index.html.

43. S. Dray, A. B. Dufour, The ade4 package: Implementing the duality diagram for ecologists. *J. Stat. Softw.* **22**, 1–20 (2007). doi:10.18637/jss.v022.i04

44. H. Schielzeth, W. Forstmeier, Conclusions beyond support: Overconfident estimates in mixed models. *Behav. Ecol.* **20**, 416–420 (2009). doi:10.1093/beheco/arn145 Medline

45. D. J. Barr, R. Levy, C. Scheepers, H. J. Tily, Random effects structure for confirmatory hypothesis testing: Keep it maximal. *J. Mem. Lang.* **68**, 255–278 (2013). doi:10.1016/j.jml.2012.11.001 Medline

46. D. Bates, M. Mächler, B. Bolker, S. Walker, Fitting linear mixed-effects models using lme4. *J. Stat. Softw.* **67**, 1–48 (2015). doi:10.18637/jss.v067.i01

47. P. I. Prado, M. D. Miranda, A. Chalom, Sads: Maximum Likelihood Models for Species Abundance Distributions. R package version 0.3.1 (2016).

48. P. A. Harcombe, Tree life tables. *Bioscience* **37**, 557–568 (1987). doi:10.2307/1310666

49. S. P. Hubbell, R. B. Foster, S. T. O'Brien, K. E. Harms, R. Condit, B. Wechsler, S. J. Wright; de Lao SL, Light-gap disturbances, recruitment limitation, and tree diversity in a

neotropical forest. *Science* **283**, 554–557 (1999). doi:10.1126/science.283.5401.554 Medline

50. S. P. Hubbell, R. Condit, R. B. Foster, Forest Census Plot on Barro Colorado Island (2005); http://ctfs.si.edu/webatlas/datasets/bci.

51. R. Condit, *Tropical Forest Census Plots* (Springer, R. G. Landes Company, 1998).

52. S. H. Su *et al*., *Fushan Subtropical Forest Dynamics Plot: Tree Species Characteristics and Distribution Patterns* (Taiwan Forestry Research Institute, 2007).

53. S. Bunyavejchewin, J. V. LaFrankie, P. J. Baker, S. J. Davies, P. S. Ashton, *Forest Trees of Huai Kha Khaeng Wildlife Sanctuarry, Thailand: Data from the 50-Hectare Forest Dynamic Plot* (National Parks, Wildlife and Plant Conservation Department, 2009).

54. S. Bunyavejchewin, P. J. Baker, J. V. LaFrankie, P. S. Ashton, Stand structure of a seasonal dry evergreen forest at Huai Kha Khaeng Wildlife Sanctuary, western Thailand. *Nat. Hist. Bull. Siam Soc.* **49**, 89–106 (2001).

55. S. Bunyavejchewin, J. V. Lafranki, P. Pattapong, M. Kanzaki, A. Itoh, T. Yamakura, P. S. Ashton, Topographic analysis of a large-scale research plot in seasonal dry evergreen forest at Huai Kha Khaeng Wildlife Sanctuary, Thailand. *Tropics* **8**, 45–60 (1998). doi:10.3759/tropics.8.45

56. G. B. Chuyong *et al*., "Korup Forest Dynamics Plot, Cameroon," in *Tropical Forest Diversity and Dynamism: Findings from a Large-Scale Plot Network*, E. Losos, E. Leigh, Eds. (Univ. of Chicago Press, 2004), pp. 506–516.

57. D. W. Thomas *et al*., *Tree Species of Southwestern Cameroon: Tree Distribution Maps, Diameter Tables and Species Documentation of the 50-ha Korup Forest Dynamics Plot* (Center for Tropical Forest Science, 2003).

58. D. Kenfack, D. W. Thomas, G. B. Chuyong, R. Condit, Rarity and abundance in a diverse African forest. *Biodivers. Conserv.* **16**, 2045–2074 (2007). doi:10.1007/s10531-006-9065-2

59. R. Ostertag, F. Inman-Narahari, S. Cordell, C. P. Giardina, L. Sack, Forest structure in low-diversity tropical forests: A study of Hawaiian wet and dry forests. *PLOS ONE* **9**, e103268 (2014). doi:10.1371/journal.pone.0103268 Medline

60. F. Inman-Narahari, R. Ostertag, S. P. Hubbell, C. P. Giardina, S. Cordell, L. Sack, Density-dependent seedling mortality varies with light availability and species abundance in wet and dry Hawaiian forests. *J. Ecol.* **104**, 773–780 (2016). doi:10.1111/1365-2745.12553

61. L. W. Chang *et al*., *Lienhuachih Subtropical Evergreen Broadleaf Forest Dynamics Plot: Tree Species Characteristics and Distribution Patterns* (Taiwan Forestry Research Institute, 2012).

62. W. Brockelman, A. Nathalang, G. Gale, The Mo Singto forest dynamics plot, Khao Yai National Park, Thailand. *Nat. Hist. Bull. Siam Soc.* **57**, 35–56 (2011).

63. L. L. Co *et al*., S. J. Davies, P. S. Ashton, *Forest Trees of Palanan, Philippines: A Study in Population Ecology* (Center for Integrative and Development Studies, University of the Philippines Diliman, 2006).

64. N. A. Bourg, W. J. McShea, J. R. Thompson, J. C. McGarvey, X. Shen, Initial census, woody seedling, seed rain, and stand structure data for the SCBI SIGEO Large Forest Dynamics Plot. *Ecology* **94**, 2111–2112 (2013). doi:10.1890/13-0010.1

65. G. Parker, S. McMahon, Tree Abundances at the Smithsonian Environmental Research Center in Edgewater, MD, USA, Census 2 [Database] (accessed 29 July 2016); www.forestgeo.si.edu.

66. R. Sukumar, S. Sathyanarayana, H. Dattaraja, R. John, N. Joshi, "Mudumalai Forest Dynamics Plot, India," in *Tropical Forest Diversity and Dynamism: Findings from a Large-Scale Plot Network*, E. Losos, E. Leigh, Eds. (Univ. of Chicago Press, 2004), pp. 551–563.

67. M. J. Spasojevic, E. A. Yablon, B. Oberle, J. A. Myers, Ontogenetic trait variation influences tree community assembly across environmental gradients. *Ecosphere* **5**, 129 (2014). doi:10.1890/ES14-000159.1

68. T. J. Furniss, "The Utah Forest Dynamics Plot: Long-term forest monitoring and theoretical ecology in a high-elevation subalpine environment," thesis, Utah State University (2016).

69. J. B. Vincent, B. Henning, S. Saulei, G. Sosanika, G. D. Weiblen, Forest carbon in lowland Papua New Guinea: Local variation and the importance of small trees. *Austral Ecol.* **40**, 151–159 (2015). doi:10.1111/aec.12187 Medline

70. J. A. Lutz, A. J. Larson, J. A. Freund, M. E. Swanson, K. J. Bible, The importance of large-diameter trees to forest structural heterogeneity. *PLOS ONE* **8**, e82784 (2013). doi:10.1371/journal.pone.0082784 Medline

71. J. A. Lutz, A. J. Larson, T. J. Furniss, D. C. Donato, J. A. Freund, M. E. Swanson, K. J. Bible, J. Chen, J. F. Franklin, Spatially nonrandom tree mortality and ingrowth maintain equilibrium pattern in an old-growth *Pseudotsuga-Tsuga* forest. *Ecology* **95**, 2047–2054 (2014). doi:10.1890/14-0157.1 Medline

72. J. A. Lutz, A. J. Larson, M. E. Swanson, J. A. Freund, Ecological importance of large-diameter trees in a temperate mixed-conifer forest. *PLOS ONE* **7**, e36131 (2012). doi:10.1371/journal.pone.0036131 Medline

73. D. Janík, K. Král, D. Adam, L. Hort, P. Šamonil, P. Unar, T. Vrška, S. M. McMahon, Tree spatial patterns of *Fagus sylvatica* expansion over 37 years. *For. Ecol. Manage.* **375**, 134–145 (2016). doi:10.1016/j.foreco.2016.05.017